Distribution Agreement

In presenting this thesis as a partial fulfillment of the requirements for a degree from Emory University, I hereby grant to Emory University and its agents the non-exclusive license to archive, make accessible, and display my thesis in whole or in part in all forms of media, now or hereafter now, including display on the World Wide Web. I understand that I may select some access restrictions as part of the online submission of this thesis. I retain all ownership rights to the copyright of the thesis. I also retain the right to use in future works (such as articles or books) all or part of this thesis.

Nishant Satapathy March 23, 2023

Analyzing white matter integrity of the basolateral amygdala and subgenual anterior cingulate cortex and its association with depression in adults with ASD using the Shannon entropy technique

by

Nishant Satapathy

Opal Ousley, Ph.D.
Adviser

Neuroscience and Behavioral Biology

Opal Ousley, Ph.D.
Adviser

Candace Fleischer, Ph.D.

Committee Member

Kristen Frenzel, Ph.D.

Committee Member

2023

Analyzing white matter integrity of the basolateral amygdala and subgenual anterior cingulate cortex and its association with depression in adults with ASD using the Shannon entropy technique

By

Nishant Satapathy

Opal Ousley, Ph.D.

Adviser

An abstract of
a thesis submitted to the Faculty of Emory College of Arts and Sciences
of Emory University in partial fulfillment
of the requirements of the degree of
Bachelor of Science with Honors

Neuroscience and Behavioral Biology

2023

Abstract

Analyzing white matter integrity of the basolateral amygdala and subgenual anterior cingulate cortex and its association with depression in adults with ASD using the Shannon entropy technique

By Nishant Satapathy

Background: Individuals with ASD are four times more likely to develop depression. Regions of the brain implicated in depression include the basolateral amygdala (BLA), subgenual anterior cingulate cortex (sgACC), and associated white matter (WM) tracts, which may also play an important role in ASD. This study evaluates Shannon entropy (SE) and fractional anisotropy (FA) as markers of WM integrity in adults with ASD and age-matched controls.

Methods: We analyzed diffusion tensor imaging (DTI) data from the Autism Brain Imaging Data Exchange II, consisting of 29 adult males with ASD (mean age = 37.5 years; *SD*=16.1; range=18-62) and 29 adult male controls with no diagnosis (CON) (mean age = 39.6 years; SD=15.1; range=18-64). FSL Version 6 and Tract-Based Spatial Statistics (TBSS) were used for DTI preprocessing and analyses. Region of interest (ROI) masks were applied to evaluate SE and FA values. Main effects of age and diagnosis on SE and FA, correlations of SE and FA with measures of depression and ASD symptom severity, and the performance of SE and FA in predicting depression were all examined.

Results: There was a main effect of age on SE values in the sgACC, with individuals aged 40 to 64 having lower SE values than individuals aged 18 to 25. The older group had higher FA than individuals the younger group. SE was positively correlated with ASD symptomatology in the right amygdala; FA in the right and left amygdala and right BLA was correlated with self-reported depression scores. Post-hoc analyses identified a main effect of diagnosis for FA in the internal capsule, with ASD individuals having higher FA values than CON individuals. Planned regression analyses yielded no significant results.

Conclusions: Primary findings include main effects of age on SE and FA values within the sgACC. The positive SE correlations with ASD symptomatology in the right amygdala are consistent with prior findings and may indicate active WM changes such as axonal remodeling, which has been shown to correlate strongly with SE in animal models (Ding et al., 2017). FA within the right and left amygdala and right BLA may provide a marker of depression.

Analyzing white matter integrity of the basolateral amygdala and subgenual anterior cingulate cortex and its association with depression in adults with ASD using the Shannon entropy technique

By

Nishant Satapathy

Opal Ousley, Ph.D.

Adviser

A thesis submitted to the Faculty of Emory College of Arts and Sciences
of Emory University in partial fulfillment
of the requirements of the degree of
Bachelor of Science with Honors

Neuroscience and Behavioral Biology

2023

Acknowledgements

I would like to thank my parents, sister, and friends for their constant support. A huge thank you to Dr. Ousley for guiding me on this journey and being such a wonderful mentor for me. Special thanks to Dr. Maurizio Bergamino from the Barrow Neurological Institute for his neuroimaging analysis insights.

Data in this study were provided by ABIDE II: The Autism Brain Imaging Data Exchange II (ABIDE II) was supported through multiple mechanisms. Adriana Di Martino was supported by grant from the National Institute of Mental Health NIMH 5R21MH107045. Michael P. Milham and team were supported by the NIMH 5R21MH107045 grant. Additional funding was provided to the Child Mind Institute, specified here: http://fcon_1000.projects.nitrc.org/indi/abide/abide_II.html. Specific Funding for the Barrow Neurological Institute/ Southwest Autism Research and Resource Center (BNI/SARRC) was provided by the State of Arizona Alzheimer's Consortium (Baxter), Barrow Neurological Foundation (Baxter) and the Department of Defense (AR140105; Baxter, Smith, and Braden).

This work uses diffusion tensor imaging (DTI) data the ABIDE II dataset, publicly available as specified above. DTI scanning parameters and phenotypic files are available for each site online. Data was accessed from ABIDE II on 09/16/2020.

Table of Contents

INTRODUCTION

According to the National Institute of Mental Health, in 2020, 8.4% of adults in the US have experienced a major depressive episode (National Institute of Mental Health, 2022). Prior meta-analyses have indicated that adults with autism spectrum disorder (ASD) are four times more likely to develop depression and have a 37% lifetime prevalence of depression (Hollocks et al., 2018; Hudson et al., 2018).

Depression in ASD is often measured by the Beck Depression Inventory, version two (BDI-II) (Cassidy et al., 2018). The BDI-II is a 21-item self-report inventory that assesses the severity of depressive symptoms (Beck et al., 1996). In a sample of 947 adults with ASD, the BDI-II reliably informed the diagnosis of depression in ASD (Williams et al., 2021). In addition to this measure, caregiver questionnaires are used in the assessment of depressive symptoms (Chandrasekhar et al., 2015). However, there are disadvantages in using assessments that rely on self- and caregiver-reporting. Such measures may be inconsistent due to patients' varied interpretation of certain questions or inaccuracy in the caregivers' recognition of symptoms (Chandrasekhar et al., 2015). Thus, neuroimaging may provide an adjunct to a behavioral diagnosis of depression in ASD by improving the accuracy of diagnoses and evaluating the effectiveness of treatment with changes in imaging markers such as white matter (WM) integrity (Dunlop and Mayberg, 2017; Wise et al., 2014).

In the general population, neuroimaging studies have found regional changes in individuals with MDD. Specifically, decreases in fractional anisotropy (FA) as a measure of WM integrity were found in adults with MDD when compared with controls both widespread and in regions such as the left anterior limb of the internal capsule, the superior longitudinal fasciculus, inferior fronto-occipital fasciculus, and corpus callosum (Zou et al., 2008; Ota et al., 2015; van Velzen et al., 2020). However, beyond these regions, the amygdala and subgenual anterior cingulate cortex (sgACC) have been involved with symptoms of depression. MRI scans showed reductions in amygdala nuclei volumes in individuals with depression (Sheline et al., 1999). Moreover, amygdala hyperactivity has also been significantly associated with symptoms of MDD (Groggans et al., 2022). Specifically, the basolateral nucleus of the amygdala (BLA) was found to have a decrease in myelin proteins such as myelin basic protein and myelin oligodendrocyte basic protein in animal models of depression (Cathomas et al., 2019). Moreover, prior studies have found the lateral nucleus of the amygdala to be larger in individuals with depression (Rubinow et al., 2016).

In addition, the sgACC is activated to a greater extent in adolescents experiencing depression (Yang et al., 2009) and a longitudinal fMRI study concluded that increases in connectivity between the amygdala and sgACC were associated with the onset of depression (Davey et al., 2014; de Kwaasteniet et al., 2013). Furthermore, despite increases in connectivity between the amygdala and sgACC, studies have found concurrent decreases in WM integrity in the uncinate fasciculus (UF), which connects the amygdala with the sgACC (Kwaasteniet et al., 2013, Kier et al., 2004). Diffusion tensor imaging (DTI) studies have also found lower FA as a measure of WM integrity in the bilateral UF (Yang, 2020). Given the importance of these regions, quantifying white matter (WM) in the BLA, sgACC, and UF may serve as an objective indicator of depression.

ASD has increasingly been classified as a WM disease. For instance, in a study of ASD individuals, voxel-based analyses found decreased WM volume in the right hemisphere and corpus callosum, the latter of which has been associated with slower processing (Alexander et al., 2007; Waiter et al., 2005). In addition, decreased WM in the dorso-lateral prefrontal cortex was correlated with severity of social impairment in children with ASD (Noriuchi et al., 2010). Furthermore, shared decreases in WM integrity in ASD and other developmental disorders, such as ADHD, provide evidence of ASD existing on a spectrum of diseases manifested due to WM alterations (Aoki et al., 2017).

In ASD, the amygdala has been a hallmark region of interest in studies analyzing changes in brain structure (Gibbard et al., 2017). For instance, comparative MRI analyses reveal a significantly larger amygdala in young adults with ASD when compared with controls (Gibbard et al., 2017). In addition, the enlargement in the amygdala has been seen to begin during the first few months of life and extend into adolescence (Shen et al., 2022). Moreover, adolescents with ASD have larger BLA volumes than their control counterparts, which correlates with impairments in social communication that are characteristic of an ASD diagnosis (Seguin et al., 2021). In terms of the sgACC, DTI studies looking at the WM integrity of the sgACC in individuals with ASD found increased mean diffusivity (MD) when compared with controls, which indicates its relationship with ASD (Nickel et al., 2017). In addition, the resting state amygdala- sgACC connectivity was concluded to have a negative relationship with the presence of ASD symptoms in adolescents (Velasquez et al., 2017).

Neuroimaging studies of depression in individuals with ASD are emerging. For instance, an fMRI study of individuals with ASD and controls aged 14 to 45 showed a significant decrease in connectivity in the BLA compared in ASD, which associated with comorbid depression (Kleinhans et al., 2015). Furthermore, a diffusion tensor imaging (DTI) study examining WM integrity in ASD and comorbid depression identified decreased fractional anisotropy (FA) and increased mean diffusivity (MD) (Mohajer et al., 2019). The high prevalence of depression in adults with ASD and involvement of the amygdala and sgACC in both conditions thus substantiates the continued need for a neuroimaging study of these regions.

While both resting state and fMRI studies have identified regions of interest in ASD and depression, the study of WM using DTI yields important information regarding physical and microstructural integrity. DTI has been used to report changes in WM in multiple conditions of the central nervous system, such as Alzheimer's disease, multiple sclerosis, or mild traumatic brain injury (Lerner et al., 2014; Rovaris et al., 2009). DTI, which measures the spatial distribution of water molecules in the WM tissues in the brain, is highly sensitive to changes at the microstructural level, particularly myelination-- differences that might not be apparent in classical MR imaging (Alexander et al., 2007; Grassi et al., 2018). DTI has been used in monitoring the development of Alzheimer's disease given its ability to detect subtle changes in WM characteristic of the onset of the condition (Lerner et al., 2014; Medina and Gaviria, 2008). In addition, post-mortem samples validated the DTI technique when compared to in vivo DTI data acquisition (Stieltjes et al., 2001).

Currently, FA derived from DTI remains one of the most reported metrics of WM integrity (Figley et al., 2022). A scalar value that describes the anisotropy, or differences due to direction of the diffusion tensor in each voxel, FA has been noted to be highly sensitive to WM injury and is suitable for cross-scanner comparisons (Basser and Pierpaoli, 1996; Luque Laguna et al., 2020; Tae et al., 2018). However, the measure is unreliable in areas with complex fiber organization or fiber crossing prevalent in WM, and regions such as the corona radiata and superior longitudinal fasciculus (Alba-Ferarra et al., 2013; Figley et al., 2022; Kochunov et al., 2022; Lebel et al, 2017; Luque Laguna et al., 2020; Penke et al.,2010; Madden et al., 2012; Zhao et al., 2022).

To complement FA, researchers have developed new metrics of quantifying WM microstructure that allow for more precise biological interpretations (Delic et al., 2016; Timmers et al., 2016). One example, Shannon entropy (SE) in WM, relies on information theory to define complexity and generate a robust marker of axonal density and remodeling while avoiding the

confounds of FA (Delic et al., 2016; Fozouni et al., 2013). In a rodent model of stroke, SE was able to detect microstructural changes in the cerebrum (Ding et al., 2017). Furthermore, SE has successfully been used in studies of depression, identifying increases in complexity of WM in the left frontoparietal network of individuals with depressive symptoms (Ho et al., 2017). SE can be used to analyze the complexity of an FA map and prior studies have concluded it to be significantly correlated with diagnosis as opposed to FA, such as in the case of myelopathy (Cui et al., 2011). SE can provide a metric that can be obtained at the individual versus group level with clinical relevance (Delic et al., 2016). Furthermore, converging evidence from autopsy and animal models reveals strong indication of axonal pathology in ASD, characterized by altered axonal density, decreased axonal diameter, oligodendroglial alterations, hypomyelination, and microglial changes (Andica et al., 2021; Graciarena et al., 2019; Wegiel et al., 2018; Zikopoulos et al, 2010). Hence, given the ability of DTI to record microlevel changes in WM and the ability of SE to quantify WM integrity without being affected by axonal fibers, unlike FA, DTI analysis using SE may serve as a valuable method in objectively quantifying WM changes in ASD.

Using DTI scans from the Autism Brain Imaging Data Exchange II (ABIDE II), this neuroimaging study focuses on younger (18-25) and older (40-64) adults with ASD to analyze the WM integrities of the BLA and sgACC and whether they are correlated with depression and age in the population, given that decreases in WM integrity have been associated with increased age and depression (Liu et al., 2017; Ouyang et al., 2021). In addition, given that prior tractography studies have concluded that white matter tracts of the UF connect the amygdala with the sgACC (Kier et al., 2004), we will also analyze the WM integrity of the region.

This study seeks to determine if SE and FA differ in the WM of the BLA, sgACC, and UF in adults with ASD and age-matched CON individuals, if age has a significant effect on the SE and FA values in the regions, whether SE and FA values in the BLA, sgACC, and UF correlate with measures of depression and ASD symptom severity, and if SE predicts depression when combined with FA and age.

In this study we hypothesize that the SE and FA values of the WM in the BLA and sgACC are lower in ASD adults compared to CON counterparts, decrease with increasing age, and associate with clinical symptom severity of depression.

Primary hypotheses are listed below:

1) SE and FA in the BLA, sgACC, and UF is lower in adults with ASD compared to age-matched CON individuals
2) SE and FA in the BLA, sgACC, and UF is lower in older individuals compared to younger subjects
3) SE and FA in the BLA, sgACC, and UF correlate with clinical symptom severity [i.e., Beck Depression Inventory, Second edition (BDI-II), Social Responsiveness Scale-2 (SRS-2), Kaufman Brief Intelligence Test- 2nd Edition (KBIT- 2)]
4) Models with age + FA + SE predict depression

Additional analyses involved:

1) Examination of SE and FA in the bilateral amygdala and whole brain WM skeleton
2) Post-hoc exploratory analysis looking at $p<.10$ results within whole brain WM skeleton to identify additional regions of interest

METHODS

Open-source data

DTI scans were retrieved from the web-accessible shared brain imaging database, Autism Brain Imaging Data Exchange II (ABIDE II). This study used a subset from the ABIDE II database (i.e., DTI scans; n=58; age range =18-64 years) provided by the Barrow Neurological Institute (BNI) and Southwest Autism Research and Resource Center (SARRC). ABIDE II is the second phase to its predecessor, ABIDE I, to investigate core ASD phenotypes and symptoms. ABIDE II is led by principal investigators Adriana D. Martino, M.D., and Michael P. Milham, M.D., Ph.D. The BNI/SARRC cohort used for this study was created and led by Leslie C. Baxter, Ph.D., Christopher Smith, Ph.D., and B. Blair Braden, Ph.D. More information regarding ABIDE II and the BNI/SARRC cohort used in this study can be found at http://fcon_1000.projects.nitrc.org/indi/abide/abide_II.html.

DTI scans from the ABIDE II cohort consisted of 29 adult males with ASD and 29 adult male controls with no diagnosis (CON). The mean age for ASD individuals was 37.5 years (*SD*=16; range=18-62), and the mean age for CON individuals was 39.6 years (*SD*=15; range=18-64). Only males were available in the BNI/SARRC cohort used in this study. All subjects were scanned on a Philips Ingenia 3T scanner with a 15-channel head coil. All scans were obtained using the echo planar imaging (EPI) fast mode. The scan voxel size was 2.93 mm (right to left (RL)) x 3mm (anterior to posterior (AP) x 3 mm (slice thickness). The reported reconstructed voxel size was 1.41 x 1.41 x 3.00. All scans had a 90-degree flip angle, a recorded echo time (TE) of 101 ms, and a recorded repetition time (TR) of 7850 ms. The reported b-value was 2500 s/mm^2. See Appendix I for detailed imaging parameters for the DTI scans in this cohort.

Imaging pre-processing

Using MRIcron, the scans were converted from DICOM to NIfTI files via the dcm2niix converter (Li et al., 2016). All further analyses for DTI images were using FSL Version 6.0 developed by the Analysis Group at FMRIB at Oxford, UK (Jenkinson et al., 2012, Smith et al., 2004, Woolrich et al., 2009).

In the files provided by ABIDE II, 33 files were included with each subject, the last being a header file. The header file was deleted using the "fslsplit" function and the remaining 32 were rejoined via "fslmerge" to generate the final composite file for analysis.

Non-zero resonances were corrected for with the FSL software's "topup" using reverse phase images provided by the dataset. Consistent with Andersson et al. (2003), induced resonances were estimated and then the two images were combined into one corrected one to be used for further analysis (Andersson et al., 2003; Smith et al., 2004). "Eddy" was then used to correct for eddy current distortion (Andersson et al., 2016; Smith et al., 2004). Extraction of the skull and white matter skeleton was completed using the dwi2mask commands of MRTrix3, which deletes any non-brain tissue and generates a binary whole brain mask (Tournier et al., 2019; VanGilder et al., 2022). A whole brain FA map was then generated using the "dtifit" function.

Tract- Based Spatial Statistics (TBSS)

Tract-based spatial statistics version 1.2 (TBSS) (Smith et al., 2006) in FSL (Smith et al., 2004) was used to generate a whole brain map of WM tracts to ensure only WM was being analyzed. TBSS, using the FA maps generated with "dtifit", aligns all subjects' FA maps into MNI space via FSL's nonlinear registration tool, FNIRT (Andersson et al., 2007a; Andersson et al., 2007b). Once aligned, TBSS generates a mean FA map based on the data from all subjects inputted. The software then thins this mean FA maps to create a mean FA skeleton upon which each subject's FA data is projected for comparative WM analysis. A threshold of FA $\geq$0.2 was applied to the mean FA skeleton to ensure no extraneous gray matter was included. All registrations and resulting FA maps and skeleton were visually inspected. In this study, we applied ROI masks on the whole brain WM FA skeletons as explained below.

Region of Interest (ROI) Analysis

To the extract regions of interest (ROIs) for our analyses, we used the Automated Anatomical Labelling Atlas 3 (AAL3), JHU ICBM-DTI-81 White-Matter Labels (JHU), Jülich Histological Atlas (JHA). All atlases are registered in standard MNI space. Regions included in the AAL3 atlas relevant for our study was the bilateral amygdala (Rolls et al., 2020). The open-source atlas was downloaded from https://www.gin.cnrs.fr/en/tools/aal/. The JHU atlas provided the ROIs for the right and left uncinate fasciculus (Mori et al., 2008). The JHA provided the

basolateral nucleus of the amygdala (BLA) mask relevant for our study and was pre-uploaded in FSL Version 6.0 (Amunts et al., 2005).

The AAL3 atlas automatically delineates regions based on connectivity and provides concrete x,y,z MNI coordinates for each region (Rolls et al., 2020) All areas labeled by the AAL3 atlas are on a standard human brain in MNI space and each region is labeled with a single value between 1 and 170 (Rolls et al., 2020). We used "fslmaths" to generate the amygdala ROIs.

Using the same method, the ROIs for the right and left uncinate fasciculus were extracted from the "JHU ICBM-DTI-81 White-Matter Labels" atlas via "fslmaths" (Duan et al., 2015). The JHU atlas, pre-uploaded in FSL Version 6.0, is a hand-segmented white matter tract atlas in stereotaxic coordinates created using DTI (Mori et al., 2008).

The JHA is a probabilistic atlas based on the cytoarchitecture of the cortical and subcortical regions of the brain (Amunts et al., 2005; Amunts et al., 2020). The atlas indicates each region by a map of 0 – 100% probability of the specific region, allowing for variability when analyzing each subject (Amunts et al., 2020). The right and left BLA map was downloaded from the atlas and a threshold of 50-100% probability was set using "fslmaths" to extract the ROI used in the study followed by visual inspection.

Unlike the bilateral amygdala and BLA ROIs, the sgACC ROIs were manually generated using the MNI and corresponding voxel coordinates from Zhan et al (Zhan et al., 2017). A 10 mm radius sphere ROI was created using "fslmaths".

Once the regions were generated, the resulting files were masked with the mean FA skeleton mask provided by TBSS and then binarized to be applied for SE and mean FA value extraction. Using "fslstats", applying the ROIs to the FA skeleton mask of each subject, the histogram analysis of the FA map was done and a region-specific SE score for the FA map was generated using the following entropy formula, postulated by Shannon in 1963:

$$H(x_1) = -\Sigma\, p(x_i)\log p(x_i)$$
$$x_i\ \varepsilon\ k$$

where $H(x_1)$ represents the SE score generated, x_i are the FA values, k is equaled to the number of bins, and $p(x_i)$ represents the probability the FA value is repeated throughout the map (Shannon, 1963; Delic et al., 2016).

Clinical and Symptom Measures

Clinical measures used in this study include the Beck Depression Inventory- II (BDI-II), Social Responsiveness Scale-Version 2 (SRS-2) and Kaufman Brief Intelligence Test- 2nd Edition (KBIT- 2).

The BDI-II was the main clinical measure of depression used in this study. The BDI-II is a 21-item self-report inventory that assesses the severity of depressive symptoms. ABIDE-II provides BDI-II scores for both CON and ASD individuals (Beck et al., 1996; Smarr et al., 2011).

To complement our analyses with an application of ASD symptomatology, the SRS-2 was used. The SRS-2 measures ASD traits based on a population sample. It contains five subtests, assessing awareness, motivation, cognition, communication, mannerisms, and overall total symptoms. A total score of 60-65 is indicative of moderate social deficits and a score of 76 or above suggests severe clinical social deficits due to an ASD diagnosis. (Constantino and Gruber, 2012; Bruni, 2014). Additionally, the KBIT-2 was used as it provides a composite IQ score with an overall score range between 40-160, mean score of 100 with a standard deviation of 15 points (Kaufman, 2004; Bain et al., 2010).

RESULTS

All statistics were completed using SPSS version 27.0 (IBM Corp, 2020). Datasets were examined for any significant outliers for each analysis and reported below. **See Table 1 for a summary of all results.**

I. Shannon entropy (SE) results:

SE in the right sgACC

A two-way ANOVA with SE as the dependent variable and age group and diagnosis held as fixed factors indicated a significant main effect for age group [$F(1,55)=13.084$, $p<.001$; $\eta_p^2=.192$] but not for diagnosis [$F(1,55)=.209$, $p=.866$; $\eta_p^2=.001$]. There was no significant interaction of age group by diagnosis. There was a significant difference ($p<.001$) in mean SE values between the older ($Mean_{AGE\geq40}=.968$; Std Err=.000; 95% CI=.969-.971) and younger ($Mean_{AGE\ 18\text{-}25}=.970$; Std Err=.000; 95% CI=.969-.971) groups. There was, however, no significant difference ($p=.866$) between CON ($Mean_{CON}=.969$; Std Err=.000; 95% CI=.968-.970) and ASD groups ($Mean_{ASD}=.969$; Std Err=.000; 95% CI=.968-.970). See Figures 1 and 2 that illustrate these findings.

SE in the left sgACC

When repeated for the left sgACC, the two-way ANOVA with SE as the dependent variable revealed a significant main effect for age group [$F(1,55)=15.811$, $p<.001$; $\eta_p^2=.223$] but not for diagnosis [$F(1,55)=.578$, $p=.450$; $\eta_p^2=.010$]. There was no significant interaction of age group by diagnosis. There was a significant difference ($p<.001$) in mean SE values between the older ($Mean_{AGE\geq40}=.969$; Std Err=.000; 95% CI=.969-.970) and younger ($Mean_{AGE\ 18\text{-}25}=.971$; Std Err=.000; 95% CI=.971-.972) groups. There was, however, no significant difference ($p=.450$) between CON ($Mean_{CON}=.971$; Std Err=.000; 95% CI=.970-.971) and ASD groups ($Mean_{ASD}=.970$; Std Err=.000; 95% CI=.969-.971). See Figures 3 and 4 that illustrate these findings.

SE in the right BLA

The two-way ANOVA for the right BLA also did not reveal any significant main effects for age group [$F(1,55)=.621$, $p=.434$; $\eta_p^2=.011$] or diagnosis [$F(1,55)=.094$, $p=.760$; $\eta_p^2=.002$] and

the age group by diagnosis interaction was not significant. The mean SE values in the older ($Mean_{AGE\geq40}$=.801; Std Err=.001; 95% CI=.799-.803) and younger groups ($Mean_{AGE\ 18\text{-}25}$=.800; Std Err=.001; 95% CI=.797-.802) were not significantly different (p=.434) from each other. Similarly, the CON ($Mean_{CON}$ =.800; Std Err=.001; 95% CI=.798-.802) and ASD groups ($Mean_{ASD}$ =.800; Std Err=.001; 95% CI=.798-.803) did not differ signicantly (p=.760) in terms of their mean SE values as well. See Figures 5 and 6 that illustrate these findings.

SE in the left BLA

For the left BLA, a two-way ANOVA with SE as the dependent variable revealed no significant main effects for age group [$F(1,55)$=.493, p=.485; η_p^2=.009] and diagnosis [$F(1,55)$=1.083, p=.303, η_p^2=.019]. The age group by diagnosis interaction was not significant. There was no significant difference (p=.485) in mean SE values between the older ($Mean_{AGE\geq40}$=.773; Std Err=.001; 95% CI=.771-.775) and younger groups ($Mean_{AGE\ 18\text{-}25}$=.774; Std Err=.001; 95% CI=.771-.777). In addition, a comparison of the mean SE values of the left BLA between CON ($Mean_{CON}$ =.773; Std Err=.001; 95% CI=.770-.775) and ASD groups ($Mean_{ASD}$ =.775; Std Err=.001; 95% CI=.772-.777) revealed no significant difference (p=.303) between the two groups. See Figures 7 and 8 that illustrate these findings.

SE in the right amygdala

A two-way ANOVA with SE as the dependent variable revealed no significant main effects for age group [$F(1,55)$=.199, p=.657; η_p^2=.004] and diagnosis [$F(1,55)$=.164, p=.687, η_p^2=.003]. The age group by diagnosis interaction was not significant. There was no significant difference (p=.657) in mean SE values between the older ($Mean_{AGE\geq40}$=.735; Std Err=.001; 95% CI=.734-.737) and younger groups ($Mean_{AGE\ 18\text{-}25}$=.735; Std Err=.001; 95% CI=.733-.737). In addition, a comparison of the mean SE values between CON ($Mean_{CON}$ =.735; Std Err=.001; 95% CI=.733-.737) and ASD groups ($Mean_{ASD}$ =.735; Std Err=.001; 95% CI=.734-.737) revealed no significant difference (p=.303) between the two groups. See Figures 9 and 10 that illustrate these findings.

SE in the left amygdala

A two-way ANOVA with SE as the dependent variable revealed no significant main effects for age group [$F(1,55)$=.076, p=.784; η_p^2=.001] and diagnosis [$F(1,55)$=.629, p=.431, η_p^2=.011].

The age group by diagnosis interaction was not significant. There was no significant difference (p=.784) in mean SE values between the older ($Mean_{AGE\geq40}$=.675; Std Err=.001; 95% CI=.672-.677) and younger groups ($Mean_{AGE\ 18\text{-}25}$=.675; Std Err=.002; 95% CI=.672-.678). In addition, there was no significant difference (p=.431) in the SE values of the left amygdala between CON ($Mean_{CON}$ =.676; Std Err=.001; 95% CI=.673-.679) and ASD groups ($Mean_{ASD}$ =.674; Std Err=.001; 95% CI=.671-.677). See Figures 11 and 12 that illustrate these findings.

SE in the right uncinate fasciculus

An examination of the SE values indicated two outliers (ASD and CON) which needed to be taken out before further analysis. Following this, a two-way ANOVA with SE as the dependent variable and age group and diagnosis held as fixed factors revealed no significant main effect for age group [$F(1,55)$=.833, p=.366; η_p^2=.015] and diagnosis [$F(1,55)$=.145, p=.705; η_p^2=.003]. There was no significant interaction of age group by diagnosis. There was no significant difference (p=.366) in mean SE values between the older ($Mean_{AGE\geq40}$=.547; Std Err=.001; 95% CI=.545-.549) and younger ($Mean_{AGE\ 18\text{-}25}$=.545; Std Err=.001; 95% CI=.542-.548) groups. There was no difference (p=.705) between CON ($Mean_{CON}$ =.546; Std Err=.001; 95% CI=.544-.549) and ASD groups ($Mean_{ASD}$ =.546; Std Err=.001; 95% CI=.543-.548). See Figures 13 and 14 that illustrate these findings.

SE in the left uncinate fasciculus

A two-way ANOVA with SE as the dependent variable and age group and diagnosis held as fixed factors revealed no significant main effect for age group [$F(1,55)$=2.985, p=.090; η_p^2=.051] and diagnosis [$F(1,55)$=2.124, p=.151; η_p^2=.037]. There was no significant interaction of age group by diagnosis. There was no significant difference (p=.090) in mean SE values between the older ($Mean_{AGE\geq40}$=.574; Std Err=.001; 95% CI=.571-.576) and younger ($Mean_{AGE\ 18\text{-}25}$=.571; Std Err=.001; 95% CI=.568-.573) groups. There was no difference (p=.151) between CON ($Mean_{CON}$ =.571; Std Err=.001; 95% CI=.569-.573) and ASD groups ($Mean_{ASD}$ =.573; Std Err=.001; 95% CI=.571-.576). See Figures 15 and 16 that illustrate these findings.

SE in the whole brain WM skeleton

A two-way ANOVA with SE as the dependent variable revealed a significant main effect for age group [$F(1,55)=17.801$, $p<.001$; $\eta_p^2=.245$] but not for diagnosis [$F(1,55)=.094$, $p=.760$, $\eta_p^2=.002$]. The age group by diagnosis interaction was not significant. There was a significant difference ($p<.001$) in mean SE values between the older ($Mean_{AGE\geq40}=.969$; Std Err=.000; 95% CI=.968-.969) and younger groups ($Mean_{AGE\ 18\text{-}25}=.971$; Std Err=.000; 95% CI=.970-.972). In addition, a comparison of the mean SE values between CON ($Mean_{CON}=.970$; Std Err=.000; 95% CI=.969-.971) and ASD groups ($Mean_{ASD}=.970$; Std Err=.000; 95% CI=.969-.970) revealed no significant difference ($p=.760$) between the two groups. See Figures 17 and 18 that illustrate these findings.

II. Fractional Anisotropy (FA) results:

FA in the right sgACC

A two-way ANOVA with FA as the dependent variable and age group and diagnosis held as fixed factors indicated a significant main effect for age group [$F(1,55)=4.128$, $p=.047$; $\eta_p^2=.070$] but not for diagnosis [$F(1,55)=.941$, $p=.336$; $\eta_p^2=.017$]. There was no significant interaction of age group by diagnosis. There was a significant difference ($p=.047$) in mean FA values between the older ($Mean_{AGE\geq40}=.472$; Std Err=.003; 95% CI=.467-.478) and younger ($Mean_{AGE\ 18\text{-}25}=.464$; Std Err=.003; 95% CI=.457-.470) groups. There was, however, no significant difference ($p=.336$) between CON ($Mean_{CON}=.466$; Std Err=.003; 95% CI=.460-.472) and ASD groups ($Mean_{ASD}=.470$; Std Err=.003; 95% CI=.464-.476). See Figures 19 and 20 that illustrate these findings.

FA in the left sgACC

A two-way ANOVA with FA as the dependent variable and age group and diagnosis held as fixed factors indicated a significant main effect for age group [$F(1,55)=4.251$, $p=.044$; $\eta_p^2=.072$] but not for diagnosis [$F(1,55)=.689$, $p=.410$; $\eta_p^2=.012$]. There was no significant interaction of age group by diagnosis. There was a significant difference ($p=.044$) in mean FA values between the older ($Mean_{AGE\geq40}=.466$; Std Err=.003; 95% CI=.461-.472) and younger ($Mean_{AGE\ 18\text{-}25}=.457$; Std Err=.003; 95% CI=.450-.464) groups. There was, however, no significant difference ($p=.410$)

between CON ($Mean_{CON}$ =.460; Std Err=.003; 95% CI=.454-.466) and ASD groups ($Mean_{ASD}$ =.457; Std Err=.003; 95% CI=.457-.469). See Figures 21 and 22 that illustrate these findings.

FA in the right BLA

The two-way ANOVA for the right BLA also did not reveal any significant main effects for age group [$F(1,55)=1.663$, $p=.203$; $\eta_p^2=.029$] or diagnosis [$F(1,55)=.226$, $p=.636$; $\eta_p^2=.004$] and the age group by diagnosis interaction was not significant. The mean FA values in the older ($Mean_{AGE\geq40}$=.336; Std Err=.003; 95% CI=.329-.342) and younger groups ($Mean_{AGE\ 18\text{-}25}$=.342; Std Err=.004; 95% CI=.334-.351) were not significantly different (p=.203) from each other. Similarly, the CON ($Mean_{CON}$ =.338; Std Err=.004; 95% CI=.330-.345) and ASD groups ($Mean_{ASD}$ =.340; Std Err=.004; 95% CI=.333-.348) did not differ significantly (p=.636) in terms of their mean SE values as well. See Figures 23 and 24 that illustrate these findings.

FA in the left BLA

For the left BLA, a two-way ANOVA with FA as the dependent variable revealed no significant main effects for age group [$F(1,55)=.538$, $p=.466$; $\eta_p^2=.010$] and diagnosis [$F(1,55)=.350$, $p=.556$, $\eta_p^2=.006$]. The age group by diagnosis interaction was not significant. There was no significant difference (p=.466) in mean FA values between the older ($Mean_{AGE\geq40}$=.265; Std Err=.003; 95% CI=.259-.270) and younger groups ($Mean_{AGE\ 18\text{-}25}$=.268; Std Err=.003; 95% CI=.261-.275). In addition, a comparison of the mean SE values of the left BLA between CON ($Mean_{CON}$ =.265; Std Err=.003; 95% CI=.259-.271) and ASD groups ($Mean_{ASD}$ =.268; Std Err=.003; 95% CI=.262-.274) revealed no significant difference (p=.556) between the two groups. See Figures 25 and 26 that illustrate these findings.

FA in the right amygdala

A two-way ANOVA with FA as the dependent variable revealed no significant main effects for age group [$F(1,55)=3.134$, $p=.082$; $\eta_p^2=.054$] and diagnosis [$F(1,55)=.234$, $p=.630$, $\eta_p^2=.004$]. The age group by diagnosis interaction was not significant. There was no significant difference (p=.657) in mean FA values between the older ($Mean_{AGE\geq40}$=.735; Std Err=.001; 95% CI=.734-.737) and younger groups ($Mean_{AGE\ 18\text{-}25}$=.735; Std Err=.001; 95% CI=.733-.737). In addition, a comparison of the mean SE values between CON ($Mean_{CON}$ =.735; Std Err=.001; 95% CI=.733-

.737) and ASD groups ($Mean_{ASD}$ =.735; Std Err=.001; 95% CI=.734-.737) revealed no significant difference (p=.303) between the two groups. See Figures 27 and 28 that illustrate these findings.

FA in the left amygdala

A two-way ANOVA with FA as the dependent variable revealed no significant main effects for age group [F(1,55)=.487, p=.488; η_p^2=.009] and diagnosis [F(1,55)=.466, p=.498, η_p^2=.008]. The age group by diagnosis interaction was not significant. There was no significant difference (p=.487) in mean FA values between the older ($Mean_{AGE\geq40}$=.277; Std Err=.003; 95% CI=.272-.283) and younger groups ($Mean_{AGE\ 18\text{-}25}$=.281; Std Err=.004; 95% CI=.273-.288). In addition, there was no significant difference (p=.498) in the SE values of the left amygdala between CON ($Mean_{CON}$ =.277; Std Err=.003; 95% CI=.271-.284) and ASD groups ($Mean_{ASD}$ =.281; Std Err=.003; 95% CI=.274-.287). See Figures 29 and 30 that illustrate these findings.

FA in the right uncinate fasciculus

A two-way ANOVA with FA as the dependent variable and age group and diagnosis held as fixed factors revealed no significant main effect for age group [F(1,55)=.330, p=.568; η_p^2=.006] and diagnosis [F(1,55)=.026, p=.872; η_p^2=.000]. There was no significant interaction of age group by diagnosis. There was no significant difference (p=.568) in mean SE values between the older ($Mean_{AGE\geq40}$=.564; Std Err=.006; 95% CI=.551-.577) and younger ($Mean_{AGE\ 18\text{-}25}$=.558; Std Err=.008; 95% CI=.543-.574) groups. There was no difference (p=.872) between CON ($Mean_{CON}$ =.560; Std Err=.007; 95% CI=.546-.575) and ASD groups ($Mean_{ASD}$ =.562; Std Err=.007; 95% CI=.548-.576). See Figures 31 and 32 that illustrate these findings.

FA in the left uncinate fasciculus

A two-way ANOVA with FA as the dependent variable and age group and diagnosis held as fixed factors revealed no significant main effect for age group [F(1,55)=2.706, p=.106; η_p^2=.047] and diagnosis [F(1,55)=1.181, p=.282; η_p^2=.021]. There was no significant interaction of age group by diagnosis. There was no significant difference (p=.106) in mean SE values between the older ($Mean_{AGE\geq40}$=.555; Std Err=.009; 95% CI=.538-.573) and younger ($Mean_{AGE\ 18\text{-}25}$=.532; Std Err=.011; 95% CI=.510-.554) groups. There was no difference (p=.282) between

CON ($Mean_{CON}$ =.536; Std Err=.010; 95% CI=.516-.556) and ASD groups ($Mean_{ASD}$ =.551; Std Err=.010; 95% CI=.532-.571). See Figures 33 and 34 that illustrate these findings.

FA in the whole brain WM skeleton

A two-way ANOVA with FA as the dependent variable revealed a significant main effect for age group [$F(1,55)=4.199$, $p=.045$; $\eta_p^2=.071$] but not for diagnosis [$F(1,55)=.759$, $p=.387$, $\eta_p^2=.014$]. The age group by diagnosis interaction was not significant. There was a significant difference ($p=.045$) in mean FA values between the older ($Mean_{AGE\geq40}$=.466; Std Err=.003; 95% CI=.460-.471) and younger groups ($Mean_{AGE\ 18\text{-}25}$=.457; Std Err=.003; 95% CI=.450-.463). In addition, a comparison of the mean SE values between CON ($Mean_{CON}$ =.459; Std Err=.003; 95% CI=.453-.465) and ASD groups ($Mean_{ASD}$ =.463; Std Err=.003; 95% CI=.457-.469) revealed no significant difference ($p=.760$) between the two groups. See Figures 35 and 36 that illustrate these findings.

III. 1-tailed Pearson correlations to identify the association of SE with measures of depression, IQ, and symptom severity:

SE in the right sgACC

There was no significant correlation between SE and depression (BDI) [$r(56) = -.147$, $p=.135$], IQ (KBIT-2) [$r(56)= -.218$, $p=.050$], awareness (SRS-2 Awareness) [$r(55)= .093$, $p=.246$], cognition (SRS-2 Cognition) [$r(55)= -.008$, $p=.476$], communication (SRS-2 Communication) [$r(55)= .054$, $p=.345$], motivation (SRS-2 Motivation) [$r(55)= .069$, $p=.304$], mannerisms (SRS-2 Mannerisms) [$r(55)= .053$, $p=.349$], and total symptom severity (SRS-2 Total) [$r(55)= .101$, $p=.228$].

SE in the left sgACC

There was no significant correlation between SE and depression (BDI) [$r(56) = -.152$, $p=.128$], IQ (KBIT-2) [$r(56)= -.172$, $p=.099$], awareness (SRS-2 Awareness) [$r(55)= .033$, $p=.405$], cognition (SRS-2 Cognition) [$r(55)= -.070$, $p=.302$], communication (SRS-2 Communication) [$r(55)= -.025$, $p=.426$], motivation (SRS-2 Motivation) [$r(55)= .016$, $p=.452$],

mannerisms (SRS-2 Mannerisms) [$r(55)= -.041$, $p=.381$], and total symptom severity (SRS-2 Total) [$r(55)= -.019$, $p=.445$].

SE in the right BLA

There was no significant correlation between SE and depression (BDI) [$r(56) = -.010$, $p=.478$], IQ (KBIT-2) [$r(56)= -.002$, $p=.493$], awareness (SRS-2 Awareness) [$r(55)= .139$, $p=.152$], cognition (SRS-2 Cognition) [$r(55)= .132$, $p=.163$], communication (SRS-2 Communication) [$r(55)= .128$, $p=.172$], mannerisms (SRS-2 Mannerisms) [$r(55)= .065$, $p=.315$], and total symptom severity (SRS-2 Total) [$r(55)= .080$, $p=.278$]. There was, however, a significant correlation between SE and motivation (SRS-2 Motivation) [$r(55)= .245$, $p=.033$].

SE in the left BLA

There was no significant correlation between SE and depression (BDI) [$r(56) = -.017$, $p=.451$], IQ (KBIT-2) [$r(56)= .181$, $p=.087$], awareness (SRS-2 Awareness) [$r(55)= -.118$, $p=.192$], cognition (SRS-2 Cognition) [$r(55)= -.154$, $p=.126$], communication (SRS-2 Communication) [$r(55)= -.114$, $p=.199$], motivation (SRS-2 Motivation) [$r(55)= -.007$, $p=.481$], mannerisms (SRS-2 Mannerisms) [$r(55)= -.155$, $p=.124$], and total symptom severity (SRS-2 Total) [$r(55)= -.116$, $p=.195$].

SE in the right amygdala

There was a significant correlation between SE and awareness (SRS-2 Awareness) [$r(55)= .347$, $p=.004$], communication (SRS-2 Communication) [$r(55)= .254$, $p=.028$], motivation (SRS-2 Motivation) [$r(55)= .222$, $p=.049$], and total symptom severity (SRS-2 Total) [$r(55)= .244$, $p=.034$]. There was no significant correlation between SE and depression (BDI) [$r(56) = -.029$, $p=.414$], IQ (KBIT-2) [$r(56)= -.047$, $p=.363$], cognition (SRS-2 Cognition) [$r(55)= .188$, $p=.080$], and mannerisms (SRS-2 Mannerisms) [$r(55)= .173$, $p=.098$]. See Figures 27-40 that illustrate these findings.

SE in the left amygdala

There was no significant correlation between SE and depression (BDI) [$r(56) = .008$, $p=.476$], IQ (KBIT-2) [$r(56)=.173$, $p=.097$], awareness (SRS-2 Awareness) [$r(55)= -.067$,

p=.311], cognition (SRS-2 Cognition) [*r*(55)= -.138, *p*=.153], communication (SRS-2 Communication) [*r*(55)= -.142, *p*=.146], motivation (SRS-2 Motivation) [*r*(55)= .011, *p*=.467], mannerisms (SRS-2 Mannerisms) [*r*(55)= -.070, *p*=.303], and total symptom severity (SRS-2 Total) [*r*(55)= -.208, *p*=.060].

SE in the right uncinate fasciculus

There was no significant correlation between SE and depression (BDI) [*r*(54) = -.086, *p*=.263], IQ (KBIT-2) [*r*(54)= .012, *p*=.465], awareness (SRS-2 Awareness) [*r*(53)= -.204, *p*=.067], cognition (SRS-2 Cognition) [*r*(53)= -.079, *p*=.282], communication (SRS-2 Communication) [*r*(53)= -.122, *p*=.187], mannerisms (SRS-2 Mannerisms) [*r*(53)= -.141, *p*=.152], and total symptom severity (SRS-2 Total) [*r*(53)= -.208, *p*=.064]. However, there was a significant correlation between SE and motivation (SRS-2 Motivation) [*r*(55)= -.245, *p*=.036].

SE in the left uncinate fasciculus

There was no significant correlation between SE and depression (BDI) [*r*(56) = .122, *p*=.181], IQ (KBIT-2) [*r*(56)= -.077, *p*=.283], awareness (SRS-2 Awareness) [*r*(55)= .170, *p*=.103], communication (SRS-2 Communication) [*r*(55)= .200, *p*=.068], motivation (SRS-2 Motivation) [*r*(55)= .083, *p*=.269], and total symptom severity (SRS-2 Total) [*r*(55)= .212, *p*=.056]. However, there was a significant correlation between SE and cognition (SRS-2 Cognition) [*r*(55)= .264, *p*=.024] and mannerisms (SRS-2 Mannerisms) [*r*(55)= .226, *p*=.046].

SE in the whole brain WM skeleton

There was no significant correlation between SE and depression (BDI) [*r*(56) = -.126, *p*=.173], IQ (KBIT-2) [*r*(56)= -.189, *p*=.077], awareness (SRS-2 Awareness) [*r*(55)= .081, *p*=.274], cognition (SRS-2 Cognition) [*r*(55)= -.028, *p*=.417], communication (SRS-2 Communication) [*r*(55)= .025, *p*=.426], motivation (SRS-2 Motivation) [*r*(55)= .061, *p*=.325], mannerisms (SRS-2 Mannerisms) [*r*(55)= .045, *p*=.370], and total symptom severity (SRS-2 Total) [*r*(55)= .057, *p*=.337].

IV. 1-tailed Pearson correlations to identify the association of FA with measures of depression, IQ, and symptom severity:

FA in the right sgACC

There was no significant correlation between FA and depression (BDI) [$r(56) = -.181$, $p=.087$], IQ (KBIT-2) [$r(56)= .113$, $p=.199$], awareness (SRS-2 Awareness) [$r(55)= .018$, $p=.448$], cognition (SRS-2 Cognition) [$r(55)= -.001$, $p=.496$], communication (SRS-2 Communication) [$r(55)= .033$, $p=.405$], motivation (SRS-2 Motivation) [$r(55)= .016$, $p=.452$], mannerisms (SRS-2 Mannerisms) [$r(55)= -.036$, $p=.396$], and total symptom severity (SRS-2 Total) [$r(55)= -.100$, $p=.229$].

FA in the left sgACC

There was no significant correlation between FA and depression (BDI) [$r(56) = -.190$, $p=.076$], IQ (KBIT-2) [$r(56)= .124$, $p=.176$], awareness (SRS-2 Awareness) [$r(55)= .002$, $p=.494$], cognition (SRS-2 Cognition) [$r(55)= -.021$, $p=.438$], communication (SRS-2 Communication) [$r(55)= .015$, $p=.457$], motivation (SRS-2 Motivation) [$r(55)= .002$, $p=.494$], mannerisms (SRS-2 Mannerisms) [$r(55)= -.060$, $p=.328$], and total symptom severity (SRS-2 Total) [$r(55)= -.126$, $p=.176$].

FA in the right BLA

There was a significant correlation between FA and depression (BDI) [$r(56) = -.245$, $p=.032$]. However, there were no significant correlations between FA and IQ (KBIT-2) [$r(56)= -.054$, $p=.342$], awareness (SRS-2 Awareness) [$r(55)= -.102$, $p=.225$], cognition (SRS-2 Cognition) [$r(55)= -.075$, $p=.289$], communication (SRS-2 Communication) [$r(55)= .010$, $p=.469$], motivation (SRS-2 Motivation) [$r(55)= -.037$, $p=.393$], mannerisms (SRS-2 Mannerisms) [$r(55)= .008$, $p=.476$], and total symptom severity (SRS-2 Total) [$r(55)= -.138$, $p=.153$].

FA in the left BLA

There was no significant correlation between FA and depression (BDI) [$r(56) = -.194$, $p=.072$], IQ (KBIT-2) [$r(56)= -.013$, $p=.461$], awareness (SRS-2 Awareness) [$r(55)= -.028$,

p=.419], cognition (SRS-2 Cognition) [*r*(55)= -.096, *p*=.239], communication (SRS-2 Communication) [*r*(55)= .062, *p*=.323], motivation (SRS-2 Motivation) [*r*(55)= .015, *p*=.456], mannerisms (SRS-2 Mannerisms) [*r*(55)= .011, *p*=.469], and total symptom severity (SRS-2 Total) [*r*(55)= -.099, *p*=.231].

FA in the right amygdala

There was a significant correlation between FA and depression (BDI) [*r*(56) = -.244, *p*=.033]. However, there were no significant correlations between FA and IQ (KBIT-2) [*r*(56)= -.161, *p*=.113], awareness (SRS-2 Awareness) [*r*(55)= .019, *p*=.443], cognition (SRS-2 Cognition) [*r*(55)= -.022, *p*=.437], communication (SRS-2 Communication) [*r*(55)= .050, *p*=.355], motivation (SRS-2 Motivation) [*r*(55)= -.003, *p*=.492], mannerisms (SRS-2 Mannerisms) [*r*(55)= .010, *p*=.470], and total symptom severity (SRS-2 Total) [*r*(55)= -.063, *p*=.321]. See Figure 41 that illustrates this finding.

FA in the left amygdala

There was a significant correlation between FA and depression (BDI) [*r*(56) = -.268, *p*=.021]. However, there were no significant correlations between FA and IQ (KBIT-2) [*r*(56)= -.103, *p*=.220], awareness (SRS-2 Awareness) [*r*(55)= .092, *p*=.247], cognition (SRS-2 Cognition) [*r*(55)= .007, *p*=.480], communication (SRS-2 Communication) [*r*(55)= .156, *p*=.123], motivation (SRS-2 Motivation) [*r*(55)= .049, *p*=.359], mannerisms (SRS-2 Mannerisms) [*r*(55)= .009 *p*=.474], and total symptom severity (SRS-2 Total) [*r*(55)= .043, *p*=.375].

FA in the right uncinate fasciculus

There was no significant correlation between FA and depression (BDI) [*r*(56) = .089, *p*=.252], IQ (KBIT-2) [*r*(56)= -.044, *p*=.373], awareness (SRS-2 Awareness) [*r*(55)= .020, *p*=.440], cognition (SRS-2 Cognition) [*r*(55)= .003, *p*=.491], communication (SRS-2 Communication) [*r*(55)= -.022, *p*=.435], motivation (SRS-2 Motivation) [*r*(55)= -.088, *p*=.257], mannerisms (SRS-2 Mannerisms) [*r*(55)= -.045, *p*=.369], and total symptom severity (SRS-2 Total) [*r*(55)= .072, *p*=.298].

FA in the left uncinate fasciculus

There was no significant correlation between FA and depression (BDI) [$r(56) = .166$, $p=.106$], IQ (KBIT-2) [$r(56)= -.026$, $p=.423$], awareness (SRS-2 Awareness) [$r(55)= .190$, $p=.078$], communication (SRS-2 Communication) [$r(55)= .152$, $p=.130$], motivation (SRS-2 Motivation) [$r(55)= .095$, $p=.241$], mannerisms (SRS-2 Mannerisms) [$r(55)= .100$, $p=.230$], and total symptom severity (SRS-2 Total) [$r(55)= .207$, $p=.062$]. However, there was a significant correlation between SE and cognition (SRS-2 Cognition) [$r(55)= .243$, $p=.034$].

FA in the whole brain WM skeleton

There was no significant correlation between SE and depression (BDI) [$r(56) = -.199$, $p=.067$], IQ (KBIT-2) [$r(56)= .117$, $p=.190$], awareness (SRS-2 Awareness) [$r(55)= -.004$, $p=.490$], cognition (SRS-2 Cognition) [$r(55)= -.022$, $p=.435$], communication (SRS-2 Communication) [$r(55)= .012$, $p=.464$], motivation (SRS-2 Motivation) [$r(55)= -.003$, $p=.491$], mannerisms (SRS-2 Mannerisms) [$r(55)= -.059$, $p=.332$], and total symptom severity (SRS-2 Total) [$r(55)= -.128$, $p=.172$].

V. Hierarchical linear regression to examine the relations of SE and FA to measures of depression:

A series of linear regression analyses were conducted to examine the relation of FA and SE to depression for each of the regions of interest, as shown in Table 2. Age was included as a covariate. The results of the analyses indicated no significant result for FA or SE in predicting depression.

VI. Post-hoc tract-based spatial statistics (TBSS) voxel wise statistical analyses:

As a post-hoc analysis, we identified regions that approached significance for the ASD vs. CON analysis of the whole brain WM skeleton ($p=.08$). We identified three major regions: the left posterior limb of the internal capsule (PLIC), the right PLIC, and the left anterior limb of the internal capsule (ALIC). See Figure 42 that illustrates these findings. 5mm wide spherical ROIs were manually generated using “fslmaths” for each of the three regions to examine SE and FA differences across age and diagnoses.

SE in the right posterior limb of the internal capsule:

A two-way ANOVA with SE as the dependent variable and age group and diagnosis held as fixed factors revealed no significant main effects for age group [$F(1,55)=.286$, $p=.595$; $\eta_p^2=.005$] or diagnosis [$F(1,55)=1.073$, $p=.305$; $\eta_p^2=.019$]. There was no significant interaction of age group by diagnosis. There was no significant difference ($p=.595$) in mean SE values between the older ($Mean_{AGE\geq40}=.657$; Std Err=.001; 95% CI=.654-.659) and younger ($Mean_{AGE\ 18\text{-}25}=.657$; Std Err=.001; 95% CI=.655-.660) groups. There was also no significant difference ($p=.305$) between CON ($Mean_{CON}=.658$; Std Err=.001; 95% CI=.655-.660) and ASD groups ($Mean_{ASD}=.656$; Std Err=.001; 95% CI=.654-.659). See Figures 43 and 44 that illustrate these findings.

SE in the left posterior limb of the internal capsule:

A two-way ANOVA with SE as the dependent variable and age group and diagnosis held as fixed factors revealed no significant main effects for age group [$F(1,55)=.398$, $p=.531$; $\eta_p^2=.007$] or diagnosis [$F(1,55)=.126$, $p=.723$; $\eta_p^2=.002$]. There was no significant interaction of age group by diagnosis. There was no significant difference ($p=.398$) in mean SE values between the older ($Mean_{AGE\geq40}=.687$; Std Err=.001; 95% CI=.685-.689) and younger ($Mean_{AGE\ 18\text{-}25}=.686$; Std Err=.001; 95% CI=.684-.689) groups. There was also no significant difference ($p=.723$) between CON ($Mean_{CON}=.687$; Std Err=.001; 95% CI=.684-.689) and ASD groups ($Mean_{ASD}=.687$; Std Err=.001; 95% CI=.685-.689). See Figures 45 and 46 that illustrate these findings.

SE in the left anterior limb of the internal capsule:

A two-way ANOVA with SE as the dependent variable and age group and diagnosis held as fixed factors revealed no significant main effects for age group [$F(1,55)=3.764$, $p=.057$; $\eta_p^2=.064$] or diagnosis [$F(1,55)=.071$, $p=.790$; $\eta_p^2=.001$]. There was no significant interaction of age group by diagnosis. There was no significant difference ($p=.057$) in mean SE values between the older ($Mean_{AGE\geq40}=.668$; Std Err=.001; 95% CI=.665-.670) and younger ($Mean_{AGE\ 18\text{-}25}=.672$; Std Err=.002; 95% CI=.669-.675) groups. There was also no significant difference ($p=.790$) between CON ($Mean_{CON}=.670$; Std Err=.001; 95% CI=.667-.673) and ASD groups ($Mean_{ASD}=.669$; Std Err=.001; 95% CI=.667-.672). See Figures 47 and 48 that illustrate these findings.

FA in the right posterior limb of the internal capsule:

Based on the distribution of the FA data, one outlier (ASD) had to be excluded to ensure normal distribution of the data. Following this, a two-way ANOVA with FA as the dependent variable and age group and diagnosis held as fixed factors revealed no significant main effects for age group [$F(1,54)=.002$, $p=.961$; $\eta_p^2=.000$] but there was a significant main effect of diagnosis [$F(1,54)= 12.073$, $p=.001$; $\eta_p^2=.183$]. There was no significant interaction of age group by diagnosis. There was no significant difference ($p=.961$) in mean FA values between the older ($Mean_{AGE\geq40}=.724$; Std Err=.005; 95% CI=.715-.734) and younger ($Mean_{AGE\ 18\text{-}25}=.724$; Std Err=.006; 95% CI=.712-.736) groups. There was a significant difference ($p=.001$) between CON ($Mean_{CON}=.711$; Std Err=.005; 95% CI=.701-.722) and ASD groups ($Mean_{ASD}=.737$; Std Err=.005; 95% CI=.727-.748). See Figures 49 and 50 that illustrate these findings.

FA in the left posterior limb of the internal capsule:

A two-way ANOVA with FA as the dependent variable and age group and diagnosis held as fixed factors revealed no significant main effect for age group [$F(1,55)=.344$, $p=.560$; $\eta_p^2=.006$] but indicated a significant main effect for diagnosis [$F(1,55)=17.903$, $p<.001$; $\eta_p^2=.246$]. There was no significant interaction of age group by diagnosis. There was no significant difference ($p=.560$) in mean FA values between the older ($Mean_{AGE\geq40}=.700$; Std Err=.006; 95% CI=.689-.711) and younger ($Mean_{AGE\ 18\text{-}25}=.705$; Std Err=.007; 95% CI=.691-.719) groups. There was, however, a significant difference ($p<.001$) between CON ($Mean_{CON}=.684$; Std Err=.006; 95% CI=.672-.697) and ASD groups ($Mean_{ASD}=.721$; Std Err=.006; 95% CI=.709-.733). See Figures 51 and 52 that illustrate these findings.

FA in the left anterior limb of the internal capsule:

A two-way ANOVA with SE as the dependent variable and age group and diagnosis held as fixed factors revealed significant main effects for age group [$F(1,55)=7.581$, $p=.008$; $\eta_p^2=.121$] and diagnosis [$F(1,55)=15.027$, $p<.001$; $\eta_p^2=.215$]. There was no significant interaction of age group by diagnosis. There was a significant difference ($p=.008$) in mean FA values between the older ($Mean_{AGE\geq40}=.678$; Std Err=.005; 95% CI=.669-.687) and younger ($Mean_{AGE\ 18\text{-}25}=.658$; Std Err=.006; 95% CI=.647-.669) groups. There was also a significant difference ($p<.001$) between

CON ($Mean_{CON}$ =.654; Std Err=.005; 95% CI=.644-.665) and ASD groups ($Mean_{ASD}$ =.682; Std Err=.005; 95% CI=.672-.692). See Figures 53 and 54 that illustrate these findings.

1-tailed Pearson correlations to identify the association of SE in the bilateral PLIC and left ALIC with measures of depression, IQ, and symptom severity:

SE in the right posterior limb of the internal capsule:

There was no significant correlation between SE and depression (BDI) [$r(56) = .064$, p=.317], IQ (KBIT-2) [$r(56)= -.027$, p=.421], awareness (SRS-2 Awareness) [$r(55)= .020$, p=.443], cognition (SRS-2 Cognition) [$r(55)= -.084$, p=.267], communication (SRS-2 Communication) [$r(55)= -.033$, p=.404], motivation (SRS-2 Motivation) [$r(55)= -.033$, p=.404], mannerisms (SRS-2 Mannerisms) [$r(55)= -.112$, p=.182], and total symptom severity (SRS-2 Total) [$r(55)= -.034$, p=.400].

SE in the left posterior limb of the internal capsule:

There was no significant correlation between SE and depression (BDI) [$r(56) = .066$, p=.313], IQ (KBIT-2) [$r(56)= -.010$, p=.470], awareness (SRS-2 Awareness) [$r(55)= .178$, p=.092], cognition (SRS-2 Cognition) [$r(55)= .042$, p=.377], communication (SRS-2 Communication) [$r(55)= .094$, p=.244], motivation (SRS-2 Motivation) [$r(55)= .067$, p=.311], mannerisms (SRS-2 Mannerisms) [$r(55)= .042$, p=.379], and total symptom severity (SRS-2 Total) [$r(55)= .031$, p=.408].

SE in the left anterior limb of the internal capsule:

There was no significant correlation between SE and depression (BDI) [$r(56) = .019$, p=.445], IQ (KBIT-2) [$r(56)= -.017$, p=.449], awareness (SRS-2 Awareness) [$r(55)= -.010$, p=.470], cognition (SRS-2 Cognition) [$r(55)= -.049$, p=.358], communication (SRS-2 Communication) [$r(55)= -.067$, p=.310], motivation (SRS-2 Motivation) [$r(55)= -.069$, p=.306], mannerisms (SRS-2 Mannerisms) [$r(55)= -.128$, p=.171], and total symptom severity (SRS-2 Total) [$r(55)= .084$, p=.268].

1-tailed Pearson correlations to identify the association of FA in the bilateral PLIC and left ALIC with measures of depression, IQ, and symptom severity:

FA in the right posterior limb of the internal capsule:

There was no significant correlation between FA and depression (BDI) [$r(55) = .071$, $p=.301$] and IQ (KBIT-2) [$r(55)= -.160$, $p=.117$]. There was, however, a significant correlation between FA and awareness (SRS-2 Awareness) [$r(54)= .279$, $p=.019$], cognition (SRS-2 Cognition) [$r(54)= .303$, $p=.012$], communication (SRS-2 Communication) [$r(54)= .428$, $p<.001$], motivation (SRS-2 Motivation) [$r(54)= .325$, $p=.007$], mannerisms (SRS-2 Mannerisms) [$r(54)= .357$, $p=.003$], and total symptom severity (SRS-2 Total) [$r(54)= .301$, $p=.012$].

FA in the left posterior limb of the internal capsule:

There was no significant correlation between FA and depression (BDI) [$r(56) = .169$, $p=.102$] and IQ (KBIT-2) [$r(56)= -.124$, $p=.176$]. There was, however, a significant correlation between FA and awareness (SRS-2 Awareness) [$r(55)= .357$, $p=.003$], cognition (SRS-2 Cognition) [$r(55)= .401$, $p<.001$], communication (SRS-2 Communication) [$r(55)= .482$, $p<.001$], motivation (SRS-2 Motivation) [$r(55)= .388$, $p=.001$], mannerisms (SRS-2 Mannerisms) [$r(55)= .405$, $p<.001$], and total symptom severity (SRS-2 Total) [$r(55)= .306$, $p=.010$].

FA in the left anterior limb of the internal capsule:

There was no significant correlation between FA and depression (BDI) [$r(56) = .117$, $p=.192$], IQ (KBIT-2) [$r(56)= -.105$, $p=.217$], and total symptom severity (SRS-2 Total) [$r(55)= .191$, $p=.078$]. However, there was a significant correlation between FA and awareness (SRS-2 Awareness) [$r(55)= .311$, $p=.009$], cognition (SRS-2 Cognition) [$r(55)= .374$, $p=.002$], communication (SRS-2 Communication) [$r(55)= .369$, $p=.002$], motivation (SRS-2 Motivation) [$r(55)= .273$, $p=.020$], and mannerisms (SRS-2 Mannerisms) [$r(55)= .304$, $p=.011$].

Hierarchical linear regression to examine the relations of SE and FA in the bilateral PLIC and left ALIC to measures of depression:

A series of linear regression analyses were conducted to examine the relation of FA and SE to depression for each of the regions of interest, as shown in Table 3. Age was included as a

covariate. The results of the analyses indicated no significant result for FA or SE in predicting depression.

Table 1. Summary of results of all regions of interest.

Region	Age main effect	Diagnosis main effect	SE	FA	Clinical correlate
right sgACC	+	-	≥ 40 ↓***	≥ 40 ↑*	none
left sgACC	+	-	≥ 40 ↓***	≥ 40 ↑*	none
right BLA	-	-	-	-	SE w/ motivation*
					FA w/ depression*
left BLA	-	-	-	-	none
right amygdala	-	-	-	-	SE w/ awareness**
					SE w/ communication*
					SE w/ motivation*
					SE w/ total ASD symptom*
					FA w/ depression*
left amygdala	-	-	-	-	FA w/ depression*
right UF	-	-	-	-	none
left UF	-	-	-	-	none
whole brain	+	-	≥ 40 ↓***	≥ 40 ↑*	none
right PLIC	-	+	-	ASD ↑**	FA w/ awareness*
					FA w/ cognition*
					FA w/ communication***
					FA w/ motivation**
					FA w/ mannerisms**
					FA w/ total ASD symptom*
left PLIC	-	+	-	ASD ↑***	FA w/ awareness**
					FA w/ cognition***
					FA w/ motivation**
					FA w/ mannerisms***
					FA w/ total ASD symptom*
left ALIC	+	+	-	≥ 40 ↑**	FA w/ awareness**
				ASD ↑***	FA w/ cognition**
					FA w/ communication**
					FA w/ motivation*
					FA w/ mannerisms*

Abbreviations: sgACC = subgenual anterior cingulate cortex; BLA = basolateral nucleus of the amygdala; PLIC = posterior limb of the internal capsule; ALIC = anterior limb of the internal capsule; UF = uncinate fasciculus; awareness = SRS-2 Awareness; communication = SRS-2 Communication; motivation = SRS-2 Motivation; total ASD symptom = SRS-2 Total; depression = BDI-II.

+ indicates presence of main effect.

- indicates no presence of main effect

≥ 40 ↑ indicates higher values for group aged ≥ 40 years

≥ 40 ↓ indicates lower values for group aged ≥ 40 years.

*p<.05, **p<.01, ***p<.001

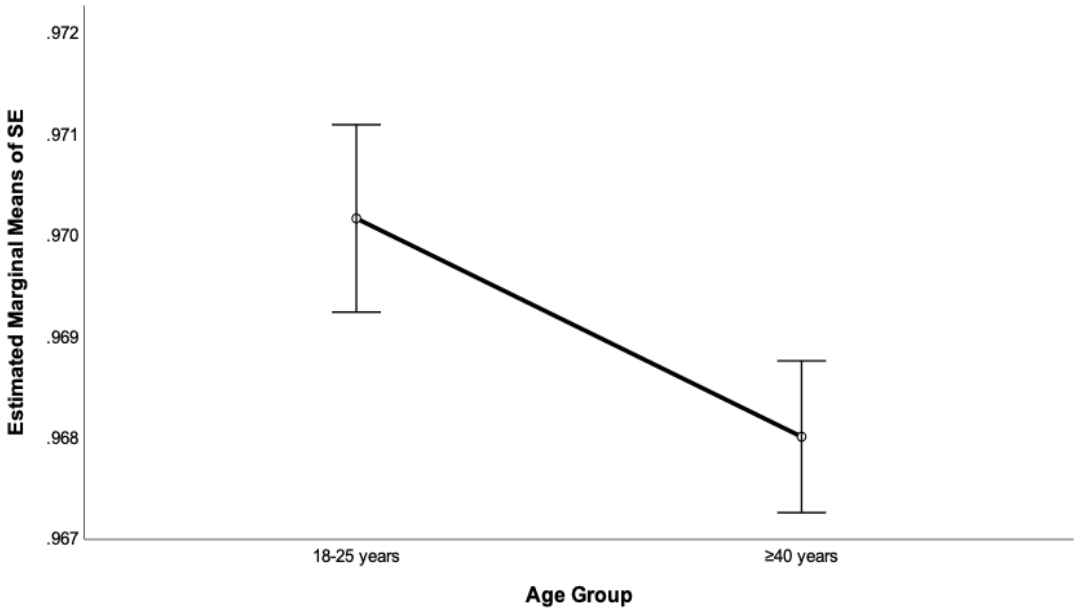

Figure 1. The main effect of age group on SE in the right sgACC.

SE differed significantly across age groups (p<.001). Error bars indicate 95% confidence intervals.

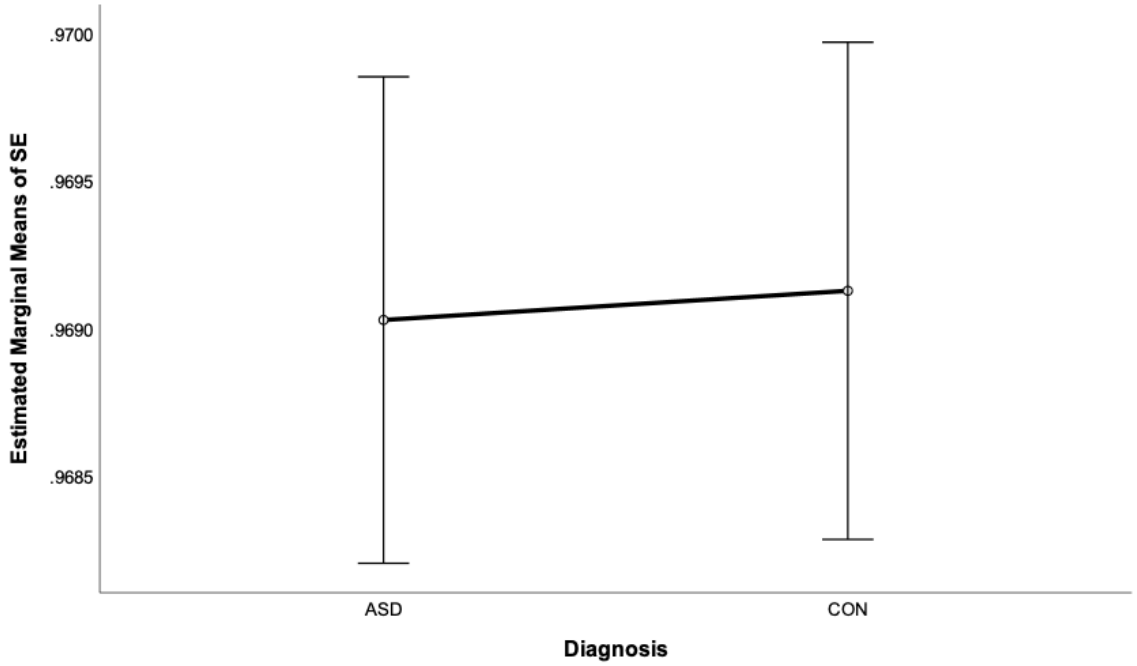

Figure 2. The main effect of diagnosis on SE in the right sgACC.

SE did not differ significantly across diagnosis (p=.866). Error bars indicate 95% confidence intervals.

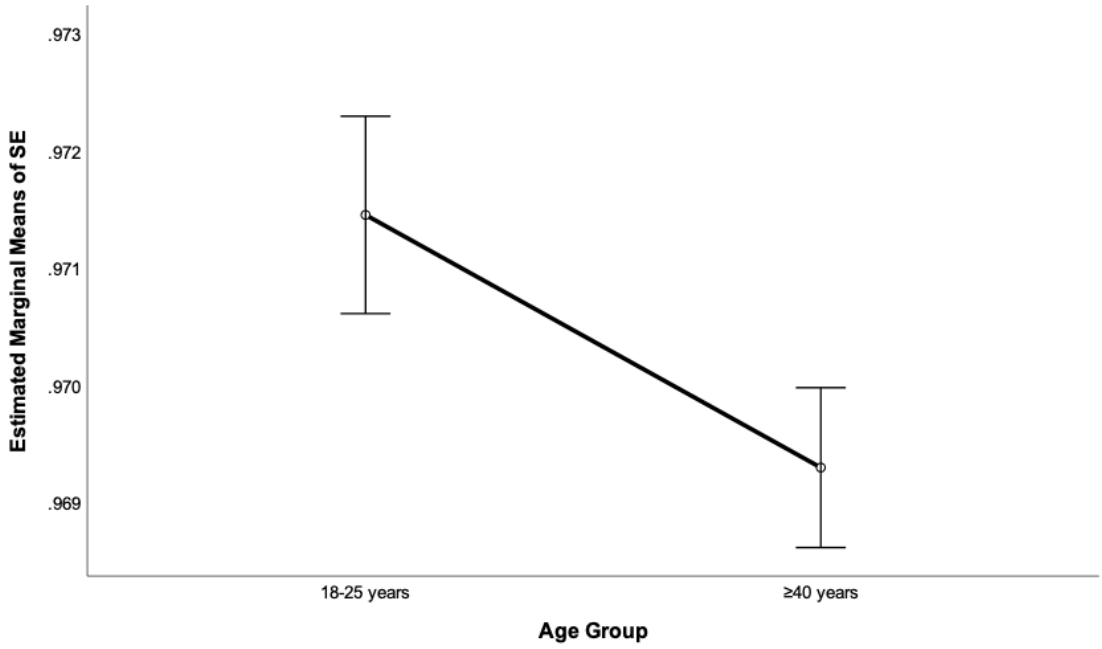

Figure 3. The main effect of age group on SE in the left sgACC.

SE differed significantly across age groups (p<.001). Error bars indicate 95% confidence intervals.

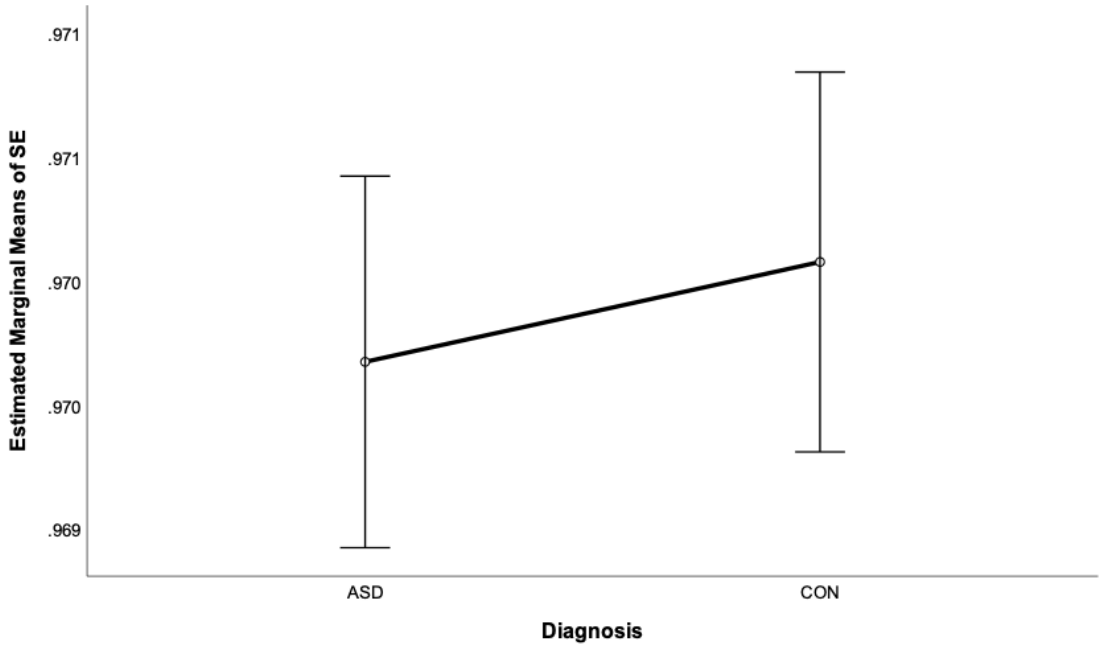

Figure 4. The main effect of diagnosis on SE in the left sgACC.

SE did not differ significantly across diagnosis (p=.450). Error bars indicate 95% confidence intervals.

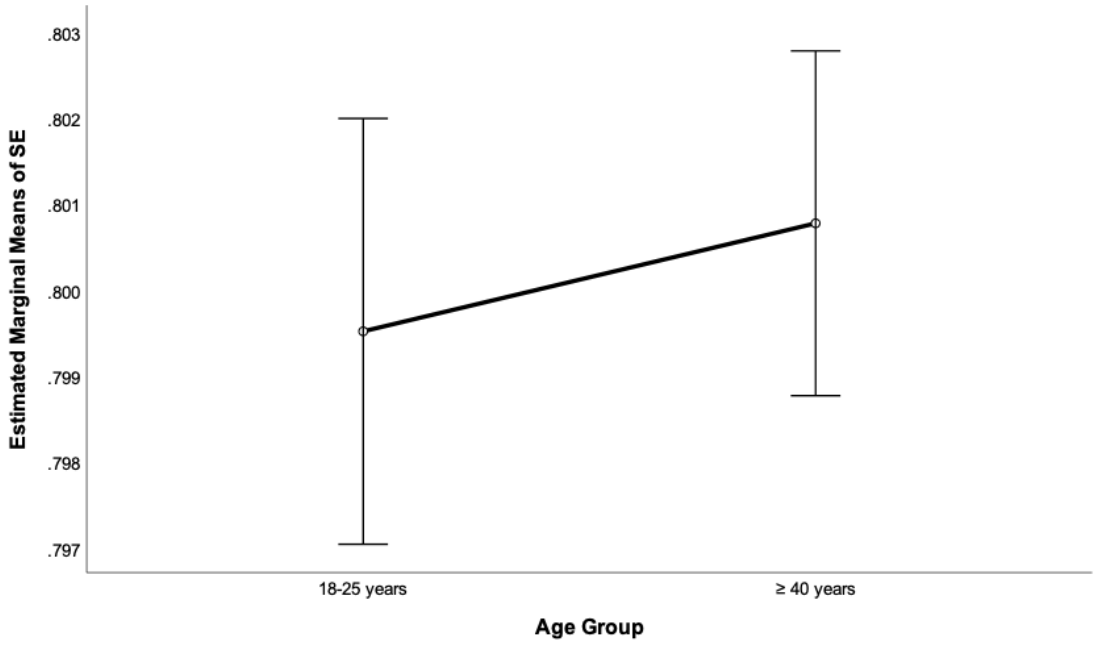

Figure 5. The main effect of age group on SE in the right BLA.

SE did not differ significantly across age groups (p=.434). Error bars indicate 95% confidence intervals.

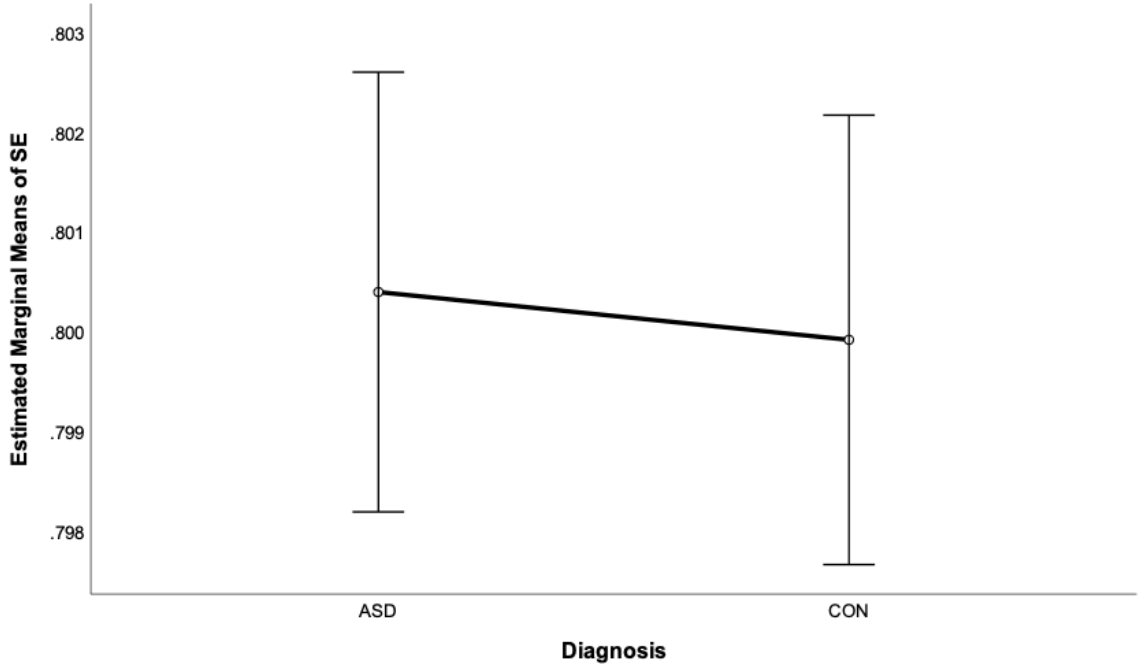

Figure 6. The main effect of diagnosis on SE in the right BLA.

SE did not differ significantly across diagnosis (p=.760). Error bars indicate 95% confidence intervals.

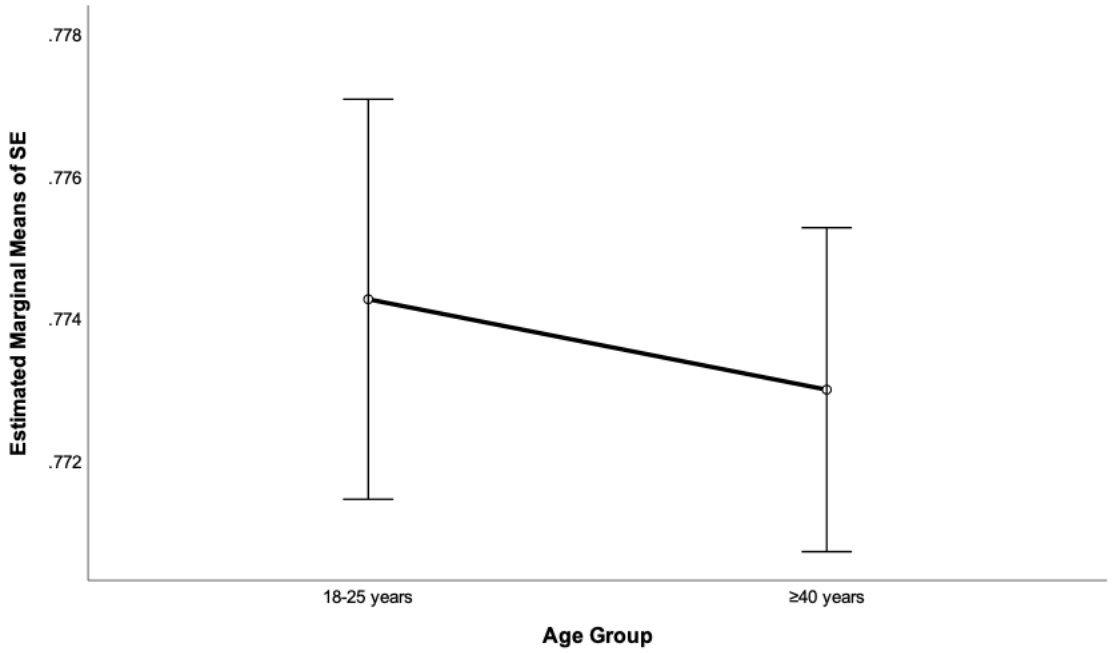

Figure 7. The main effect of age group on SE in the left BLA.

SE did not differ significantly across age groups (p=.485). Error bars indicate 95% confidence intervals.

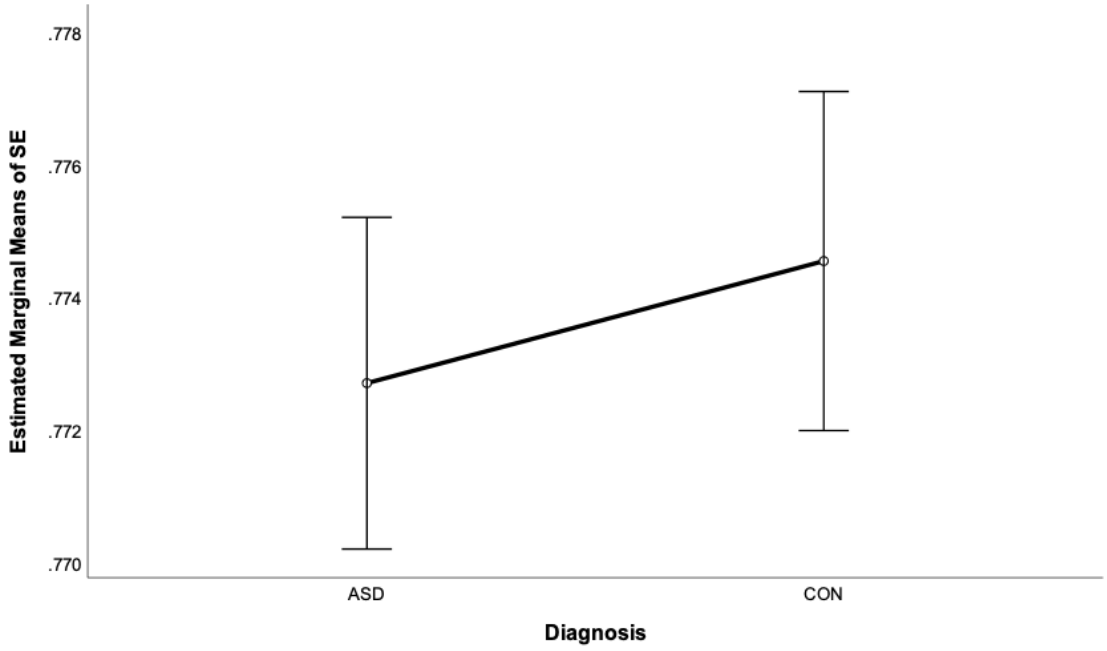

Figure 8. The main effect of diagnosis on SE in the left BLA.

SE did not differ significantly across diagnosis (p=.303). Error bars indicate 95% confidence intervals.

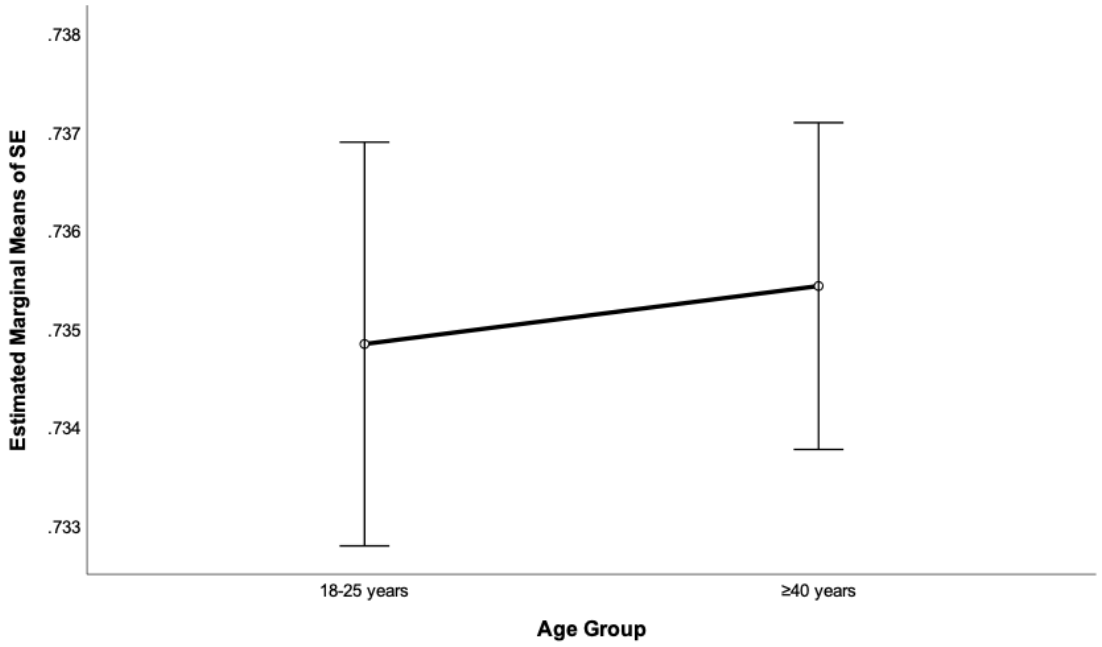

Figure 9. The main effect of age group on SE in the right amygdala.

SE did not differ significantly across age groups (p=.657). Error bars indicate 95% confidence intervals.

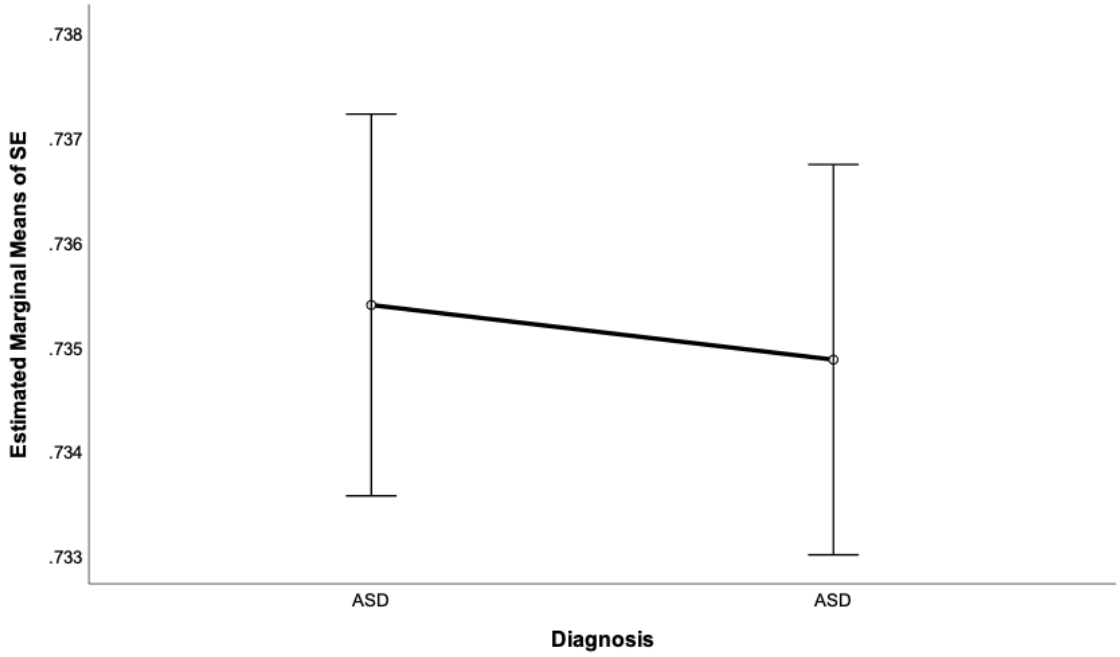

Figure 10. The main effect of diagnosis on SE in the right amygdala.

SE did not differ significantly across diagnosis (p=.687). Error bars indicate 95% confidence intervals.

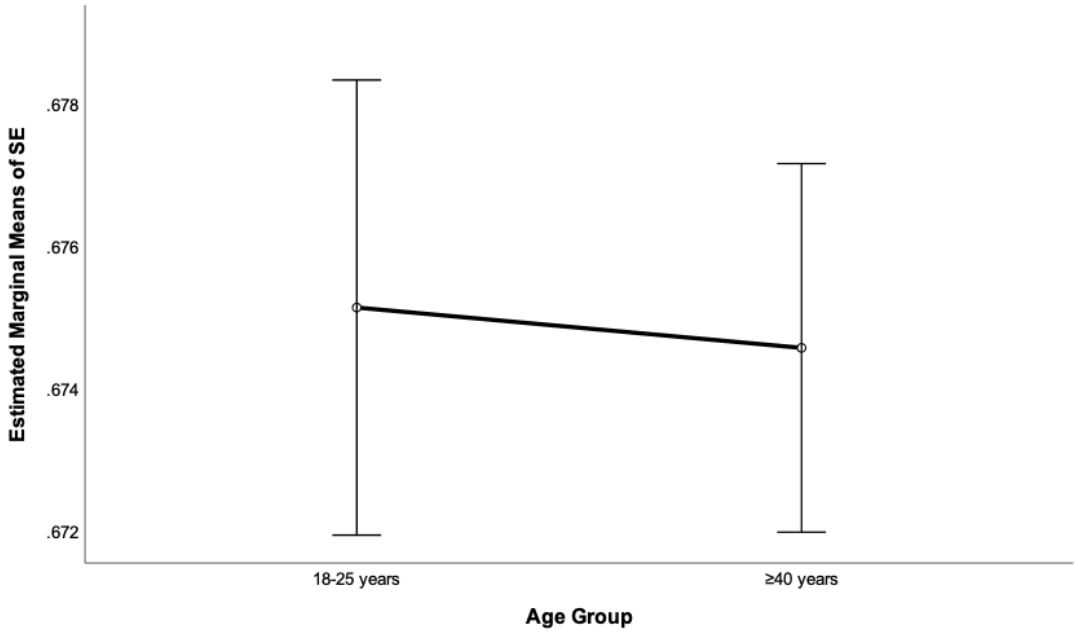

Figure 11. The main effect of age group on SE in the left amygdala.

SE did not differ significantly across age groups (p=.784). Error bars indicate 95% confidence intervals.

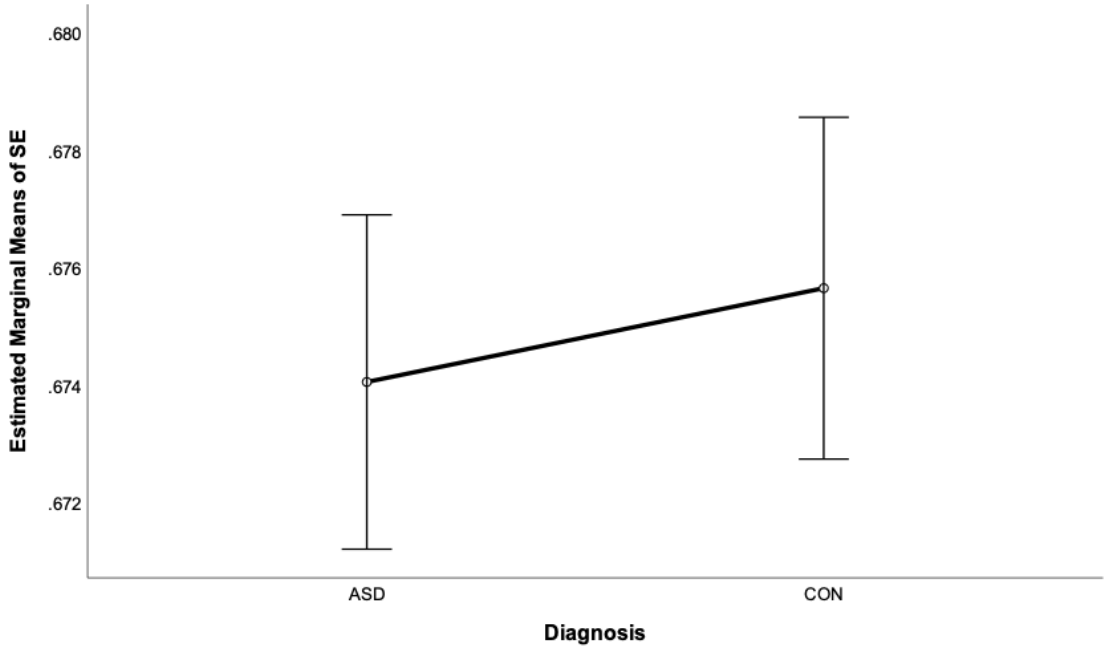

Figure 12. The main effect of diagnosis on SE in the left amygdala.

SE did not differ significantly across diagnosis (p=.431). Error bars indicate 95% confidence intervals.

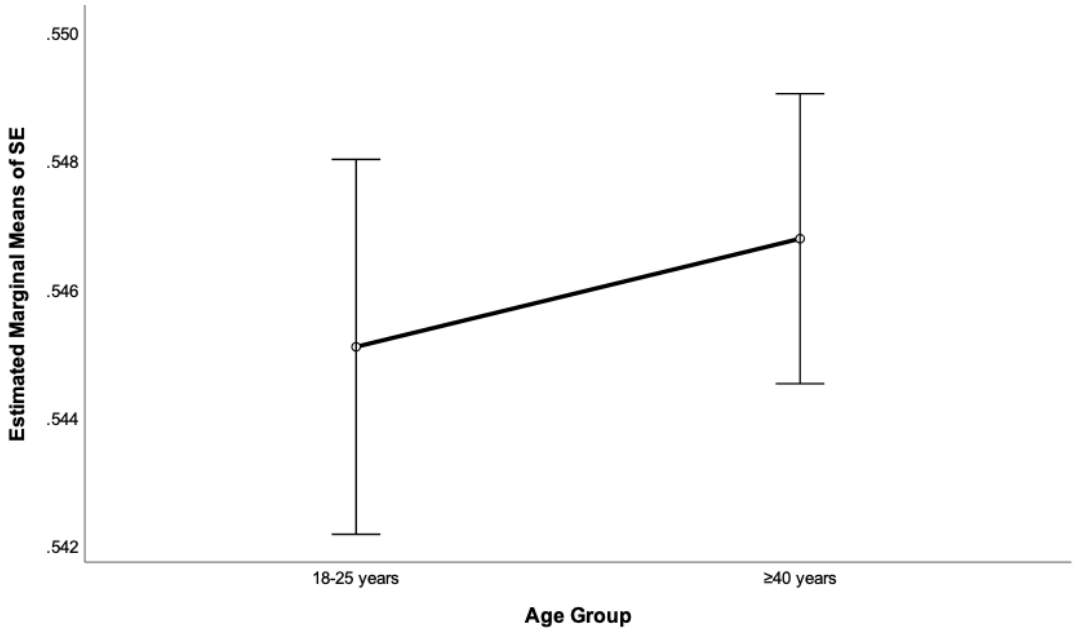

Figure 13. The main effect of age group on SE in the right uncinate fasciculus.

SE did not differ significantly across age group (p=.366). Error bars indicate 95% confidence intervals.

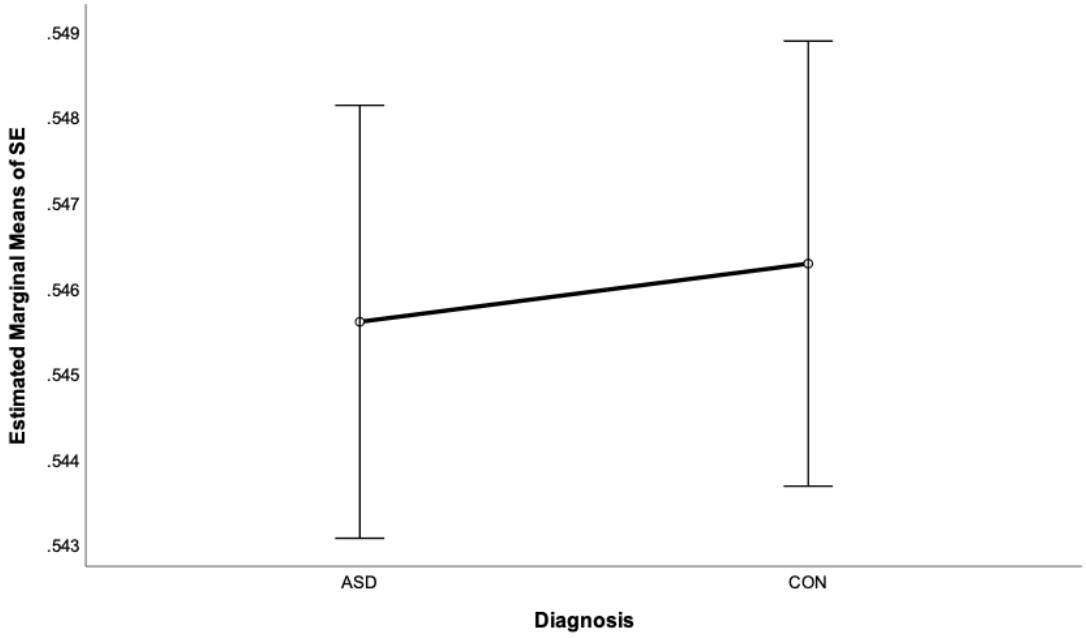

Figure 14. The main effect of diagnosis on SE in the right uncinate fasciculus.

SE did not differ significantly across diagnosis (p=.705). Error bars indicate 95% confidence intervals.

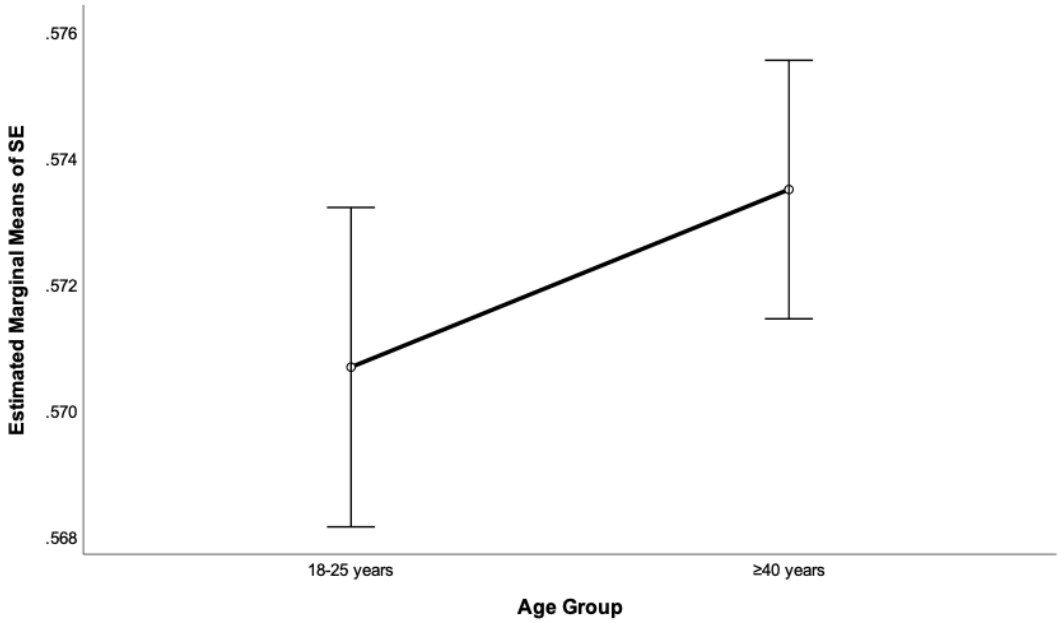

Figure 15. The main effect of age group on SE in the left uncinate fasciculus.

SE did not differ significantly across age group (p=.090). Error bars indicate 95% confidence intervals.

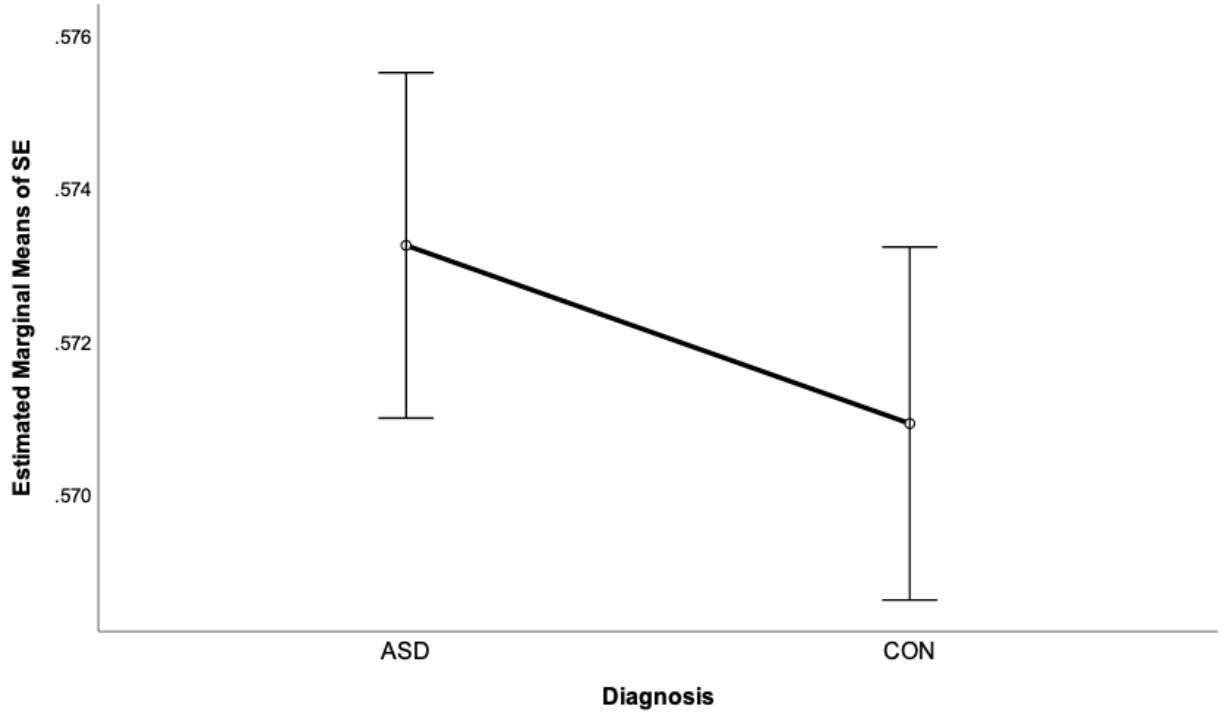

Figure 16. The main effect of diagnosis on SE in the left uncinate fasciculus.

SE did not differ significantly across diagnosis (p=.151). Error bars indicate 95% confidence intervals.

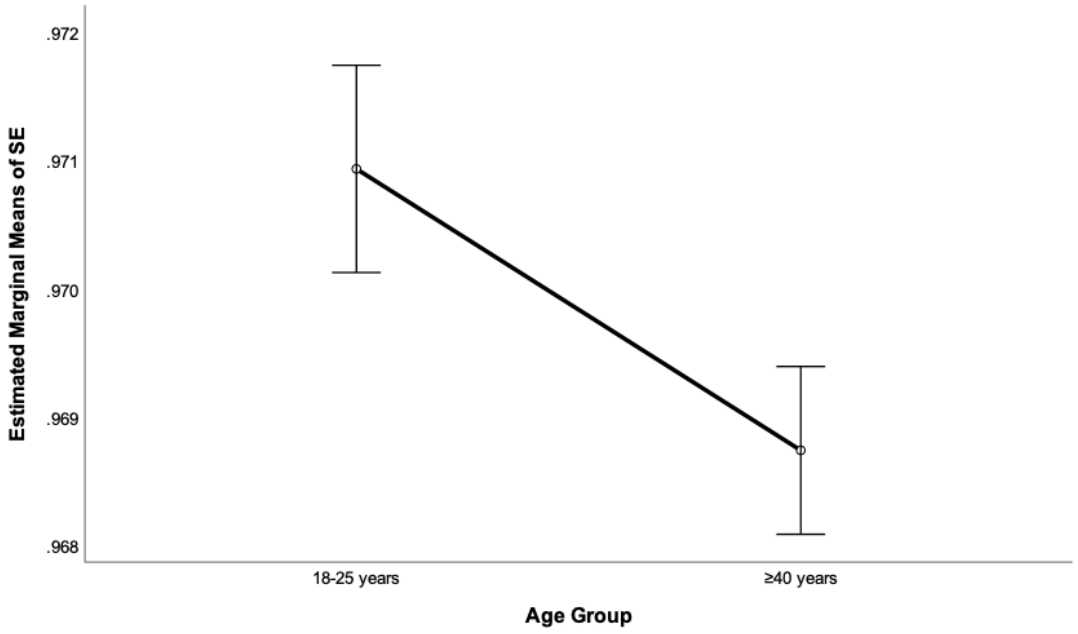

Figure 17. The main effect of age group on SE in the whole brain WM skeleton.
SE differed significantly across age groups (p<.001). Error bars indicate 95% confidence intervals.

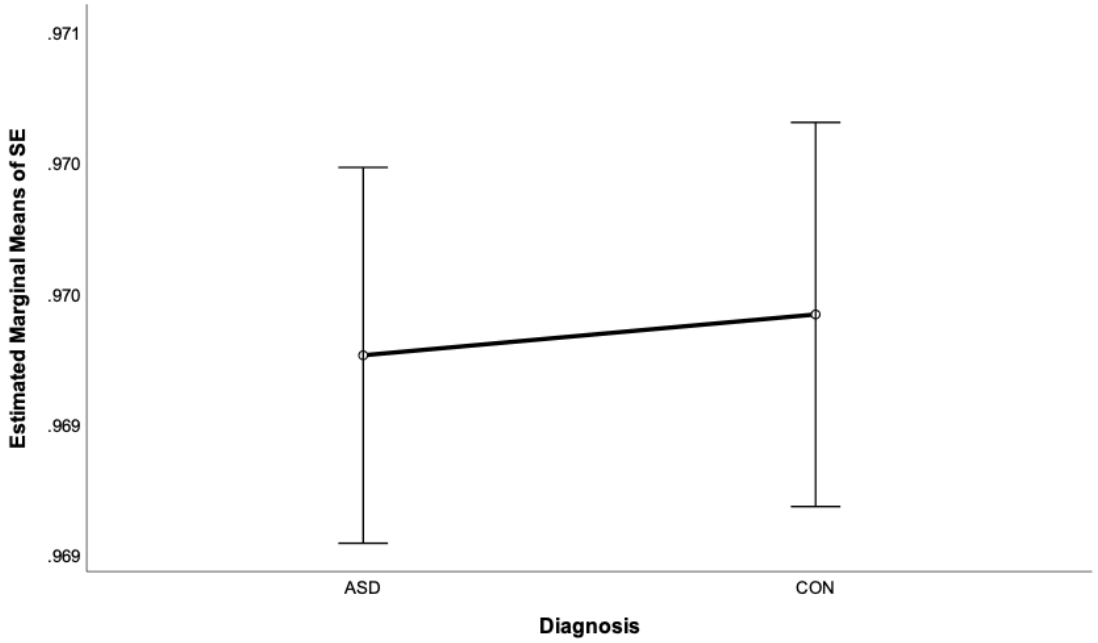

Figure 18. The main effect of diagnosis on SE in whole brain WM skeleton.
SE did not differ significantly across diagnosis (p=.760). Error bars indicate 95% confidence intervals.

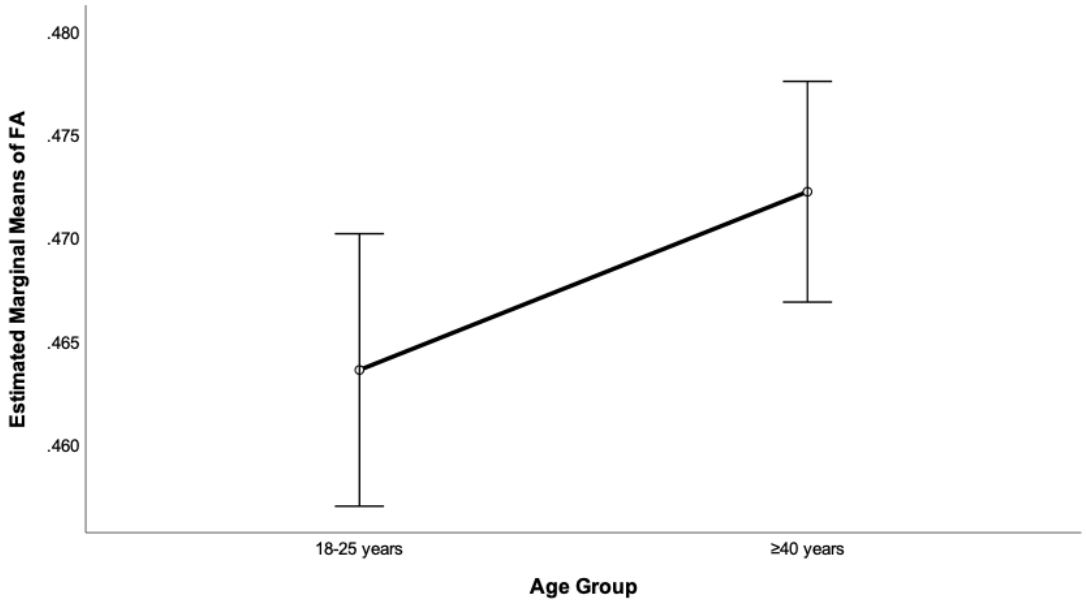

Figure 19. The main effect of age group on FA in the right sgACC.

FA differed significantly across age groups (p=.047). Error bars indicate 95% confidence intervals.

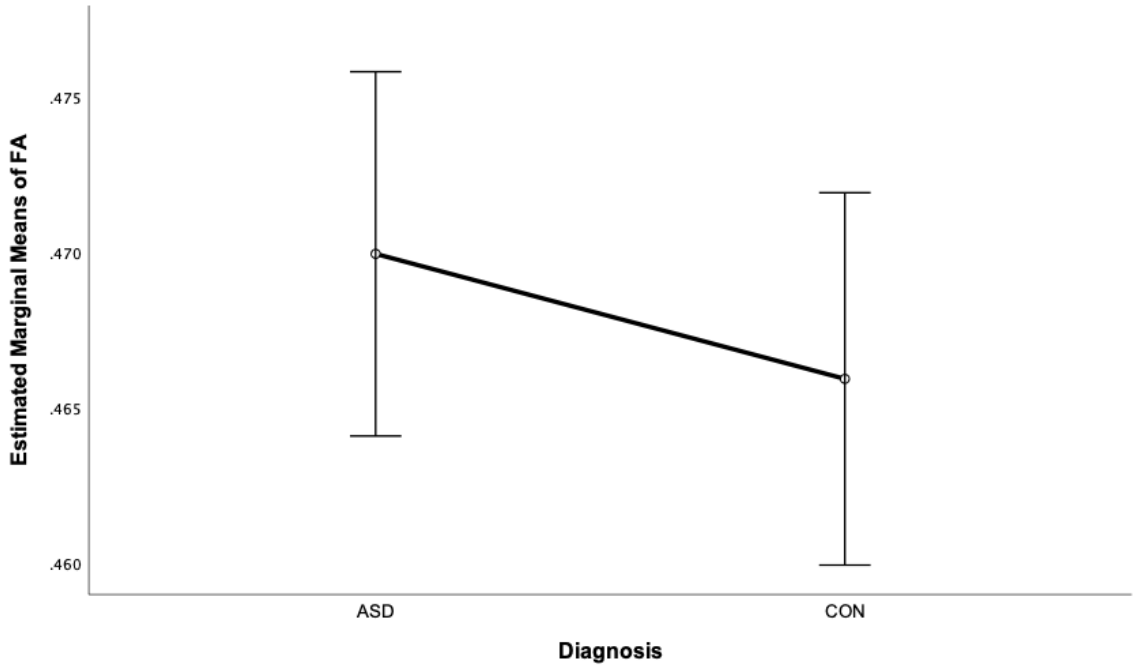

Figure 20. The main effect of diagnosis on FA in the right sgACC.

FA did not differ significantly across diagnosis (p=.336). Error bars indicate 95% confidence intervals.

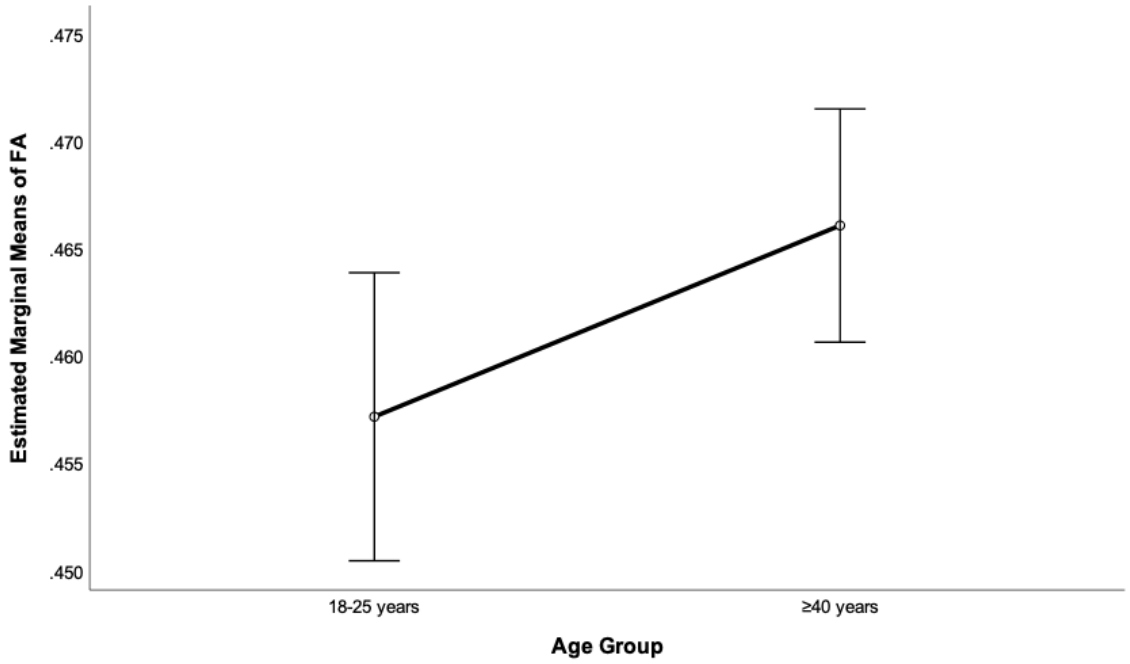

Figure 21. The main effect of age group on FA in the left sgACC.

FA differed significantly across age groups (p=.044). Error bars indicate 95% confidence intervals.

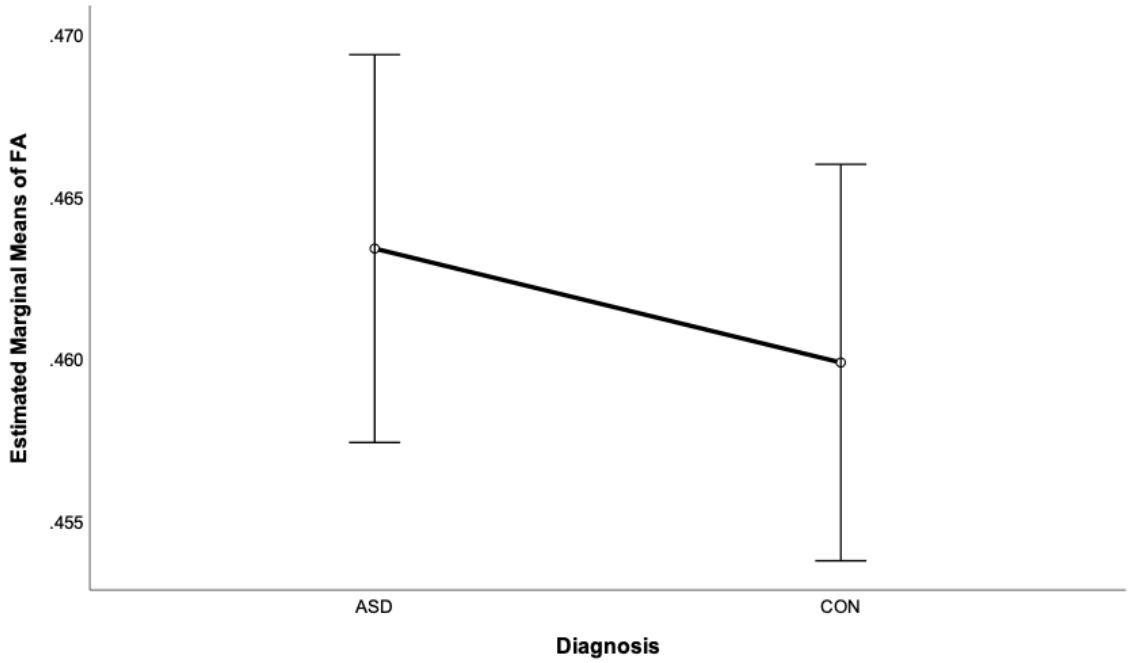

Figure 22. The main effect of diagnosis on FA in the left sgACC.

FA did not differ significantly across diagnosis (p=.410). Error bars indicate 95% confidence intervals.

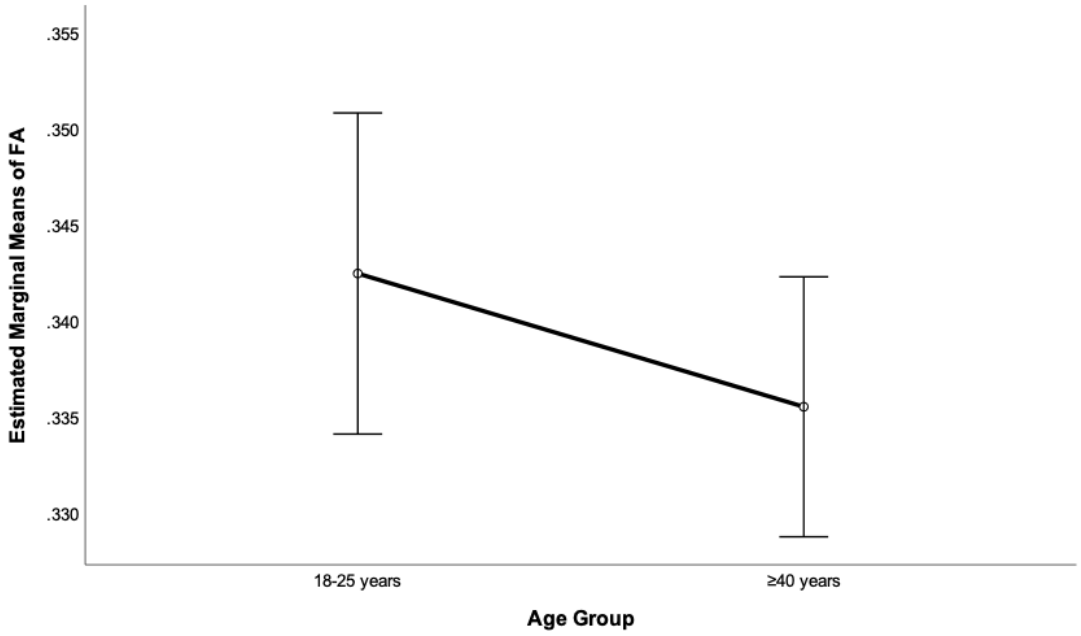

Figure 23. The main effect of age group on FA in the right BLA.

FA did not differ significantly across age groups (p=.485). Error bars indicate 95% confidence intervals.

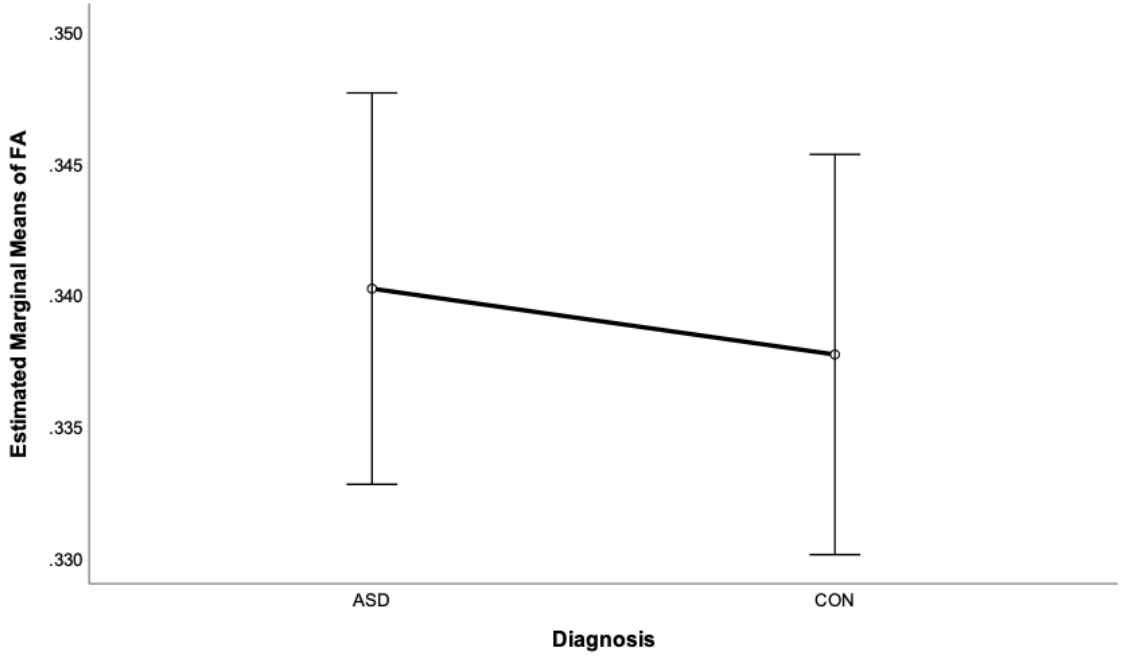

Figure 24. The main effect of diagnosis on FA in the right BLA.

FA did not differ significantly across diagnosis (p=.303). Error bars indicate 95% confidence intervals.

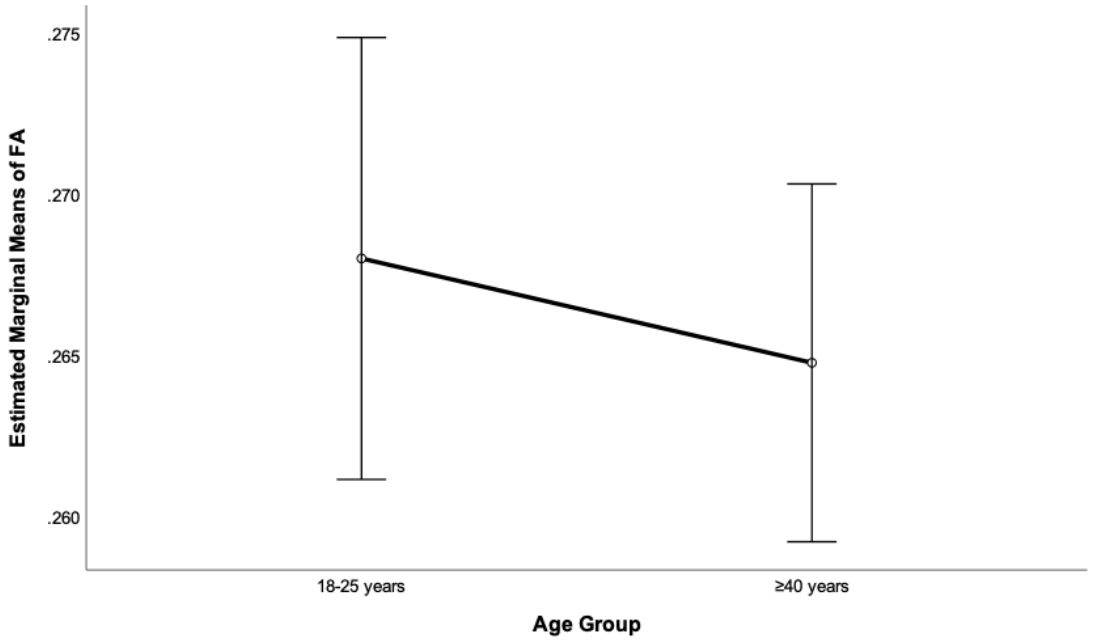

Figure 25. The main effect of age group on FA in the left BLA.

FA did not differ significantly across age groups (p=.466). Error bars indicate 95% confidence intervals.

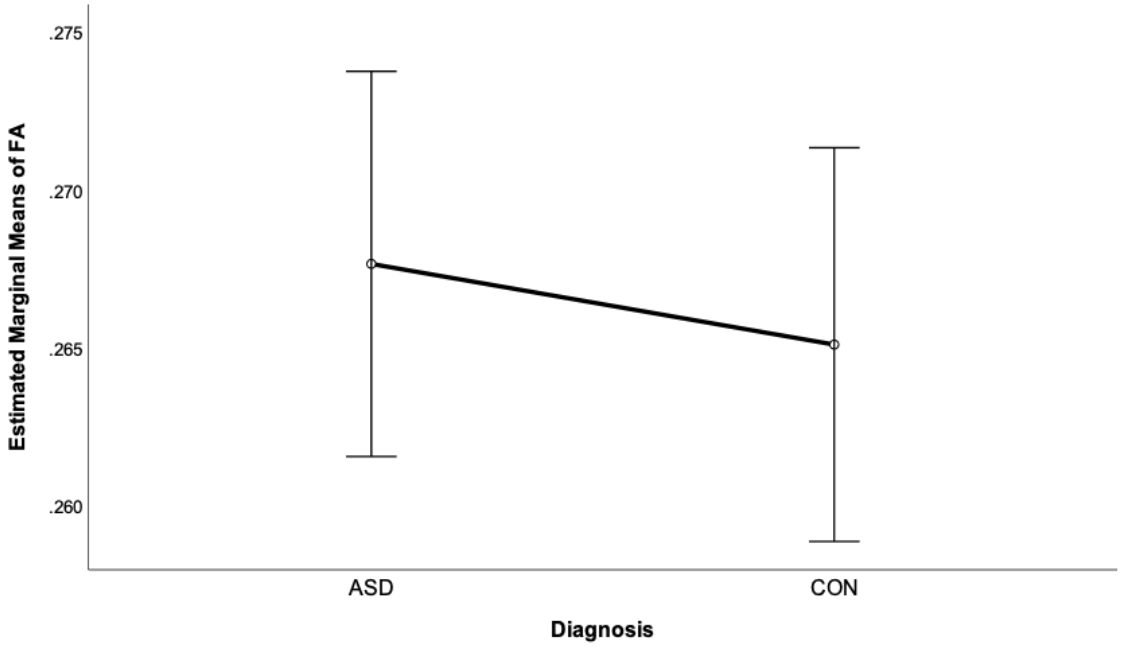

Figure 26. The main effect of diagnosis on FA in the left BLA.

FA did not differ significantly across diagnosis (p=.556). Error bars indicate 95% confidence intervals.

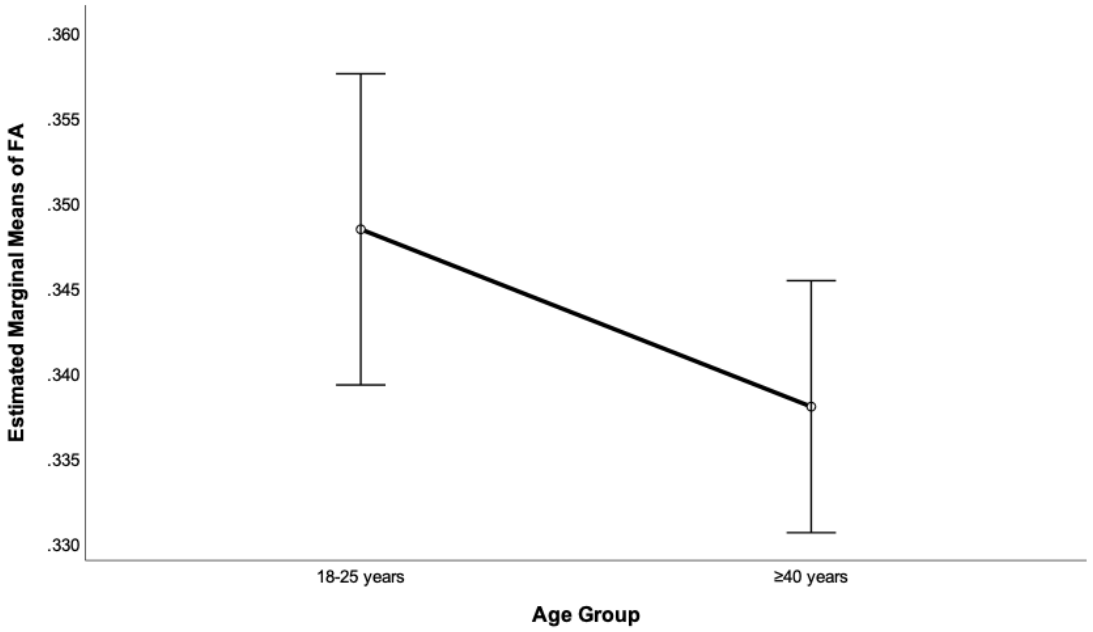

Figure 27. The main effect of age group on FA in the right amygdala.

FA did not differ significantly across age groups (p=.082). Error bars indicate 95% confidence intervals.

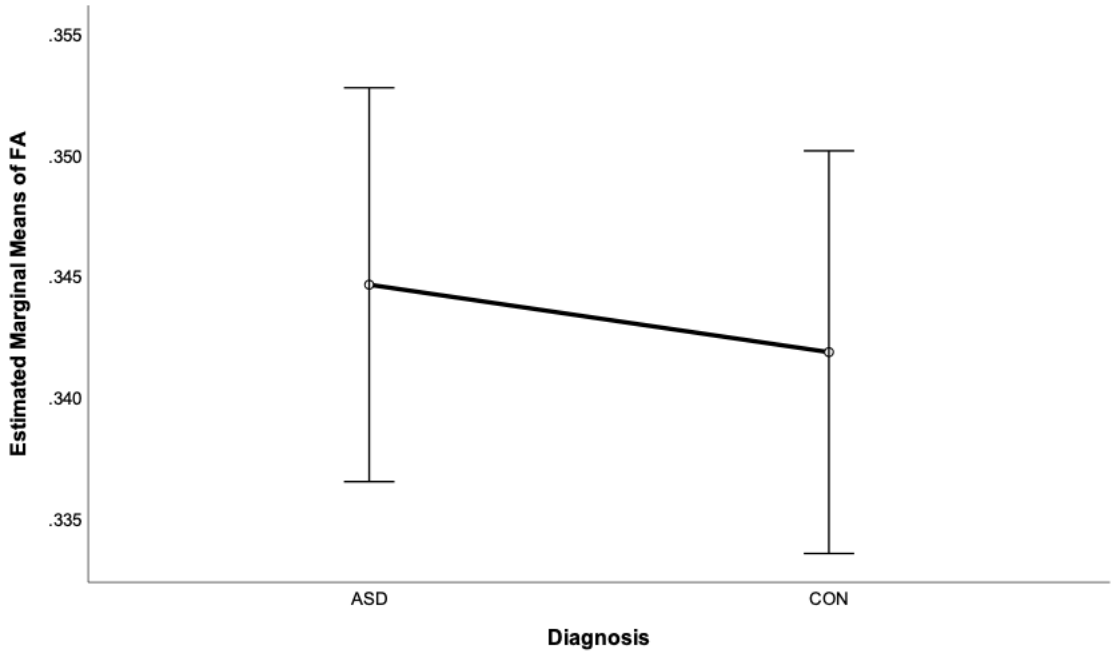

Figure 28. The main effect of diagnosis on FA in the right amygdala.

FA did not differ significantly across diagnosis (p=.630). Error bars indicate 95% confidence intervals.

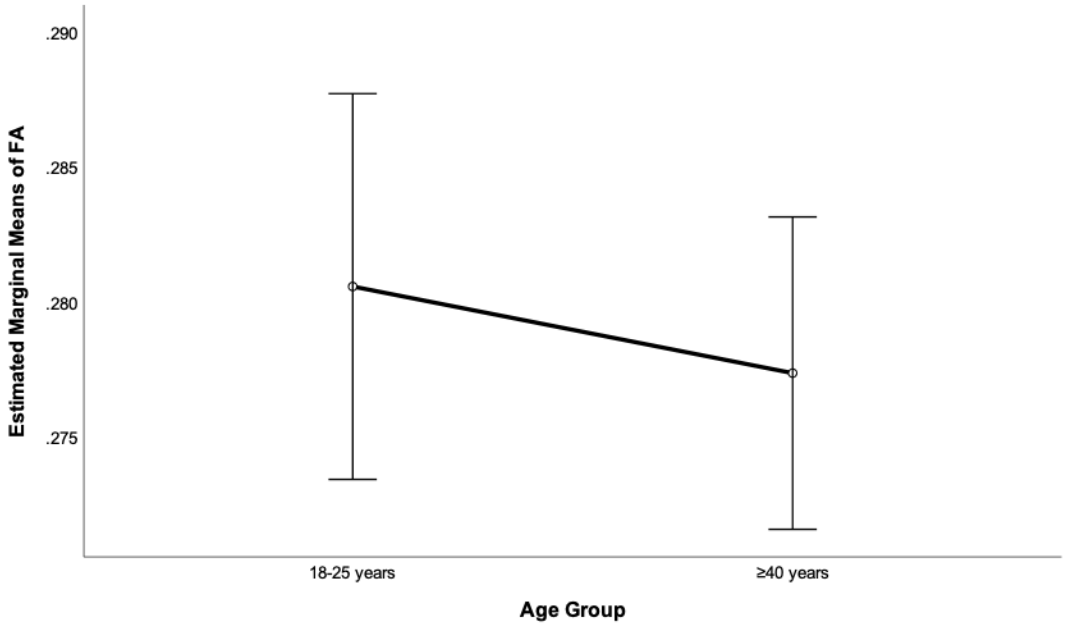

Figure 29. The main effect of age group on FA in the left amygdala.

FA did not differ significantly across age groups (p=.488). Error bars indicate 95% confidence intervals.

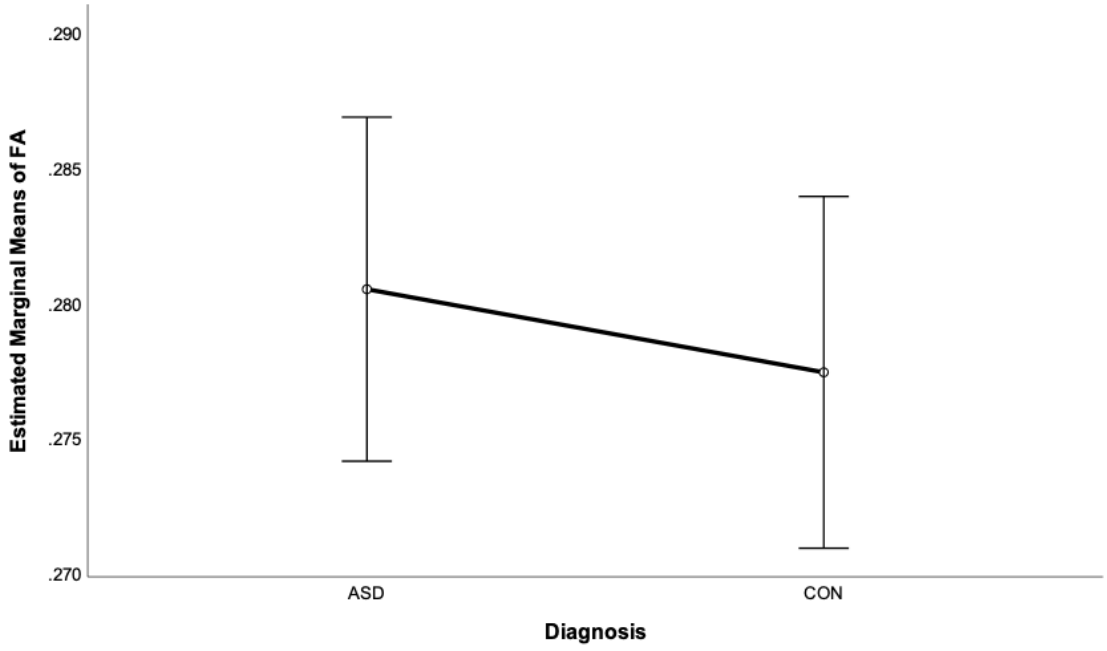

Figure 30. The main effect of diagnosis on FA in the left amygdala.

FA did not differ significantly across diagnosis (p=.498). Error bars indicate 95% confidence intervals.

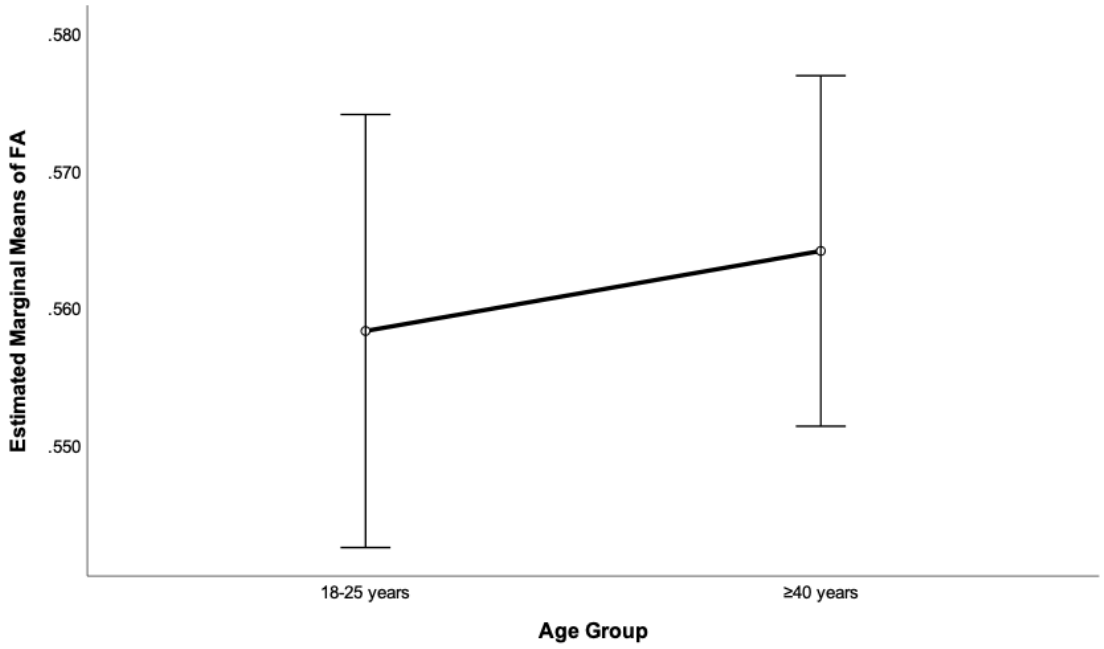

Figure 31. The main effect of age group on FA in the right uncinate fasciculus.

FA did not differ significantly across age group (p=.568). Error bars indicate 95% confidence intervals.

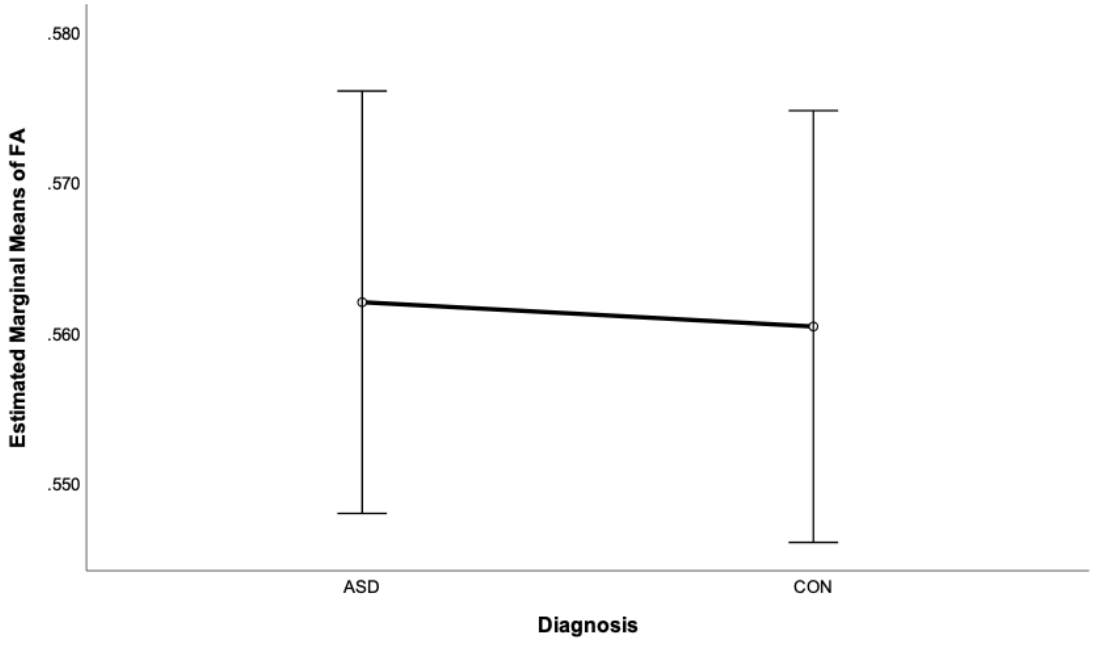

Figure 32. The main effect of diagnosis on FA in the right uncinate fasciculus.

FA did not differ significantly across diagnosis (p=.872). Error bars indicate 95% confidence intervals.

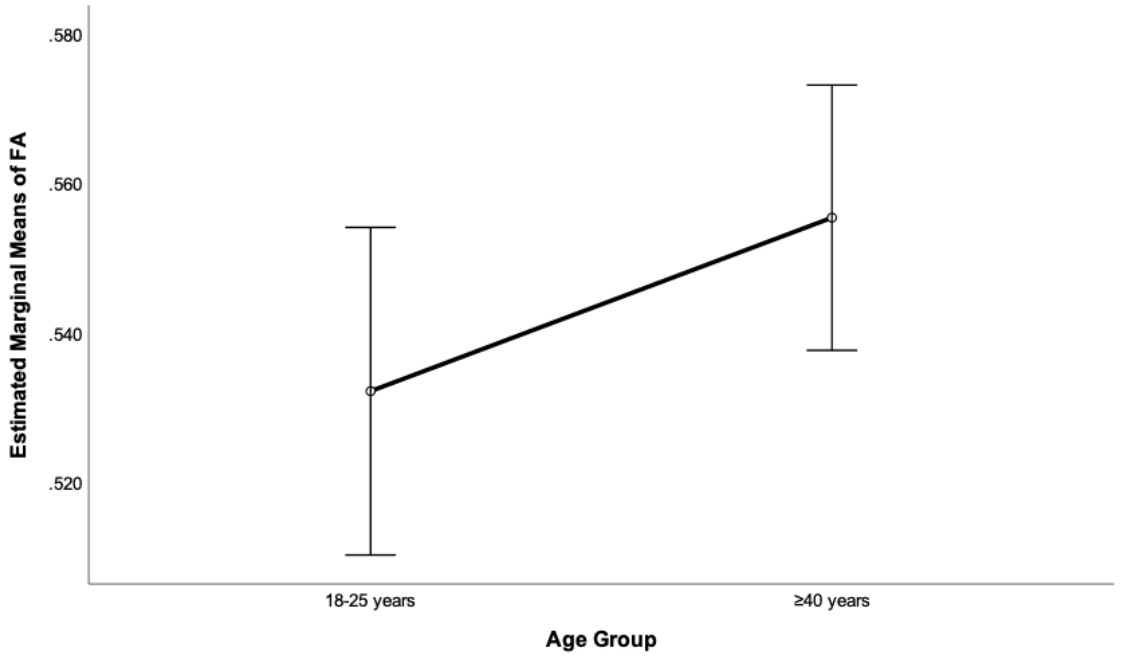

Figure 33. The main effect of age group on FA in the left uncinate fasciculus.

FA did not differ significantly across age group (p=.106). Error bars indicate 95% confidence intervals.

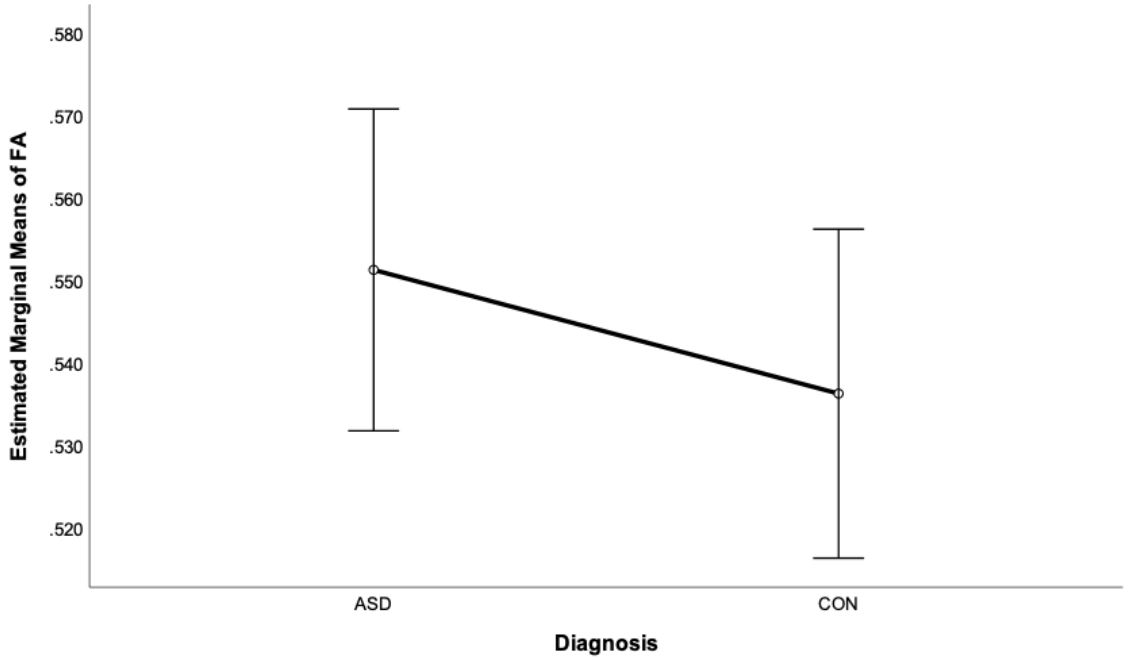

Figure 34. The main effect of diagnosis on FA in the left uncinate fasciculus.

FA did not differ significantly across diagnosis (p=.282). Error bars indicate 95% confidence intervals.

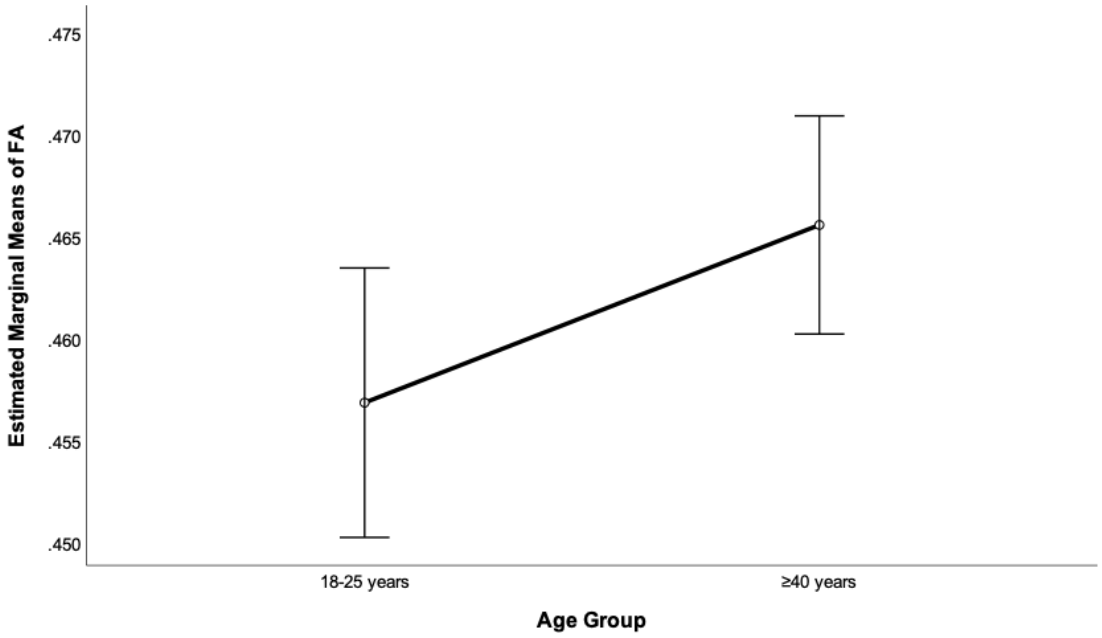

Figure 35. The main effect of age group on FA in the whole brain WM skeleton.

SE differed significantly across age groups (p=.045). Error bars indicate 95% confidence intervals.

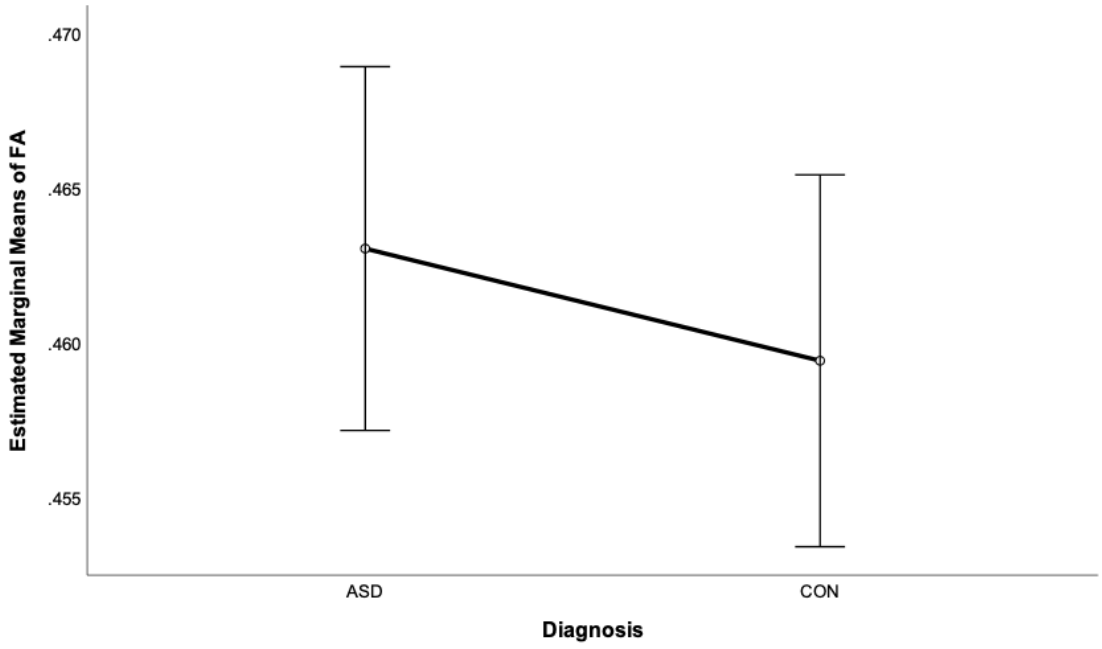

Figure 36. The main effect of diagnosis on FA in the whole brain WM skeleton

SE did not differ significantly across diagnosis (p=.387). Error bars indicate 95% confidence intervals.

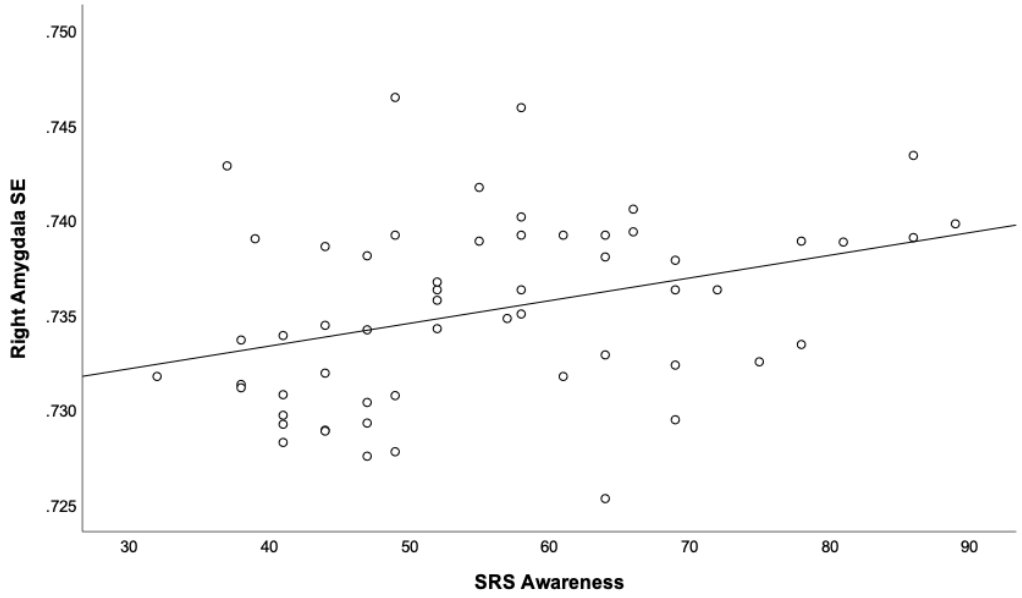

Figure 37. The correlation of SE in the right amygdala with SRS-2 Awareness scores.
SE significantly correlated with SRS-2 Awareness scores [r(55)= .347, p=.004, R^2 = .120].

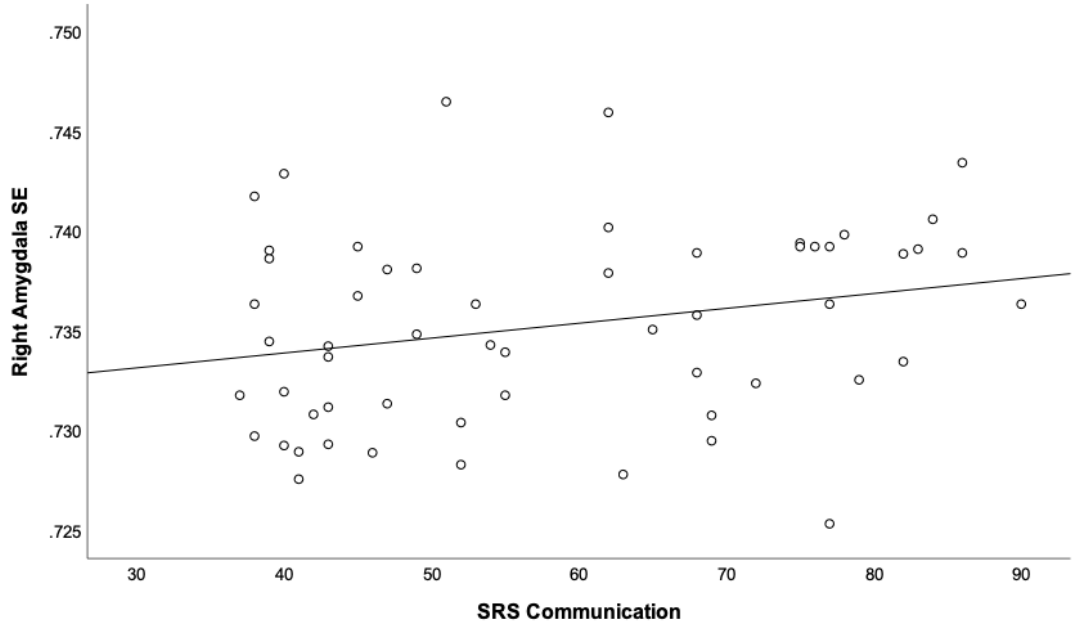

Figure 38. The correlation of SE in the right amygdala with SRS-2 Communication scores.
SE significantly correlated with SRS-2 Communication scores [r(55)= .254, p=.028, R^2 = .065].

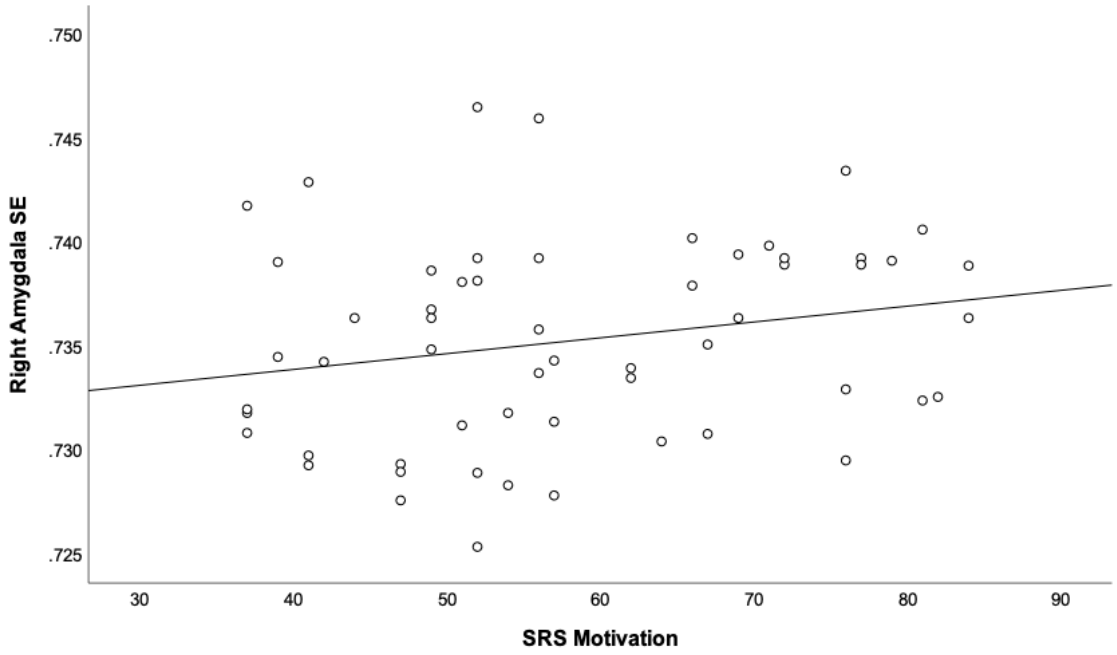

Figure 39. The correlation of SE in the right amygdala with SRS-2 Motivation scores.
SE significantly correlated with SRS-2 Motivation scores [$r(55)= .222$, $p=.049$, $R^2 = .049$].

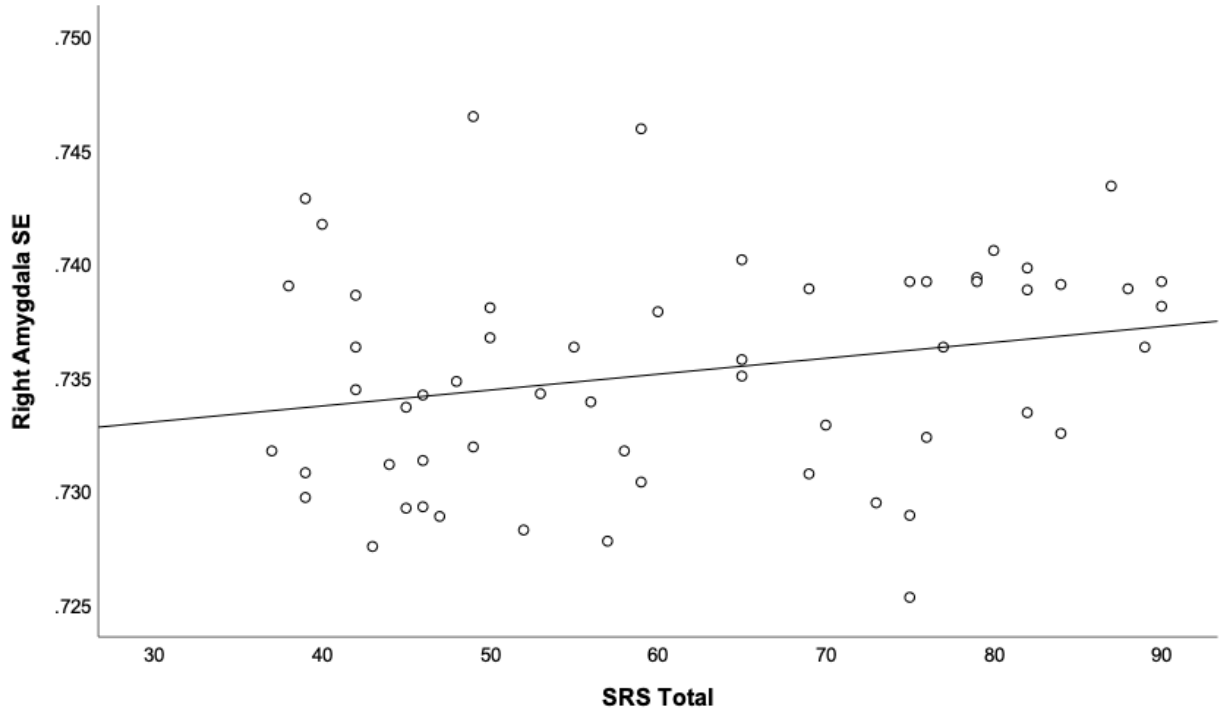

Figure 40. The correlation of SE in the right amygdala with SRS-2 Total scores.
SE significantly correlated with SRS-2 Total scores [$r(55)= .244$, $p=.034$, $R^2 = .060$].

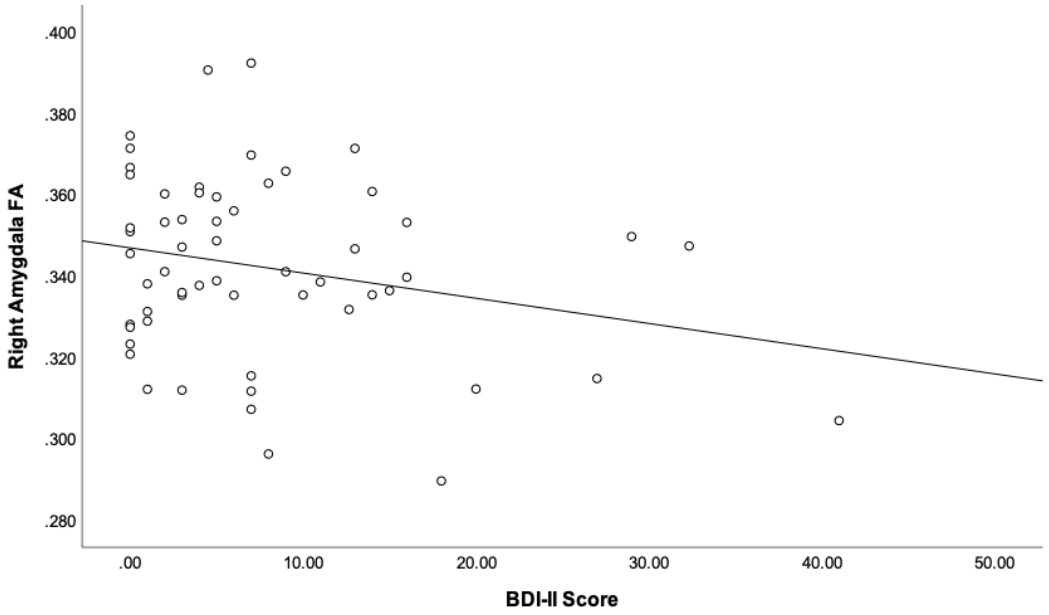

Figure 41. The correlation of FA in the right amygdala with BDI-II scores.

SE significantly correlated with BDI-II scores [r(56) = -.244, p=.033, R^2 = .059].

Table 2. Results of hierarchical regression analyses: Examining age, FA, and SE as predictors of depression (BDI-II) for each region of interest.

ROI	sgACC_R[a]	sgACC_L[a]	BLA_R[a]	BLA_L[a]	amyg_R[a]	amyg_L[a]	UF_R[b]	UF_L[a]	WB[a]
Step 1:									
Age	.105	.105	.105	.105	.105	.105	.116	.105	.105
R^2	.011	.011	.011	.011	.011	.011	.014	.011	.011
F	.622	.622	.622	.622	.622	.622	.739	.622	.622
Step 2:									
FA	-.221	-.233	-.234	-.185	-.232	-.260	.123	.151	-.242
ΔR^2	.046	.051	.053	.034	.051	.067	.015	.022	.055
ΔF	2.676	2.960	3.113	1.952	2.971	3.993	.827	1.252	3.215
Step 3:									
SE	-.101	-.087	-.032	-.029	-.008	.185	-.105	.084	-.063
ΔR^2	.008	.051	.001	.001	.000	.033	.011	.007	.003
ΔF	.469	.330	.059	.047	.004	2.008	.591	.371	.170

Standard coefficients from each step of the analysis are reported. Age is a categorical variable, consisting of two values: 18-25 years or ≥40 years. Analyses did not yield significant results. Abbreviations: BDI-II=Beck Depression Inventory, Second edition; sgACC_R = right sgACC; sgACC_L = left sgACC; BLA_R = right BLA; BLA_L = left BLA; amyg_R = right amygdala; amyg_L = left amygdala; UF_R = right uncinate fasciculus; UF_L = left uncinate fasciculus; WB = whole brain white matter skeleton

[a]*n*=58, [b]*n*=56

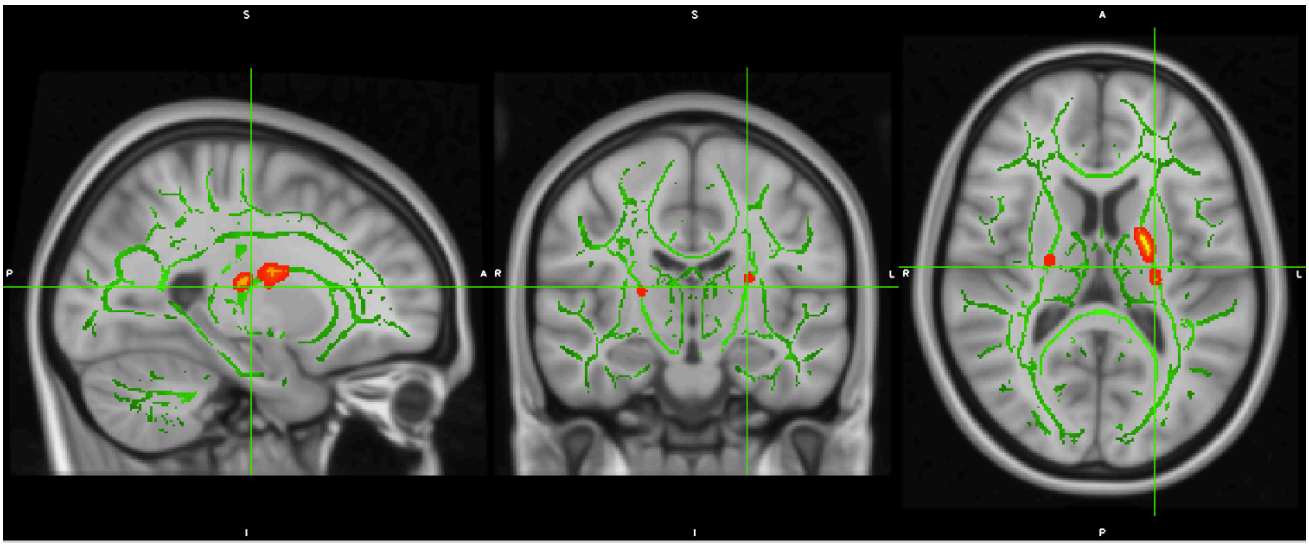

Figure 42. Visualization of tract based spatial statistics (TBSS) results.

Regions (bilateral posterior limb of the internal capsule, right anterior limb of internal capsule) labeled in red-yellow were identified by TBSS as having difference between ASD and CON individuals (p=.09).

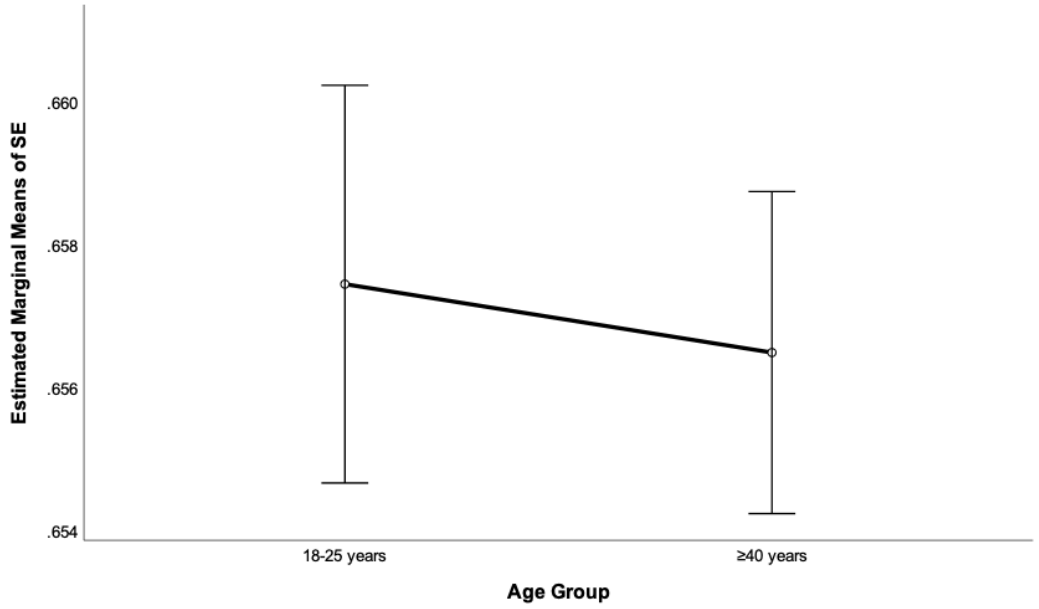

Figure 43. The main effect of age group on SE in the right posterior limb of the internal capsule.

SE did not differ significantly across age group (p=.595). Error bars indicate 95% confidence intervals.

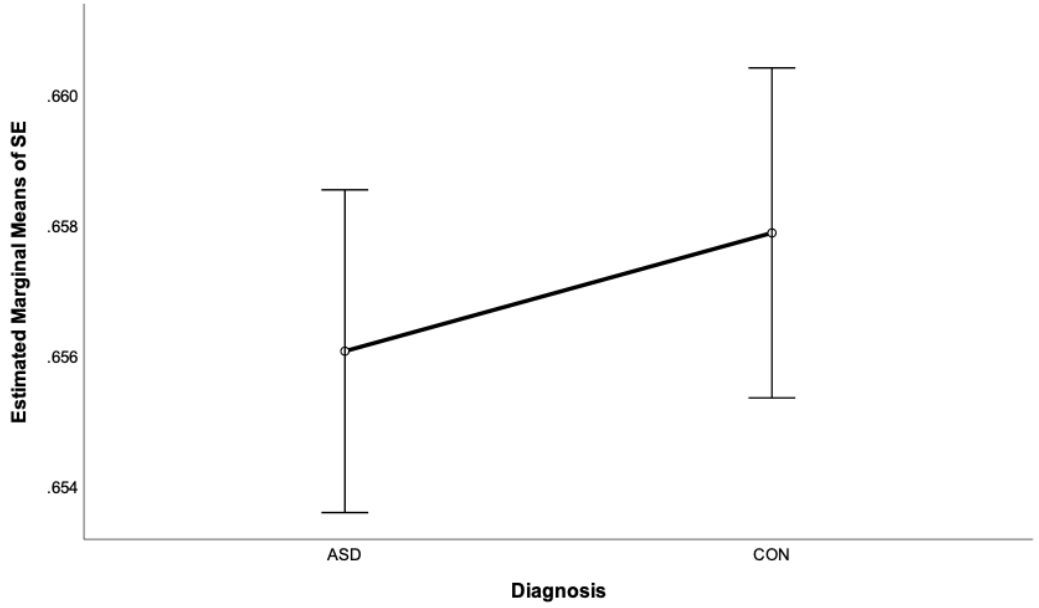

Figure 44. The main effect of diagnosis on SE in the right posterior limb of the internal capsule.

SE did not differ significantly across diagnosis (p=.305). Error bars indicate 95% confidence intervals.

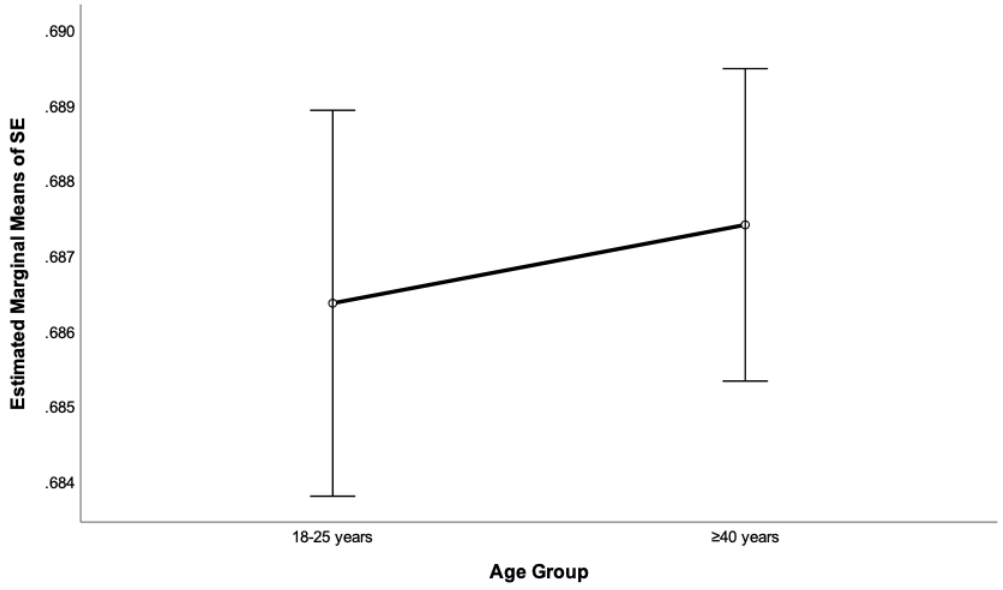

Figure 45. The main effect of age group on SE in the left posterior limb of the internal capsule.

SE did not differ significantly across age group (p=.531). Error bars indicate 95% confidence intervals.

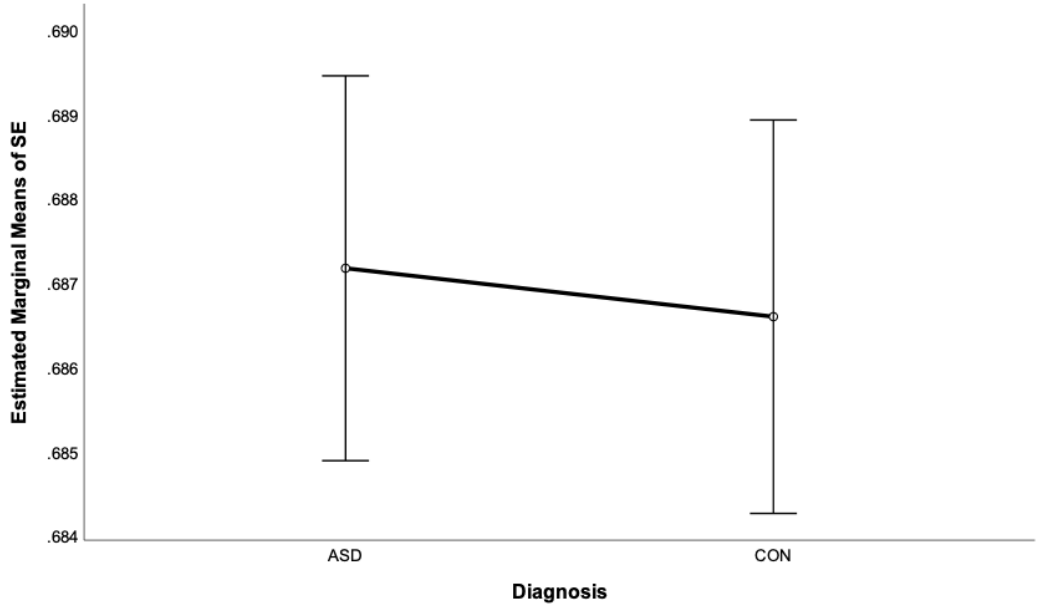

Figure 46. The main effect of diagnosis on SE in the left posterior limb of the internal capsule.

SE did not differ significantly across diagnosis (p=.723). Error bars indicate 95% confidence intervals.

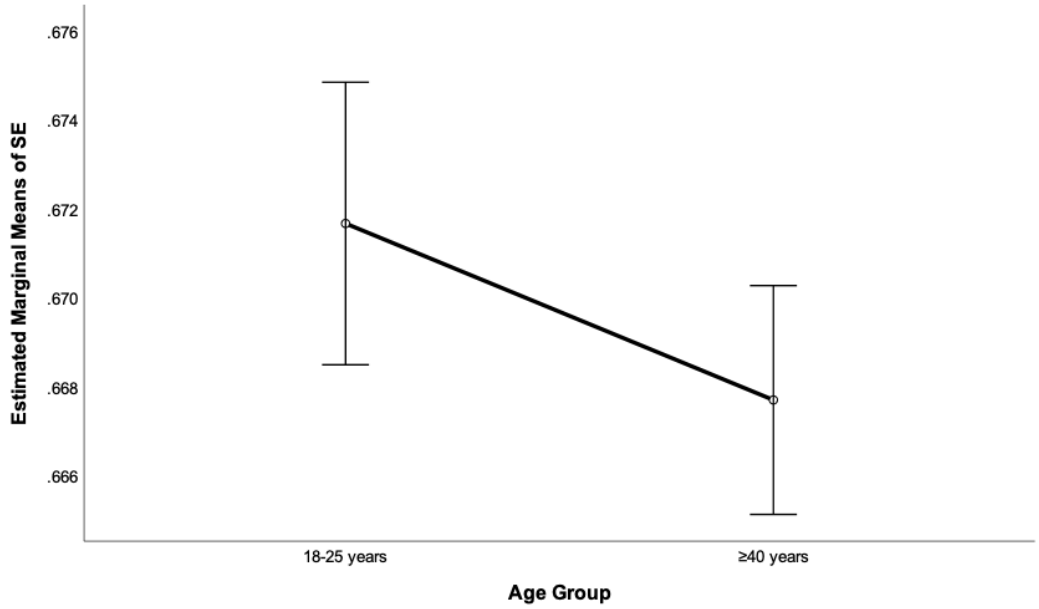

Figure 47. The main effect of age group on SE in the left anterior limb of the internal capsule.

SE did not differ significantly across age group (p=.057). Error bars indicate 95% confidence intervals.

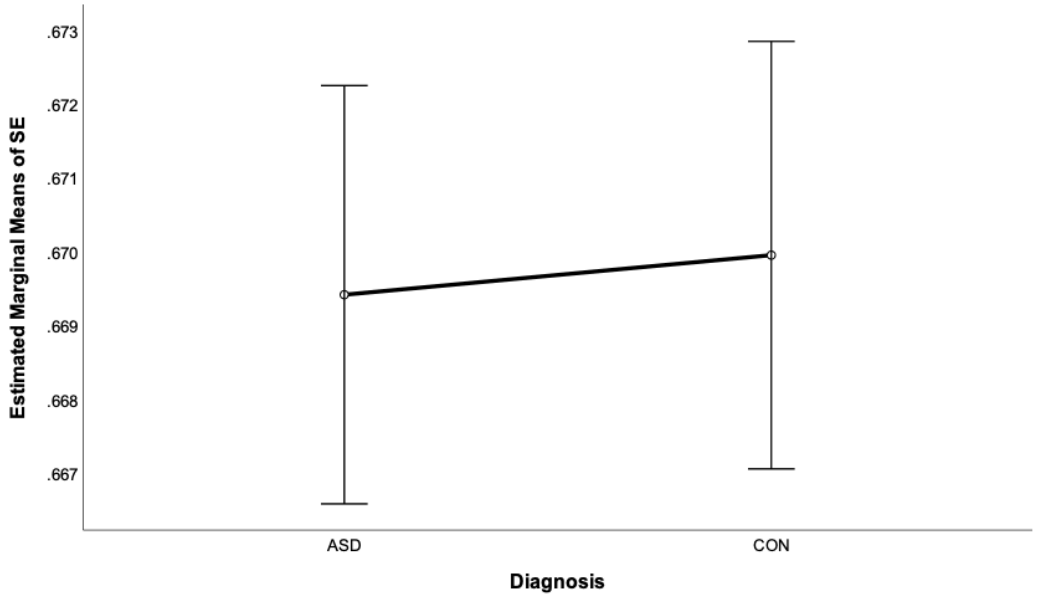

Figure 48. The main effect of diagnosis on SE in the left anterior limb of the internal capsule.

SE did not differ significantly across diagnosis (p=.790). Error bars indicate 95% confidence intervals.

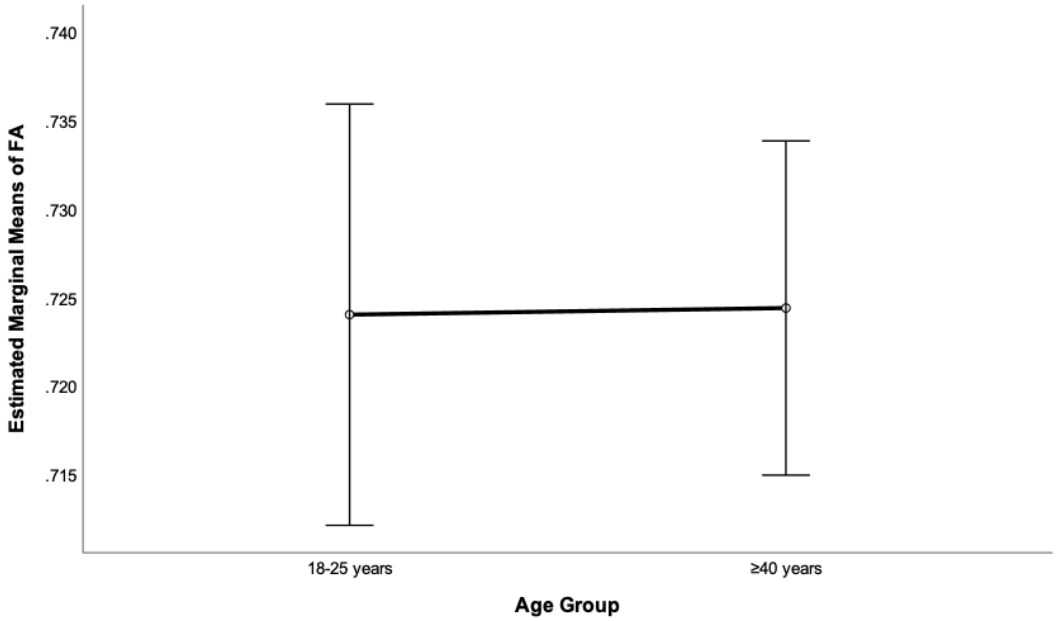

Figure 49. The main effect of age group on FA in the right posterior limb of the internal capsule.

FA did not differ significantly across age group (p=.961). Error bars indicate 95% confidence intervals.

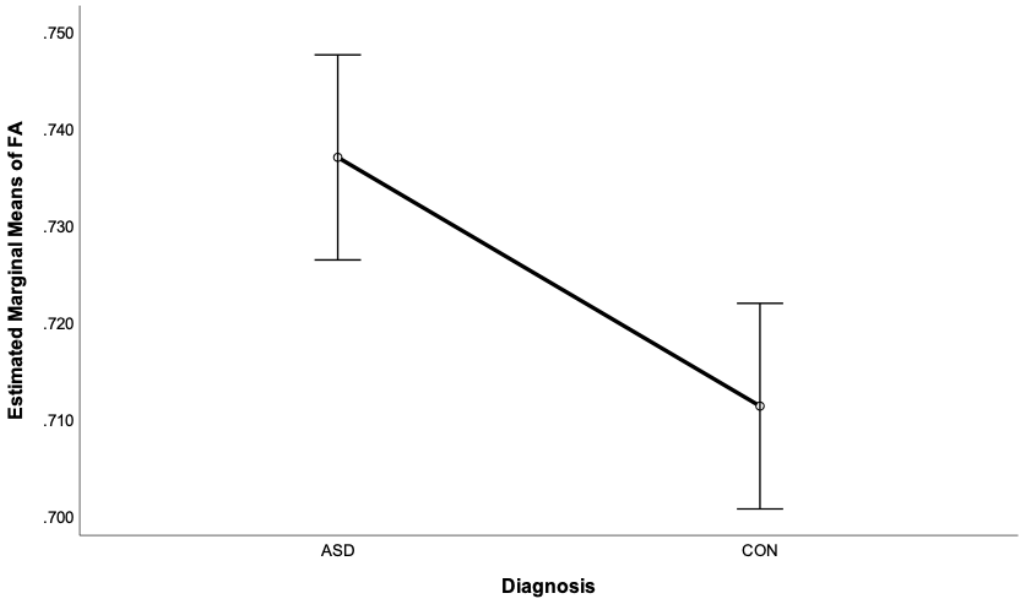

Figure 50. The main effect of diagnosis on FA in the right posterior limb of the internal capsule.

FA differed significantly across diagnosis (p=.001). Error bars indicate 95% confidence intervals.

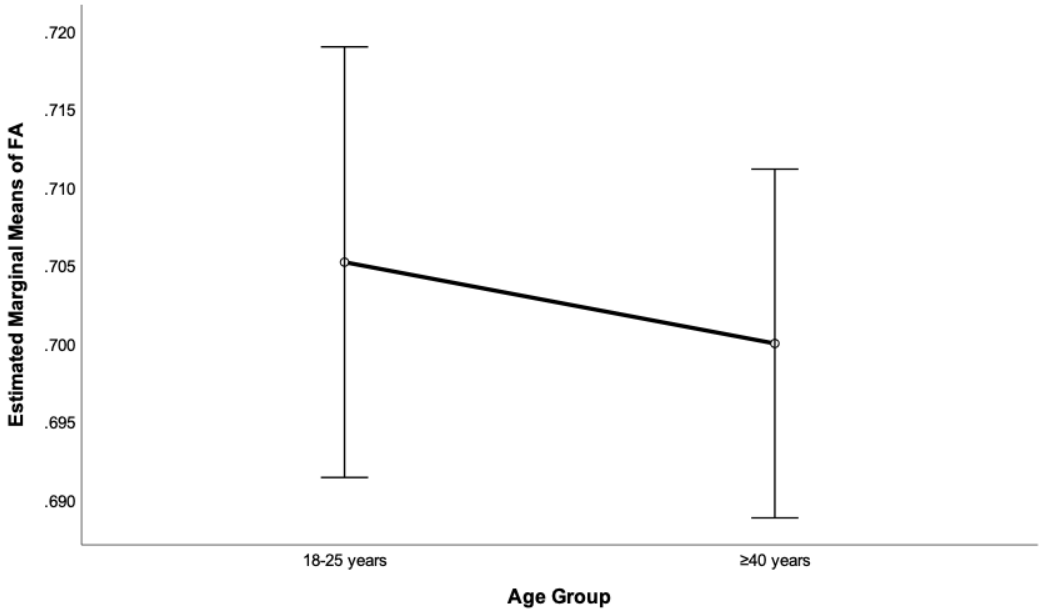

Figure 51. The main effect of age group on FA in the left posterior limb of the internal capsule.

FA did not differ significantly across age group (p=.560). Error bars indicate 95% confidence intervals.

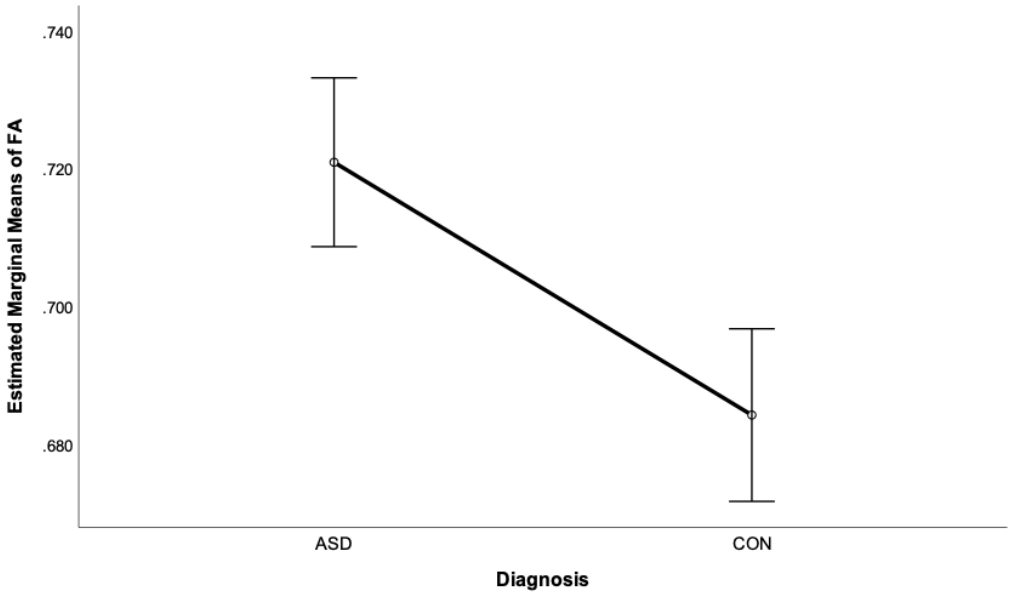

Figure 52. The main effect of diagnosis on FA in the left posterior limb of the internal capsule.

FA differed significantly across diagnosis (p<.001). Error bars indicate 95% confidence intervals.

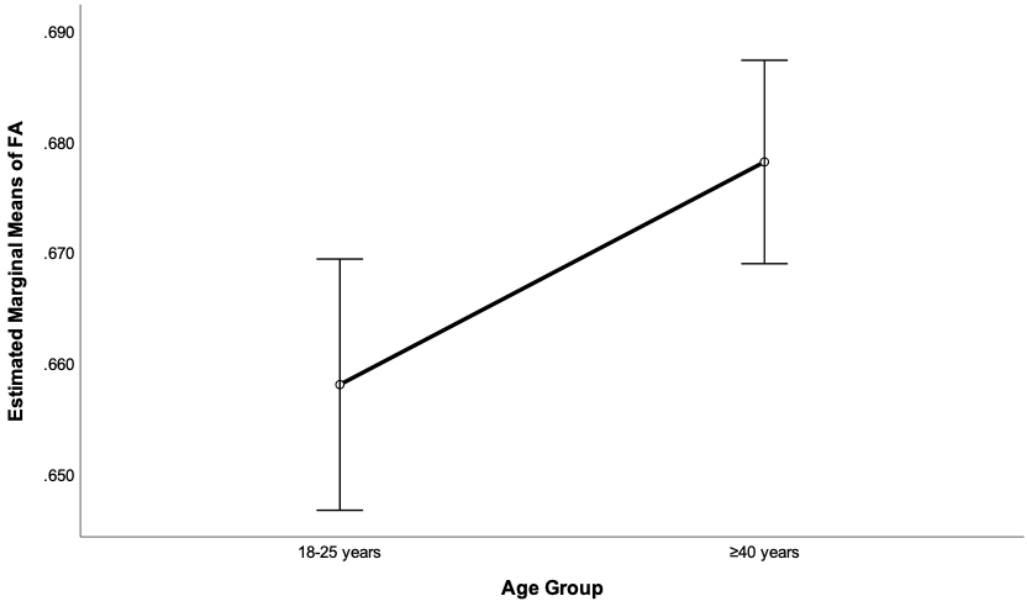

Figure 53. The main effect of age group on FA in the left anterior limb of the internal capsule.

FA differed significantly across age group (p=.008). Error bars indicate 95% confidence intervals.

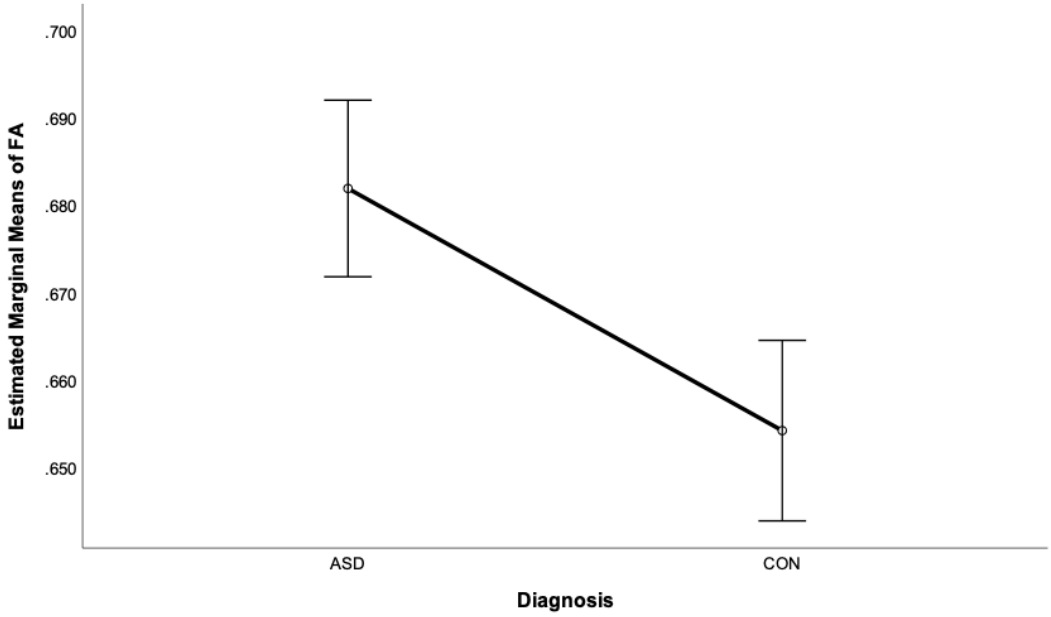

Figure 54. The main effect of diagnosis on FA in the left anterior limb of the internal capsule.

FA differed significantly across diagnosis (p<.001). Error bars indicate 95% confidence intervals.

Table 3. Results of hierarchical regression analyses: Examining age, FA, and SE as predictors of depression (BDI-II) in post-hoc regions of interest.

ROI	PLIC_R[a]	PLIC_L[b]	ALIC_L[b]
Step 1: Age			
	.120	.105	.105
R^2	.014	.011	.011
F	.807	.622	.622
Step 2: FA			
	.074	.184	.095
ΔR^2	.006	.033	.008
ΔF	.305	1.926	.471
Step 3: SE			
	.080	.056	.068
ΔR^2	.006	.003	.004
ΔF	.347	.174	.230

Standard coefficients from each step of the analysis are reported. Age is a categorical variable, consisting of two values: 18-25 years or ≥40 years. Analyses did not yield significant results. Abbreviations: BDI-II=Beck Depression Inventory, Second edition; PLIC_R = right posterior limb of internal capsule; PLIC_L = left posterior limb of internal capsule; ALIC_L = left anterior limb of internal capsule.

[a]n=58, [b]*n*=56

DISCUSSION

This neuroimaging study examined the use of SE and FA as measures of WM integrity in various regions of interest in individuals with ASD using DTI data from an ASD database (ABIDE II). The primary findings revealed main effects of age on measures of WM integrity with medium to large effect sizes. The study results indicated that there was a significant main effect of age group on SE in the left [$\eta_p^2 = .223$] and right [$\eta_p^2 = .192$] subgenual anterior cingulate cortices (sgACC). SE was significantly lower in both left and right sgACC in individuals aged ≥40 (i.e., 40-64) years compared to the younger group aged 18-25 years old. There was also a main effect of age group on FA in the left [$\eta_p^2 = .072$] and right [$\eta_p^2 = .070$] sgACC. However, the ≥40 years group had significantly higher FA values than the younger group. These effects of age on SE [$\eta_p^2 = .245$] and FA [$\eta_p^2 = .014$] values were also present in the whole brain WM skeleton. There were no other regions for which there was a significant main effect for either age or diagnosis.

These findings suggest that the WM integrity of the sgACC may be affected by aging in individuals with ASD. SE being lower in individuals aged greater than 40 goes in line with prior studies that have found that decreased SE is associated with decreased axonal density that occurs with aging and is found in individuals with atypical brain development or functioning, such as multiple sclerosis (Huang et al., 2019).

The result of higher FA in older individuals unexpected. However, this finding may be because many brain biomarkers follow an inverted U-shaped developmental trajectory (Snook et al., 2005; Sullivan et al., 2010; Westlye et al., 2010). Prior studies of FA in young adults have shown that FA increases from childhood through early adulthood, with whole brain FA values reaching their maximum FA by 29.1 years, followed by decline in FA values, representing strong quadratic age effects (Snook et al., 2005; Sullivan et al., 2010; Westlye et al., 2010). Given the mean age for the younger group (i.e., mean age= 20.78; *SD*=2.32), it is possible that these individuals had not yet reached their FA peak, accounting for the lower FA score compared to the older group (i.e., mean age =50.17; *SD*=6.82). A larger dataset with representation at each age as well as longitudinal follow-up will be needed to determine if SE and FA changes follow a quadratic pattern.

With respect to clinical correlations, SE in the right amygdala was significantly associated with general ASD symptomatology [$r(55)= .244$], in addition to awareness [$r(55)= .347$], communication [$r(55)= .254$], and motivation [$r(55)= .222$]. This finding indicates that SE is

positively correlated with ASD symptomatology, as higher scores of the SRS-2 reveal increase in severity of ASD symptoms. These results do not support our hypothesis of higher SE being associated less severe ASD.

Given that we proposed using SE as a measure of WM integrity, we had originally postulated SE to be lower in individuals with ASD. This was based on Delic et al. (2016), which had shown individuals with TBI to have lower SE compared to controls. However, the results in this study indicate that SE is higher in individuals with more severe ASD symptoms in contrast to prior studies that have concluded that decreased WM in the right amygdala was associated with severity of ASD (Gibbard et al., 2018). One possible explanation for this could be in axonal remodeling. A study examining SE in type 2 diabetes rats post stroke concludes that increased fiber crossing can be found at the site of injury and since SE is more sensitive to microlevel restructuring in WM, it may cause higher SE values and lower FA values (Ding et al., 2017). In addition, SE has been shown to detect new axonal remodeling after injury or onset of disease (Fozouni et al., 2013). Thus, despite these findings contradicting our idea of higher SE associating with better brain health, in adults with ASD, axonal remodeling may be occurring to a greater degree as a compensatory mechanism than controls, thereby causing SE to be associated with increased ASD symptom severity. We are only starting to understand how SE operates as a measure of WM integrity, and thus these results may provide more insight into the information we can obtain from SE as a biomarker.

FA in the left [$r(56) = -.268$] and right [$r(56) = -.244$] amygdala and right BLA [$r(56) = -.245$] was significantly associated with depression, thus suggesting an overlap in the role of the amygdala. OFC-amygdala WM disruption has been linked to the onset of depressive symptoms and the relationship between decreased FA and increased depression, as found in this study, is further evidence of such occurrences (Zheng et al., 2018). These results also indicate that SE and FA may provide different types of information—one more related to axonal integrity in neurodevelopmental conditions while the other with psychiatric symptoms, respectively.

Post-hoc analyses with TBSS revealed significant main effects of diagnosis on FA in the left [$\eta_p^2=.246$] and right [$\eta_p^2=.183$] posterior limb of the internal capsule and left anterior limb of the internal capsule [$\eta_p^2=.215$]. There was also a main effect for age on FA in the left anterior limb of the internal capsule [$\eta_p^2=.121$]. Individuals with ASD had higher FA values compared to controls. These results replicate previously found WM tract differences between ASD and CON

diagnoses in the left and right posterior and left anterior limbs of the internal capsule (Shukla et al., 2011). Similar results for FA in the anterior limb of the internal capsule have been found in individuals with OCD (Lochner et al., 2012).

FA in the right and left posterior limbs of the internal capsule was significantly associated with awareness [$r(54)= .279$; $r(55)= .357$], cognition [$r(54)= .303$; $r(55)= .401$], communication [$r(54)= .428$; $r(55)= .482$], motivation [$r(54)= .325$; $r(55)= .388$], mannerisms [$r(54)= .357$; $r(55)= .405$], and total symptomatology scores [$r(54)= .301$; $r(55)= .306$]. FA in the anterior limb of the internal capsule was correlated with awareness [$r(55)= .311$], cognition [$r(55)= .374$], communication [$r(55)= .369$], motivation [$r(55)= .273$], and mannerisms [$r(55)= .304$] scores. Microstructural and functional alterations in the left posterior limb of the internal capsule have been shown to associate with ASD symptoms (Ma et al., 2022).

Limitations of this study include the fact that this study is cross-sectional. To truly investigate the role of aging in WM development in adults, we would need to conduct a longitudinal study with individuals of each age to better identify trends in aging and WM integrity. This study also only included 58 individuals and thus replication with a larger sample size is needed. There were also two age groups in this study (18-25 and 40-64), whereas individuals between 26 to 39 years old were omitted. Future studies should include this age range to fully understand aging trajectory in ASD. In addition, only males were available in the cohort which also prevents understanding sex-specific differences. While some of our results had large effect sizes ($\eta_p^2= .070 - .246$), the relatively small study sample size ($N = 58$) may have limited the power for identifying results with small effect sizes.

Furthermore, the technique of TBSS has its own limitations. For instance, the registration technique of FNIRT in TBSS is not fully error free and the tracts generated may not be completely at the center of the WM tracts (Eikenes et al., 2023). In addition, the technique is not able to detect smaller tracts, such the fornix (Bach et al., 2014). However, this did not apply to this study as we focused on the uncinate fasciculus, which is the largest WM tract (Bhatia et. al., 2014; Von Der Heide et al., 2013).

From this study, we were able to identify that age affects the WM integrity of regions involved in depression, specifically the sgACC. However, neither SE nor FA in the sgACC correlated with the clinical measure of depression, suggesting more studies are needed to understand the role of the sgACC in depression in ASD. In comparison, there was no main effect

of age for SE or FA in the right amygdala. However, FA in the right and left amygdala correlated with depression and the right amygdala correlated with ASD symptom severity, suggesting that regional FA metrics may be an important psychiatric biomarker. Future studies may also expand the number of imaging metrics used, such as diffusion kurtosis imaging, which extends the impact of DTI to analyze axonal water improving the resolution of our results (Henriques et al., 2021). In addition, given previous studies that have linked grey matter density in the whole brain and in the amygdala with ASD diagnoses, grey matter ROIs may be of interest in performing SE analysis to examine how the grey matter complexity is affected by diagnoses of ASD and possible associations with depression in adults (Arunachalam Chandran et al., 2021; Gennatas et al., 2017; Sato et al., 2017). Thus, future longitudinal studies could incorporate ASD and depression measures and a large age range to understand the amygdala-sgACC circuitry and their respective contributions to symptom presentation.

REFERENCES

Aoki, Y., Yoncheva, Y. N., Chen, B., Nath, T., Sharp, D., Lazar, M., Velasco, P., Milham, M. P., & Di Martino, A. (2017). Association of White Matter Structure With Autism Spectrum Disorder and Attention-Deficit/Hyperactivity Disorder. *JAMA Psychiatry, 74*(11), 1120-1128. doi:10.1001/jamapsychiatry.2017.2573

Alba-Ferrara, L., & de Erausquin, G. (2013). What does anisotropy measure? Insights from increased and decreased anisotropy in selective fiber tracts in schizophrenia. *Frontiers in integrative neuroscience, 7*, 9. doi:10.3389/fnint.2013.00009

Alexander, A. L., Lee, J. E., Lazar, M., & Field, A. S. (2007). Diffusion tensor imaging of the brain. *Neurotherapeutics, 4*(3), 316-329. doi:10.1016/j.nurt.2007.05.011

Alexander, A. L., Lee, J. E., Lazar, M., Boudos, R., DuBray, M. B., Oakes, T. R., Miller, J. N., Lu, J., Jeong, E.-K., McMahon, W. M., Bigler, E. D., & Lainhart, J. E. (2007). Diffusion tensor imaging of the corpus callosum in Autism. *NeuroImage, 34*(1), 61-73. doi:https://doi.org/10.1016/j.neuroimage.2006.08.032

Amunts, K., Kedo, O., Kindler, M., Pieperhoff, P., Mohlberg, H., Shah, N. J., Habel, U., Schneider, F., & Zilles, K. (2005). Cytoarchitectonic mapping of the human amygdala, hippocampal region and entorhinal cortex: intersubject variability and probability maps. *Anatomy and Embryology, 210*(5), 343-352. doi:10.1007/s00429-005-0025-5

Amunts, K., Mohlberg, H., Bludau, S., & Zilles, K. (2020). Julich-Brain: A 3D probabilistic atlas of the human brain's cytoarchitecture. *Science, 369*(6506), 988-992. doi:doi:10.1126/science.abb4588

Andersson, J. L. R., Skare, S., & Ashburner, J. (2003). How to correct susceptibility distortions in spin-echo echo-planar images: application to diffusion tensor imaging. *NeuroImage, 20*(2), 870-888. doi:https://doi.org/10.1016/S1053-8119(03)00336-7

Andersson, J. L. R., & Sotiropoulos, S. N. (2016). An integrated approach to correction for off-resonance effects and subject movement in diffusion MR imaging. *NeuroImage, 125*, 1063-1078. doi:https://doi.org/10.1016/j.neuroimage.2015.10.019

Andersson, J.L.R., Jenkinson, M., Smith, S. Non-linear optimisation. *FMRIB technical report TR07JA1* from *www.fmrib.ox.ac.uk/analysis/techrep*

Andica, C., Kamagata, K., Kirino, E., Uchida, W., Irie, R., Murata, S., & Aoki, S. (2021). Neurite orientation dispersion and density imaging reveals white matter microstructural alterations in adults with autism. *Molecular Autism, 12*(1), 48. doi:10.1186/s13229-021-00456-4

Arunachalam Chandran, V., Pliatsikas, C., Neufeld, J., O'Connell, G., Haffey, A., DeLuca, V., & Chakrabarti, B. (2021). Brain structural correlates of autistic traits across the diagnostic divide: A grey matter and white matter microstructure study. *Neuroimage Clin, 32*, 102897. doi:10.1016/j.nicl.2021.102897

Avants, B. B., Tustison, N. J., Song, G., Cook, P. A., Klein, A., & Gee, J. C. (2011). A reproducible evaluation of ANTs similarity metric performance in brain image registration. *NeuroImage, 54*(3), 2033-2044. doi:https://doi.org/10.1016/j.neuroimage.2010.09.025

Bain, S. K., & Jaspers, K. E. (2010). Test review: review of Kaufman brief intelligence test, Second Edition:Kaufman, A. S., & Kaufman, N. L. (2004). Kaufman Brief Intelligence Test, Second Edition. Bloomington, MN: Pearson, Inc. *Journal of Psychoeducational Assessment, 28*(2), 167-174. doi:10.1177/0734282909348217

Basser, P. J., & Pierpaoli, C. (1996). Microstructural and physiological features of tissues elucidated by quantitative-diffusion-tensor MRI. *J Magn Reson B, 111*(3), 209-219. doi:10.1006/jmrb.1996.0086

Beck, A. T., Steer, R. A., & Brown, G. K. (1996). Manual for the beck depression inventory-II. In: San Antonio, TX: Psychological Corporation.

Bhatia, K., Henderson, L., Yim, M., Hsu, E., & Dhaliwal, R. (2017). Diffusion Tensor Imaging Investigation of Uncinate Fasciculus Anatomy in Healthy Controls: Description of a Subgenual Stem. *Neuropsychobiology, 75*(3), 132-140. doi:10.1159/000485111

Bollinger, J. L., Collins, K. E., Patel, R., & Wellman, C. L. (2017). Behavioral stress alters corticolimbic microglia in a sex- and brain region-specific manner. *PLOS ONE, 12*(12), e0187631. doi:10.1371/journal.pone.0187631

Bruni, T. P. (2014). Test Review: Social Responsiveness Scale–Second Edition (SRS-2). *Journal of Psychoeducational Assessment, 32*(4), 365-369. doi:10.1177/0734282913517525

Bürgel, U., Amunts, K., Hoemke, L., Mohlberg, H., Gilsbach, J. M., & Zilles, K. (2006). White matter fiber tracts of the human brain: Three-dimensional mapping at microscopic resolution, topography and intersubject variability. *NeuroImage, 29*(4), 1092-1105. doi:https://doi.org/10.1016/j.neuroimage.2005.08.040

Cassidy, S. A., Bradley, L., Bowen, E., Wigham, S., & Rodgers, J. (2018). Measurement properties of tools used to assess depression in adults with and without autism spectrum conditions: A systematic review. *Autism Res, 11*(5), 738-754. doi:10.1002/aur.1922

Castanheira, L., Silva, C., Cheniaux, E., & Telles-Correia, D. (2019). Neuroimaging Correlates of Depression—Implications to Clinical Practice. *Frontiers in Psychiatry, 10*. doi:10.3389/fpsyt.2019.00703

Cathomas, F., Azzinnari, D., Bergamini, G., Sigrist, H., Buerge, M., Hoop, V., Wicki, B., Goetze, L., Soares, S., Kukelova, D., Seifritz, E., Goebbels, S., Nave, K.-A., Ghandour, M. S., Seoighe, C., Hildebrandt, T., Leparc, G., Klein, H., Stupka, E., Hengerer, B., & Pryce, C. R. (2019). Oligodendrocyte gene expression is reduced by and influences effects of chronic social stress in mice. *Genes, Brain and Behavior, 18*(1), e12475. doi:https://doi.org/10.1111/gbb.12475

Chandrasekhar, T., & Sikich, L. (2015). Challenges in the diagnosis and treatment of depression in autism spectrum disorders across the lifespan. *Dialogues Clin Neurosci, 17*(2), 219-227. doi:10.31887/DCNS.2015.17.2/tchandrasekhar

Constantino, J. N., & Gruber, C. P. (2012). *Social responsiveness scale: SRS-2*: Western psychological services Torrance, CA.

Cui, J.-L., Wen, C.-Y., Hu, Y., Li, T.-H., & Luk, K. D.-K. (2011). Entropy-based analysis for diffusion anisotropy mapping of healthy and myelopathic spinal cord. *NeuroImage, 54*(3), 2125-2131. doi:https://doi.org/10.1016/j.neuroimage.2010.10.018

Davey, C., Whittle, S., Harrison, B., Simmons, J., Byrne, M., Schwartz, O., & Allen, N. (2014). Functional brain-imaging correlates of negative affectivity and the onset of first-episode depression. *Psychological Medicine, 45*, 1-9. doi:10.1017/S0033291714002001

De Erausquin, G., & Alba-Ferrara, L. (2013). What does anisotropy measure? Insights from increased and decreased anisotropy in selective fiber tracts in schizophrenia. *Frontiers in integrative neuroscience, 7*. doi:10.3389/fnint.2013.00009

de Kwaasteniet, B., Ruhe, E., Caan, M., Rive, M., Olabarriaga, S., Groefsema, M., Heesink, L., van Wingen, G., & Denys, D. (2013). Relation between structural and functional

connectivity in major depressive disorder. *Biol Psychiatry, 74*(1), 40-47. doi:10.1016/j.biopsych.2012.12.024

Delic, J., Alhilali, L. M., Hughes, M. A., Gumus, S., & Fakhran, S. (2016). White Matter Injuries in Mild Traumatic Brain Injury and Posttraumatic Migraines: Diffusion Entropy Analysis. *Radiology, 279*(3), 859-866. doi:10.1148/radiol.2015151388

Ding, G., Chen, J., Chopp, M., Li, L., Yan, T., Davoodi-Bojd, E., Li, Q., Davarani, S. P., & Jiang, Q. (2017). White matter changes after stroke in type 2 diabetic rats measured by diffusion magnetic resonance imaging. *Journal of Cerebral Blood Flow & Metabolism, 37*(1), 241-251. doi:10.1177/0271678x15622464

Duan, F., Zhao, T., He, Y., & Shu, N. (2015). Test-Retest Reliability of Diffusion Measures in Cerebral White Matter: A Multiband Diffusion MRI Study. *Journal of magnetic resonance imaging : JMRI, 42*. doi:10.1002/jmri.24859

Dunlop, B. W., & Mayberg, H. S. (2017). Neuroimaging Advances for Depression. *Cerebrum, 2017*.

Evans, A. C., Janke, A. L., Collins, D. L., & Baillet, S. (2012). Brain templates and atlases. *NeuroImage, 62*(2), 911-922. doi:https://doi.org/10.1016/j.neuroimage.2012.01.024

Feldman, H. M., Yeatman, J. D., Lee, E. S., Barde, L. H. F., & Gaman-Bean, S. (2010). Diffusion tensor imaging: a review for pediatric researchers and clinicians. *Journal of developmental and behavioral pediatrics : JDBP, 31*(4), 346-356. doi:10.1097/DBP.0b013e3181dcaa8b

Ferrara, N. C., Trask, S., & Rosenkranz, J. A. (2021). Maturation of amygdala inputs regulate shifts in social and fear behaviors: A substrate for developmental effects of stress. *Neuroscience & Biobehavioral Reviews, 125*, 11-25. doi:https://doi.org/10.1016/j.neubiorev.2021.01.021

Fozouni, N., Chopp, M., Nejad-Davarani, S. P., Zhang, Z. G., Lehman, N. L., Gu, S., Ueno, Y., Lu, M., Ding, G., Li, L., Hu, J., Bagher-Ebadian, H., Hearshen, D., & Jiang, Q. (2013). Characterizing Brain Structures and Remodeling after TBI Based on Information Content, Diffusion Entropy. *PLOS ONE, 8*(10), e76343. doi:10.1371/journal.pone.0076343

Gennatas, E. D., Avants, B. B., Wolf, D. H., Satterthwaite, T. D., Ruparel, K., Ciric, R., Hakonarson, H., Gur, R. E., & Gur, R. C. (2017). Age-Related Effects and Sex Differences in Gray Matter Density, Volume, Mass, and Cortical Thickness from Childhood to Young Adulthood. *J Neurosci, 37*(20), 5065-5073. doi:10.1523/jneurosci.3550-16.2017

Gibbard, C. R., Ren, J., Skuse, D. H., Clayden, J. D., & Clark, C. A. (2018). Structural connectivity of the amygdala in young adults with autism spectrum disorder. *Human Brain Mapping, 39*(3), 1270-1282. doi:https://doi.org/10.1002/hbm.23915

Graciarena, M., Seiffe, A., Nait-Oumesmar, B., & Depino, A. M. (2019). Hypomyelination and Oligodendroglial Alterations in a Mouse Model of Autism Spectrum Disorder. *Frontiers in Cellular Neuroscience, 12*(517). doi:10.3389/fncel.2018.00517

Grassi, D. C., Conceição, D. M. d., Leite, C. d. C., & Andrade, C. S. (2018). Current contribution of diffusion tensor imaging in the evaluation of diffuse axonal injury. *Arquivos de Neuro-Psiquiatria, 76*.

Haigh, S. M., Keller, T. A., Minshew, N. J., & Eack, S. M. (2020). Reduced White Matter Integrity and Deficits in Neuropsychological Functioning in Adults With Autism Spectrum Disorder. *Autism Research, 13*(5), 702-714. doi:https://doi.org/10.1002/aur.2271

Henriques, R. N., Correia, M. M., Marrale, M., Huber, E., Kruper, J., Koudoro, S., Yeatman, J. D., Garyfallidis, E., & Rokem, A. (2021). Diffusional Kurtosis Imaging in the Diffusion

Imaging in Python Project. *Frontiers in Human Neuroscience, 15*. Retrieved from https://www.frontiersin.org/articles/10.3389/fnhum.2021.675433

Ho, P. S., Lin, C., Chen, G. Y., Liu, H. L., Huang, C. M., Lee, T. M. C., Lee, S. H., & Wu, S. C. (2017, 11-15 July 2017). *Complexity analysis of resting state fMRI signals in depressive patients.* Paper presented at the 2017 39th Annual International Conference of the IEEE Engineering in Medicine and Biology Society (EMBC).

Hollocks, M. J., Lerh, J. W., Magiati, I., Meiser-Stedman, R., & Brugha, T. S. (2019). Anxiety and depression in adults with autism spectrum disorder: a systematic review and meta-analysis. *Psychological Medicine, 49*(4), 559-572. doi:10.1017/S0033291718002283

Huang, S. Y., Fan, Q., Machado, N., Eloyan, A., Bireley, J. D., Russo, A. W., Tobyne, S. M., Patel, K. R., Brewer, K., Rapaport, S. F., Nummenmaa, A., Witzel, T., Sherman, J. C., Wald, L. L., & Klawiter, E. C. (2019). Corpus callosum axon diameter relates to cognitive impairment in multiple sclerosis. *Annals of Clinical and Translational Neurology, 6*(5), 882-892. doi:10.1002/acn3.760

Hudson, C. C., Hall, L., & Harkness, K. L. (2019). Prevalence of Depressive Disorders in Individuals with Autism Spectrum Disorder: a Meta-Analysis. *Journal of Abnormal Child Psychology, 47*(1), 165-175. doi:10.1007/s10802-018-0402-1

IBM Corp. Released 2020. IBM SPSS Statistics for Windows, Version 27.0. Armonk, NY: IBM Corp

Jenkinson, M., Beckmann, C. F., Behrens, T. E. J., Woolrich, M. W., & Smith, S. M. (2012). FSL. *NeuroImage, 62*(2), 782-790. doi:https://doi.org/10.1016/j.neuroimage.2011.09.015

Kaufman, A. S. (2004). Kaufman brief intelligence test–second edition (KBIT-2). *Circle Pines, MN: American Guidance Service*.

Kier, E. L., Staib, L. H., Davis, L. M., & Bronen, R. A. (2004). MR imaging of the temporal stem: anatomic dissection tractography of the uncinate fasciculus, inferior occipitofrontal fasciculus, and Meyer's loop of the optic radiation. *AJNR Am J Neuroradiol, 25*(5), 677-691.

Kochunov, P., Hong, L. E., Dennis, E. L., Morey, R. A., Tate, D. F., Wilde, E. A., Logue, M., Kelly, S., Donohoe, G., Favre, P., Houenou, J., Ching, C. R. K., Holleran, L., Andreassen, O. A., van Velzen, L. S., Schmaal, L., Villalón-Reina, J. E., Bearden, C. E., Piras, F., Spalletta, G., van den Heuvel, O. A., Veltman, D. J., Stein, D. J., Ryan, M. C., Tan, Y., van Erp, T. G. M., Turner, J. A., Haddad, L., Nir, T. M., Glahn, D. C., Thompson, P. M., & Jahanshad, N. (2022). ENIGMA-DTI: Translating reproducible white matter deficits into personalized vulnerability metrics in cross-diagnostic psychiatric research. *Human Brain Mapping, 43*(1), 194-206. doi:https://doi.org/10.1002/hbm.24998

Kroenke, K., Spitzer, R. L., & Williams, J. B. (2001). The PHQ-9: validity of a brief depression severity measure. *J Gen Intern Med, 16*(9), 606-613. doi:10.1046/j.1525-1497.2001.016009606.x

Lebel, C., Treit, S., & Beaulieu, C. (2019). A review of diffusion MRI of typical white matter development from early childhood to young adulthood. *NMR in Biomedicine, 32*(4), e3778. doi:https://doi.org/10.1002/nbm.3778

Lerner, A., Mogensen, M. A., Kim, P. E., Shiroishi, M. S., Hwang, D. H., & Law, M. (2014). Clinical applications of diffusion tensor imaging. *World Neurosurg, 82*(1-2), 96-109. doi:10.1016/j.wneu.2013.07.083

Li, X., Morgan, P. S., Ashburner, J., Smith, J., & Rorden, C. (2016). The first step for neuroimaging data analysis: DICOM to NIfTI conversion. *Journal of Neuroscience Methods, 264*, 47-56. doi:https://doi.org/10.1016/j.jneumeth.2016.03.001

Liu, H., Yang, Y., Xia, Y., Zhu, W., Leak, R. K., Wei, Z., Wang, J., & Hu, X. (2017). Aging of cerebral white matter. *Ageing Res Rev, 34*, 64-76. doi:10.1016/j.arr.2016.11.006

Lochner, C., Fouché, J.-P., du Plessis, S., Spottiswoode, B., Seedat, S., Fineberg, N., Chamberlain, S. R., & Stein, D. J. (2012). Evidence for fractional anisotropy and mean diffusivity white matter abnormalities in the internal capsule and cingulum in patients with obsessive–compulsive disorder. *Journal of Psychiatry and Neuroscience, 37*(3), 193-199.

Luque Laguna, P. A., Combes, A. J. E., Streffer, J., Einstein, S., Timmers, M., Williams, S. C. R., & Dell'Acqua, F. (2020). Reproducibility, reliability and variability of FA and MD in the older healthy population: A test-retest multiparametric analysis. *NeuroImage: Clinical, 26*, 102168. doi:https://doi.org/10.1016/j.nicl.2020.102168

Ma, L., Liu, M., Xue, K., Ye, C., Man, W., Cheng, M., Liu, Z., Zhu, D., Liu, F., & Wang, J. (2022). Abnormal Regional Spontaneous Brain Activities in White Matter in Patients with Autism Spectrum Disorder. *Neuroscience, 490*, 1-10. doi:https://doi.org/10.1016/j.neuroscience.2022.02.022

Madden, D. J., Bennett, I. J., Burzynska, A., Potter, G. G., Chen, N.-k., & Song, A. W. (2012). Diffusion tensor imaging of cerebral white matter integrity in cognitive aging. *Biochimica et Biophysica Acta (BBA) - Molecular Basis of Disease, 1822*(3), 386-400. doi:https://doi.org/10.1016/j.bbadis.2011.08.003

Maximo, J. O., Nelson, C. M., & Kana, R. K. (2021). "Unrest while Resting"? Brain entropy in autism spectrum disorder. *Brain Research, 1762*, 147435. doi:https://doi.org/10.1016/j.brainres.2021.147435

Medina, D. A., & Gaviria, M. (2008). Diffusion tensor imaging investigations in Alzheimer's disease: the resurgence of white matter compromise in the cortical dysfunction of the aging brain. *Neuropsychiatr Dis Treat, 4*(4), 737-742. doi:10.2147/ndt.s3381

Mori, S., Oishi, K., Jiang, H., Jiang, L., Li, X., Akhter, K., Hua, K., Faria, A. V., Mahmood, A., Woods, R., Toga, A. W., Pike, G. B., Neto, P. R., Evans, A., Zhang, J., Huang, H., Miller, M. I., van Zijl, P., & Mazziotta, J. (2008). Stereotaxic white matter atlas based on diffusion tensor imaging in an ICBM template. *NeuroImage, 40*(2), 570-582. doi:https://doi.org/10.1016/j.neuroimage.2007.12.035

National Institute of Mental Health. (2022, January). *Major depression*. National Institute of Mental Health. Retrieved October 14, 2022, from https://www.nimh.nih.gov/health/statistics/major-depression

Nickel, K., Tebartz van Elst, L., Perlov, E., Endres, D., Müller, G. T., Riedel, A., Fangmeier, T., & Maier, S. (2017). Altered white matter integrity in adults with autism spectrum disorder and an IQ >100: a diffusion tensor imaging study. *Acta Psychiatrica Scandinavica, 135*(6), 573-583. doi:https://doi.org/10.1111/acps.12731

Noriuchi, M., Kikuchi, Y., Yoshiura, T., Kira, R., Shigeto, H., Hara, T., Tobimatsu, S., & Kamio, Y. (2010). Altered white matter fractional anisotropy and social impairment in children with autism spectrum disorder. *Brain Research, 1362*, 141-149. doi:https://doi.org/10.1016/j.brainres.2010.09.051

Ota, M., Noda, T., Sato, N., Hattori, K., Hori, H., Sasayama, D., Teraishi, T., Nagashima, A., Obu, S., Higuchi, T., & Kunugi, H. (2015). White matter abnormalities in major depressive disorder with melancholic and atypical features: A diffusion tensor imaging study.

Psychiatry and Clinical Neurosciences, 69(6), 360-368. doi:https://doi.org/10.1111/pcn.12255

Ouyang, Y., Cui, D., Yuan, Z., Liu, Z., Jiao, Q., Yin, T., & Qiu, J. (2021). Analysis of Age-Related White Matter Microstructures Based on Diffusion Tensor Imaging. *Frontiers in Aging Neuroscience, 13*. doi:10.3389/fnagi.2021.664911

Penke, L., Maniega, S. M., Murray, C., Gow, A. J., Valdés Hernández, M. C., Clayden, J. D., Starr, J. M., Wardlaw, J. M., Bastin, M. E., & Deary, I. J. (2010). A General Factor of Brain White Matter Integrity Predicts Information Processing Speed in Healthy Older People. *The Journal of Neuroscience, 30*(22), 7569-7574. doi:10.1523/jneurosci.1553-10.2010

Rolls, E. T., Huang, C.-C., Lin, C.-P., Feng, J., & Joliot, M. (2020). Automated anatomical labelling atlas 3. *NeuroImage, 206*, 116189. doi:https://doi.org/10.1016/j.neuroimage.2019.116189

Rovaris, M., Agosta, F., Pagani, E., & Filippi, M. (2009). Diffusion Tensor MR Imaging. *Neuroimaging Clinics of North America, 19*(1), 37-43. doi:https://doi.org/10.1016/j.nic.2008.08.001

Rubinow, M. J., Mahajan, G., May, W., Overholser, J. C., Jurjus, G. J., Dieter, L., Herbst, N., Steffens, D. C., Miguel-Hidalgo, J. J., Rajkowska, G., & Stockmeier, C. A. (2016). Basolateral amygdala volume and cell numbers in major depressive disorder: a postmortem stereological study. *Brain Structure and Function, 221*(1), 171-184. doi:10.1007/s00429-014-0900-z

Sato, W., Kochiyama, T., Uono, S., Yoshimura, S., Kubota, Y., Sawada, R., Sakihama, M., & Toichi, M. (2017). Reduced Gray Matter Volume in the Social Brain Network in Adults with Autism Spectrum Disorder. *Front Hum Neurosci, 11*, 395. doi:10.3389/fnhum.2017.00395

Seguin, D., Pac, S., Wang, J., Nicolson, R., Martinez-Trujillo, J., & Duerden, E. G. (2021). Amygdala subnuclei development in adolescents with autism spectrum disorder: Association with social communication and repetitive behaviors. *Brain and Behavior, 11*(8), e2299. doi:https://doi.org/10.1002/brb3.2299

Shannon, C. E. (1997). The mathematical theory of communication. 1963. *MD computing: computers in medical practice, 14*(4), 306-317.

Shannon E. Grogans, M.S. ,, Andrew S. Fox, Ph.D. ,, & Alexander J. Shackman, Ph.D. (2022). The Amygdala and Depression: A Sober Reconsideration. *American Journal of Psychiatry, 179*(7), 454-457. doi:10.1176/appi.ajp.20220412

Sheline, Y. I., Sanghavi, M., Mintun, M. A., & Gado, M. H. (1999). Depression duration but not age predicts hippocampal volume loss in medically healthy women with recurrent major depression. *J Neurosci, 19*(12), 5034-5043. doi:10.1523/jneurosci.19-12-05034.1999

Shen, M. D., Swanson, M. R., Wolff, J. J., Elison, J. T., Girault, J. B., Kim, S. H., Smith, R. G., Graves, M. M., Weisenfeld, L. A. H., Flake, L., MacIntyre, L., Gross, J. L., Burrows, C. A., Fonov, V. S., Collins, D. L., Evans, A. C., Gerig, G., McKinstry, R. C., Pandey, J., St. John, T., Zwaigenbaum, L., Estes, A. M., Dager, S. R., Schultz, R. T., Styner, M. A., Botteron, K. N., Hazlett, H. C., & Piven, J. (2022). Subcortical Brain Development in Autism and Fragile X Syndrome: Evidence for Dynamic, Age- and Disorder-Specific Trajectories in Infancy. *American Journal of Psychiatry, 179*(8), 562-572. doi:10.1176/appi.ajp.21090896

Shukla, D. K., Keehn, B., & Müller, R. A. (2011). Tract-specific analyses of diffusion tensor imaging show widespread white matter compromise in autism spectrum disorder. *J Child Psychol Psychiatry, 52*(3), 286-295. doi:10.1111/j.1469-7610.2010.02342.x

Smarr, K. L., & Keefer, A. L. (2011). Measures of depression and depressive symptoms: Beck Depression Inventory-II (BDI-II), Center for Epidemiologic Studies Depression Scale (CES-D), Geriatric Depression Scale (GDS), Hospital Anxiety and Depression Scale (HADS), and Patient Health Questionnaire-9 (PHQ-9). *Arthritis Care & Research, 63*(S11), S454-S466. doi:https://doi.org/10.1002/acr.20556

Smith, S. M. (2002). Fast robust automated brain extraction. *Hum Brain Mapp, 17*(3), 143-155. doi:10.1002/hbm.10062

Smith, S. M., Jenkinson, M., Woolrich, M. W., Beckmann, C. F., Behrens, T. E. J., Johansen-Berg, H., Bannister, P. R., De Luca, M., Drobnjak, I., Flitney, D. E., Niazy, R. K., Saunders, J., Vickers, J., Zhang, Y., De Stefano, N., Brady, J. M., & Matthews, P. M. (2004). Advances in functional and structural MR image analysis and implementation as FSL. *NeuroImage, 23*, S208-S219. doi:https://doi.org/10.1016/j.neuroimage.2004.07.051

Smith, S. M., Jenkinson, M., Johansen-Berg, H., Rueckert, D., Nichols, T. E., Mackay, C. E., Watkins, K. E., Ciccarelli, O., Cader, M. Z., Matthews, P. M., & Behrens, T. E. (2006). Tract-based spatial statistics: voxelwise analysis of multi-subject diffusion data. *NeuroImage, 31*(4), 1487-1505. doi:10.1016/j.neuroimage.2006.02.024

Snook, L., Paulson, L.A., Roy, D., Phillips, L., & Beaulieu, C. (2005). Diffusion tensor imaging of neurodevelopment in children and young adults. *NeuroImage, 26*(4), 1164-1173. doi:https://doi.org/10.1016/j.neuroimage.2005.03.016

Stieltjes, B., Kaufmann, W. E., van Zijl, P. C. M., Fredericksen, K., Pearlson, G. D., Solaiyappan, M., & Mori, S. (2001). Diffusion Tensor Imaging and Axonal Tracking in the Human Brainstem. *NeuroImage, 14*(3), 723-735. doi:https://doi.org/10.1006/nimg.2001.0861

Sullivan, E. V., Rohlfing, T., & Pfefferbaum, A. (2010). Longitudinal study of callosal microstructure in the normal adult aging brain using quantitative DTI fiber tracking. *Developmental Neuropsychology, 35*(3), 233-256. doi:10.1080/87565641003689556

Tae, W. S., Ham, B. J., Pyun, S. B., Kang, S. H., & Kim, B. J. (2018). Current Clinical Applications of Diffusion-Tensor Imaging in Neurological Disorders. *J Clin Neurol, 14*(2), 129-140. doi:10.3988/jcn.2018.14.2.129

Tang, Y., Kong, L., Wu, F., Womer, F., Jiang, W., Cao, Y., Ren, L., Wang, J., Fan, G., Blumberg, H. P., Xu, K., & Wang, F. (2013). Decreased functional connectivity between the amygdala and the left ventral prefrontal cortex in treatment-naive patients with major depressive disorder: a resting-state functional magnetic resonance imaging study. *Psychological Medicine, 43*(9), 1921-1927. doi:10.1017/S0033291712002759

Timmers, I., Roebroeck, A., Bastiani, M., Jansma, B., Rubio-Gozalbo, E., & Zhang, H. (2016). Assessing Microstructural Substrates of White Matter Abnormalities: A Comparative Study Using DTI and NODDI. *PLOS ONE, 11*(12), e0167884. doi:10.1371/journal.pone.0167884

Tournier, J. D., Smith, R., Raffelt, D., Tabbara, R., Dhollander, T., Pietsch, M., Christiaens, D., Jeurissen, B., Yeh, C.-H., & Connelly, A. (2019). MRtrix3: A fast, flexible and open software framework for medical image processing and visualisation. *NeuroImage, 202*, 116137. doi:https://doi.org/10.1016/j.neuroimage.2019.116137

van Velzen, L. S., Kelly, S., Isaev, D., Aleman, A., Aftanas, L. I., Bauer, J., Baune, B. T., Brak, I. V., Carballedo, A., Connolly, C. G., Couvy-Duchesne, B., Cullen, K. R., Danilenko, K. V.,

Dannlowski, U., Enneking, V., Filimonova, E., Förster, K., Frodl, T., Gotlib, I. H., Groenewold, N. A., Grotegerd, D., Harris, M. A., Hatton, S. N., Hawkins, E. L., Hickie, I. B., Ho, T. C., Jansen, A., Kircher, T., Klimes-Dougan, B., Kochunov, P., Krug, A., Lagopoulos, J., Lee, R., Lett, T. A., Li, M., MacMaster, F. P., Martin, N. G., McIntosh, A. M., McLellan, Q., Meinert, S., Nenadić, I., Osipov, E., Penninx, B. W. J. H., Portella, M. J., Repple, J., Roos, A., Sacchet, M. D., Sämann, P. G., Schnell, K., Shen, X., Sim, K., Stein, D. J., van Tol, M.-J., Tomyshev, A. S., Tozzi, L., Veer, I. M., Vermeiren, R., Vives-Gilabert, Y., Walter, H., Walter, M., van der Wee, N. J. A., van der Werff, S. J. A., Schreiner, M. W., Whalley, H. C., Wright, M. J., Yang, T. T., Zhu, A., Veltman, D. J., Thompson, P. M., Jahanshad, N., & Schmaal, L. (2020). White matter disturbances in major depressive disorder: a coordinated analysis across 20 international cohorts in the ENIGMA MDD working group. *Molecular Psychiatry, 25*(7), 1511-1525. doi:10.1038/s41380-019-0477-2

Velasquez, F., Wiggins, J. L., Mattson, W. I., Martin, D. M., Lord, C., & Monk, C. S. (2017). The influence of 5-HTTLPR transporter genotype on amygdala-subgenual anterior cingulate cortex connectivity in autism spectrum disorder. *Developmental Cognitive Neuroscience, 24*, 12-20. doi:https://doi.org/10.1016/j.dcn.2016.12.002

Von Der Heide, R. J., Skipper, L. M., Klobusicky, E., & Olson, I. R. (2013). Dissecting the uncinate fasciculus: disorders, controversies and a hypothesis. *Brain, 136*(Pt 6), 1692-1707. doi:10.1093/brain/awt094

Waiter, G. D., Williams, J. H. G., Murray, A. D., Gilchrist, A., Perrett, D. I., & Whiten, A. (2005). Structural white matter deficits in high-functioning individuals with autistic spectrum disorder: a voxel-based investigation. *NeuroImage, 24*(2), 455-461. doi:https://doi.org/10.1016/j.neuroimage.2004.08.049

Wegiel, J., Kaczmarski, W., Flory, M., Martinez-Cerdeno, V., Wisniewski, T., Nowicki, K., Kuchna, I., & Wegiel, J. (2018). Deficit of corpus callosum axons, reduced axon diameter and decreased area are markers of abnormal development of interhemispheric connections in autistic subjects. *Acta Neuropathologica Communications, 6*(1), 143. doi:10.1186/s40478-018-0645-7

Westlye, L. T., Walhovd, K. B., Dale, A. M., Bjørnerud, A., Due-Tønnessen, P., Engvig, A., Grydeland, H., Tamnes, C. K., Østby, Y., & Fjell, A. M. (2009). Life-Span Changes of the Human Brain White Matter: Diffusion Tensor Imaging (DTI) and Volumetry. *Cerebral Cortex, 20*(9), 2055-2068. doi:10.1093/cercor/bhp280

Williams, Z. J., Everaert, J., & Gotham, K. O. (2021). Measuring Depression in Autistic Adults: Psychometric Validation of the Beck Depression Inventory-II. *Assessment, 28*(3), 858-876. doi:10.1177/1073191120952889

Wise, T., Cleare, A. J., Herane, A., Young, A. H., & Arnone, D. (2014). Diagnostic and therapeutic utility of neuroimaging in depression: an overview. *Neuropsychiatr Dis Treat, 10*, 1509-1522. doi:10.2147/ndt.S50156

Woolrich, M. W., Jbabdi, S., Patenaude, B., Chappell, M., Makni, S., Behrens, T., Beckmann, C., Jenkinson, M., & Smith, S. M. (2009). Bayesian analysis of neuroimaging data in FSL. *NeuroImage, 45*(1, Supplement 1), S173-S186. doi:https://doi.org/10.1016/j.neuroimage.2008.10.055

Yang, T. (2014). EPA-0625 – White Matter Diffusion Tensor Imaging Microstructure Correlates of Adolescent Depression: Structural Evidence for Frontolimbic Disconnectivity. *European Psychiatry, 29*(S1), 1-1. doi:10.1016/S0924-9338(14)78003-4

Yang, T. T., Simmons, A. N., Matthews, S. C., Tapert, S. F., Frank, G. K., Bischoff-Grethe, A., Lansing, A. E., Wu, J., Brown, G. G., & Paulus, M. P. (2009). Depressed adolescents demonstrate greater subgenual anterior cingulate activity. *Neuroreport, 20*(4), 440-444. doi:10.1097/WNR.0b013e3283262e10

Yarger, H. A. (2022). Anxiety-Amygdala Associations: Novel Insights From the First Longitudinal Study of Autistic Youth With Distinct Anxiety. *Biological Psychiatry, 91*(11), e41-e43. doi:10.1016/j.biopsych.2022.03.016

Zhan, C. Liu, Y., Wu, K., Gao, Y., Li, X. (2017). Structural and Functional Abnormalities in Children with Attention-Deficit/Hyperactivity Disorder: A Focus on Subgenual Anterior Cingulate Cortex. (2017). *Brain Connectivity, 7*(2), 106-114. doi:10.1089/brain.2016.0444

Zhang, W., & Rosenkranz, J. A. (2012). Repeated restraint stress increases basolateral amygdala neuronal activity in an age-dependent manner. *Neuroscience, 226*, 459-474. doi:https://doi.org/10.1016/j.neuroscience.2012.08.051

Zheng, K. Z., Wang, H. N., Liu, J., Xi, Y. B., Li, L., Zhang, X., Li, J. M., Yin, H., Tan, Q. R., Lu, H. B., & Li, B. J. (2018). Incapacity to control emotion in major depression may arise from disrupted white matter integrity and OFC-amygdala inhibition. *CNS Neurosci Ther, 24*(11), 1053-1062. doi:10.1111/cns.12800

Zhao, Y., Yang, L., Gong, G., Cao, Q., & Liu, J. (2022). Identify aberrant white matter microstructure in ASD, ADHD and other neurodevelopmental disorders: A meta-analysis of diffusion tensor imaging studies. *Progress in Neuro-Psychopharmacology and Biological Psychiatry, 113*, 110477. doi:https://doi.org/10.1016/j.pnpbp.2021.110477

Zou, K., Huang, X., Li, T., Gong, Q., Li, Z., Ou-yang, L., Deng, W., Chen, Q., Li, C., Ding, Y., & Sun, X. (2008). Alterations of white matter integrity in adults with major depressive disorder: a magnetic resonance imaging study. *J Psychiatry Neurosci, 33*(6), 525-530.

Appendix I. DTI scan parameters in the BNI/SARRC cohort*
*Taken directly from ABIDE II website on February 15, 2023.
http://fcon_1000.projects.nitrc.org/indi/abide/scan_params/ABIDEII-BNI_1/dti.txt

Nucleus =	"H1";
SmartSelect =	"yes";
Coil 1 (exclude) =	"None";
Uniformity =	"CLEAR";
FOV	
RL (mm) =	270;
AP (mm) =	270;
FH (mm) =	144;
Voxel size	
RL (mm) =	3;
AP (mm) =	3;
Slice thickness (mm) =	3;
Recon voxel size (mm) =	1.40625;
Small FOV imaging =	"no";
Fold-over suppression =	"no";
Reconstruction matrix =	192;
SENSE =	"yes";
P reduction (AP) =	2;
k-t BLAST =	"no";
Stacks =	1;

```
    type =                          "parallel";
    slices =                        48;
    slice gap =                     "user defined";
        gap (mm) =                  0;
    slice orientation =             "transverse";
    fold-over direction =           "AP";
    fat shift direction =           "P";
Stack Offc.
        AP (P=+mm) =                -46.8054733;
        RL (L=+mm) =                -5.90813494;
        FH (H=+mm) =                23.3194065;
    Ang.
        AP (deg) =                  2.83938247e-021;
        RL (deg) =                  -0;
        FH (deg) =                  -0;
    Free rotatable =                "no";
Minimum number of packages =        1;
Slice scan order =                  "default";
Large table movement =              "no";
PlanAlign =                         "no";
REST slabs =                        0;
Catheter tracking =                 "no";
Interactive positioning =           "no";
Allow table movement =              "no";
Patient position =                  "head first";
      orientation =                 "supine";
Scan type =                         "Imaging";
Scan mode =                         "MS";
    technique =                     "SE";
```

Modified SE = "no";

Acquisition mode = "cartesian";

Fast Imaging mode = "EPI";

shot mode = "single-shot";

Echoes = 1;

partial echo = "no";

TE = "shortest";

Flip angle (deg) = 90;

TR = "shortest";

Halfscan = "no";

Water-fat shift = "minimum";

RF Shims = "fixed";

Shim = "auto";

mDIXON = "no";

Fat suppression = "SPIR";

strength = "strong";

frequency offset = "default";

Grad Rev Fat suppr = "no";

Water suppression = "no";

BB pulse = "no";

MTC = "no";

Research prepulse = "no";

Diffusion mode = "DTI";

sequence = "SE";

gradient duration = "maximum";

gradient overplus = "no";

directional resolution = "high (32)";

nr of b-factors = 2;

b-factor order = "ascending";

max b-factor = 2500;

average high b = "no";

Elastography mode = "no";

Transmit channels = "both";

SAR mode = "high";

B1 mode = "default";

SAR Patient data = "auto";

PNS mode = "moderate";

Gradient mode = "default";

SofTone mode = "no";

Cardiac synchronization = "no";

Heart rate > 250 bpm = "no";

Respiratory compensation = "no";

Navigator respiratory comp = "no";

Flow compensation = "no";

Temporal slice spacing = "default";

NSA = 1;

Manual start = "no";

Dynamic study = "no";

dyn stabilization = "no";

Arterial Spin labeling = "no";

Preparation phases = "auto";

Interactive F0 = "no";

SmartPlan survey = "no";

B0 field map = "no";

B1 field map = "no";

MIP/MPR = "no";

Images = "M", (3) "no";

Autoview image = "M";

Calculated images = (4) "no";

Reference tissue = "White matter";

EPI 2D phase correction = "no";

Recon compression = "No";

Preset window contrast = "soft";

Reconstruction mode = "immediate";

Save raw data = "no";

Hardcopy protocol = "no";

Image filter = "system default";

Geometry correction = "default";

IF_info_seperator = 1634755923;

Total scan duration = "04:34.8";

Rel. SNR = 1;

Act. TR (ms) = "7850";

Act. TE (ms) = "101";

ACQ matrix M x P = "92 x 90";

ACQ voxel MPS (mm) = "2.93 / 3.00 / 3.00";

REC voxel MPS (mm) = "1.41 / 1.41 / 3.00";

Scan percentage (%) = 97.826088;

Packages = 1;

Min. slice gap (mm) = -0;

Diffusion gradient timing DELTA / delta (ms) = "50.7 / 29.8";

EPI factor = 45;

WFS (pix) / BW (Hz) = "11.988 / 36.2";

BW in EPI freq. dir. (Hz) = "2621.1";

SAR / head = "< 24 %";

Whole body / level =	"< 0.1 W/kg / normal";
SED =	" 0.0 kJ/kg";
B1+rms / Coil Power =	"1.13 uT / 23 %";
Max B1+rms =	"1.13 uT";
PNS / level =	"67 % / normal";
dB/dt =	"62.4 T/s";
Sound Pressure Level (dB) =	9.9297514;